ENGINEERING

JOURNAL OF FLUID MECHANICS

VOLUME 3 PART 5

FEBRUARY 1958

Published by

CAMBRIDGE UNIVERSITY PRESS

BENTLEY HOUSE, 200 EUSTON ROAD, LONDON, N.W.1
AMERICAN BRANCH: 32 EAST 57th STREET, NEW YORK 22, N.Y.

Price 20*s*. (*U.S.A.* $3.25)

The JOURNAL OF FLUID MECHANICS exists for the publication of theoretical and experimental investigations of all aspects of the mechanics of fluids, and is issued in six parts per volume.

Editor

Dr. G. K. BATCHELOR, Cavendish Laboratory, University of Cambridge, Cambridge, England.

Assistant Editors

Dr. T. B. BENJAMIN, Dr. I. PROUDMAN, Dr. P. G. SAFFMAN.

Associate Editors

Prof. G. F. CARRIER, Pierce Hall, Harvard University, Cambridge 38, Massachusetts, U.S.A.

Dr. W. C. GRIFFITH, Research and Development Laboratory, Missile Systems Division, Lockheed Aircraft Corporation, Palo Alto, California, U.S.A.

Prof. M. J. LIGHTHILL, Department of Mathematics, The University, Manchester, England.

Authors wishing to have papers published in the JOURNAL should communicate them to any one of the persons named above, choosing one in their own country where possible.

Authors are urged to ensure that their papers are written clearly and attractively, in order that their work will be readily accessible to readers.

Manuscripts should be typed in double spacing on one side of the paper only, with references listed at the end in alphabetical order of authors. Drawings should be done on a large scale in Indian ink on tracing cloth or drawing paper, with the list of captions typed at the end of the manuscript. Proofs of papers from overseas will usually be despatched to authors by airmail. Authors are entitled to receive 50 offprints of a paper in the JOURNAL free of charge, and additional offprints can be purchased from the publisher.

SUBSCRIPTIONS

The subscription price for a volume of six parts is £5 10*s.* net, post free, payable in advance. Separate parts 20*s.* net, plus postage. Subscriptions may be sent to any bookseller, or to the Cambridge University Press, Bentley House, 200 Euston Road, London, N.W.1.

Subscribers in the United States should send their orders to the Cambridge University Press, American Branch, 32 East 57th Street, New York 22. Subscription price per volume $18.50 post free, payable in advance; separate parts $3.25, plus postage.

The behaviour of a Pitot tube in transverse shear

By P. O. A. L. DAVIES
Aeronautical Engineering Department, University of Southampton

(*Received* 30 *August* 1957)

SUMMARY

This paper presents an experimental investigation of the displacement of the total-head profile in a shear flow from its true position when it is measured with a flat-ended round Pitot tube. The experiments showed that at least two forms of displacement may exist depending on the flow conditions.

In a wake the displacement of the effective centre of pressure towards the higher velocity was found to obey the law deduced theoretically by Hall (1956), provided that changes in flow direction were not large. In the presence of large eddies the behaviour of the Pitot is further modified by its characteristics in yaw. This introduces a total-head error reducing the observed total head.

In a turbulent boundary layer the experiments showed that the displacements were an order of magnitude smaller than in a wake and could be regarded as negligible for a round Pitot, even when it was touching the wall.

An empirical method for correcting the observations made with a round Pitot which is of the same width as the wake is given in an appendix.

1. INTRODUCTION

In the experimental studies of boundary layers and wakes, the velocity profile is generally established by a Pitot traverse. The displacement of the effective centre of pressure recorded by a total-head Pitot tube in a wake has been studied experimentally by Young & Maas (1936) and theoretically by Hall (1956). A more exact theoretical study has just been published by Lighthill (1957) and his results substantiate Hall's simplified theory.

Young & Maas studied the wake close behind a symmetrical aerofoil, and found a displacement towards the region of higher velocity that could be expressed as a constant fraction of the Pitot diameter and was independent of the velocity gradient. However, as Young & Maas pointed out, this implies a sharp discontinuity in the displacement correction as the velocity gradient approaches zero, which is not physically plausible. Their observations indicate a velocity correction at the centre of the wake, but they did not discuss this in their paper.

Halls' theoretical investigation was based on the consideration of the vorticity field alone and neglected viscosity. He pointed out that in front of a three-dimensional object in uniform shear the vortex tube must be stretched, giving a local increase in vorticity. This gives a larger displacement of the stagnation streamline than pure two-dimensional flow alone. He then calculated the displacement of the stagnation streamline for a sphere in uniform shear, and showed it was a function of the velocity gradient as well as the mean velocity and the diameter of the Pitot. This avoids the discontinuity described in the previous paragraph.

This paper first describes an experimental investigation of the validity of Hall's assumptions, to resolve the discrepancy with the results of Young & Maas. Further experiments are described which were undertaken to establish the form of corrections which apply to other examples of shear flow. The experiments indicated that the different conditions existing in other forms of shear flow introduce different corrections. Examples of shear flow where conditions may differ significantly include (*a*) flow in a wake after large eddies have decayed; (*b*) flow in a wake just downstream of the trailing edge; (*c*) flow in a turbulent boundary layer; (*d*) flow in a laminar boundary layer; (*e*) flow where compressibility is important; (*f*) pulsating flow.

These experiments were confined to the first three of the above examples. Hall's work is confined to the first shear flow example, which is discussed in § 2 of this paper. The results of Young & Maas may be classed with example (*b*), which is discussed in § 3. Flow of the type in example (*c*) is discussed in § 4.

Other experimental work on displacement corrections has been published. Livesey (1956) has studied the corrections for cylindrical Pitots, and also gives some results for flat-ended Pitots of the conventional pattern. All his results were obtained in a turbulent boundary layer after it had been thickened by a wire cloth screen. Mawson & Lilley (1956) include results for high speed flow, and also include some observations for low speed flow which may be classed with examples (*a*) or (*b*). They were, however, primarily concerned with corrections for total-head tubes larger than the wake. Macmillan (1957) gives careful measurements which may be classed with example (*c*) both for a pipe and a flat plate. The effect of flow pulsations on total-head tube readings has been investigated by several authors, although very few observations have been recorded.

2. Total head measurements in a wake

Hall (1956) has shown that, when the vorticity field alone is considered, the displacement δ of the stagnation streamline from its position at infinity for a sphere in uniform shear can be expressed by

$$\delta/D = 0{\cdot}6200K - 0{\cdot}5786K^3 + O(K^5), \tag{1}$$

where D is the sphere diameter, and K represents the maximum difference between the velocities at the edges of the sphere divided by twice the mean velocity. (Lighthill's (1957) asymptotically exact theory for flows with

small shear (i.e. small K) gives $\delta/D = 0{\cdot}45K - CK^3$, where C is probably greater than 1·35. In his paper, K is expressed as Aa/u.) Hall suggested that a conventional flat-ended round Pitot tube may be represented by a sphere of slightly larger diameter.

It still remains to test Hall's two assumptions, namely that the viscosity may be neglected, and that a round Pitot of slightly smaller diameter may replace the sphere. To this end, traverses were made through a wake by a series of flat-ended round Pitots of graded size but constant shape, the ratio of bore to outer diameter being 0·6. Other experiments were made to investigate the effect of changing this ratio.

The traverses were carried out behind two models in a N.P.L. wind tunnel of 3 ft. × 2 ft. working section, the maximum available wind speed being 70 ft./sec. One of these was a two-dimensional symmetrical aerofoil of 10 in. chord and 5% thick. To permit the use of larger tubes an axi-symmetric double ogive (cigar-shaped), of 40 in. chord and 7 in. maximum diameter, was also employed. This form was chosen for the larger model to minimize the effects of tunnel interference. It was considered that at radii large compared with the Pitot diameter the flow could be considered for practical purposes two-dimensional. For checking Hall's assumptions, the traverses were carried out several wake widths downstream to allow for the decay of the large eddies produced by oscillation of the rear stagnation point, particularly in two-dimensional flow. Most of the measurements were made at a fixed wind speed, though check traverses made at other speeds gave similar results.

The undisturbed velocity head p_0 was measured with a standard round-nosed N.P.L. Pitot-static combination, of 0·5 in. outside diameter, placed well clear of the wake and just downstream of the trailing edge. The reading p of the total-head tube under test was compared with that from the standard total-head tube tapping, the difference $(p_0 - p)$ being observed. Care was taken to ensure this difference was exactly zero when the tube under test was outside the wake. This provided a check on the uniformity of the flow in the tunnel, and of the absence of leaks. The tunnel was an open N.P.L. type, and it was found that any leaks into the tunnel disturbed the flow there considerably.

The measurements were made in regions of appreciable turbulence, and therefore the pressure differences observed within the wake were fluctuating. To investigate a Pitot's behaviour it was essential to establish that the mean observed pressure was unaffected by changes in the dynamic behaviour of the manometer system due to changes of Pitot bore. It would have been ideal if the manometer system always recorded the true mean Pitot pressure, but it was not possible to establish that it did so in turbulent flow. Experiments did show, however, that variation of the manometer system response by throttling the leads produced no change in the recorded mean pressure in turbulent flow. This indicated that for the purpose of comparison of Pitot performance, variation of the dynamic behaviour of the manometer could be neglected.

Small temperature variations also limit the minimum Pitot bore which may be used satisfactorily with a given manometer system in unsteady conditions. It only requires a temperature change of 0·01° C to produce pressure variations of 0·015 in. of water in a constant volume system at atmospheric pressure. When the Pitot bore was 0·018 in., the manometer system would respond to a small disturbance of approximately $\frac{1}{4}$ second period. When the bore was reduced to 0·005 in., however, the period rose to 40 seconds, which was considered too long.

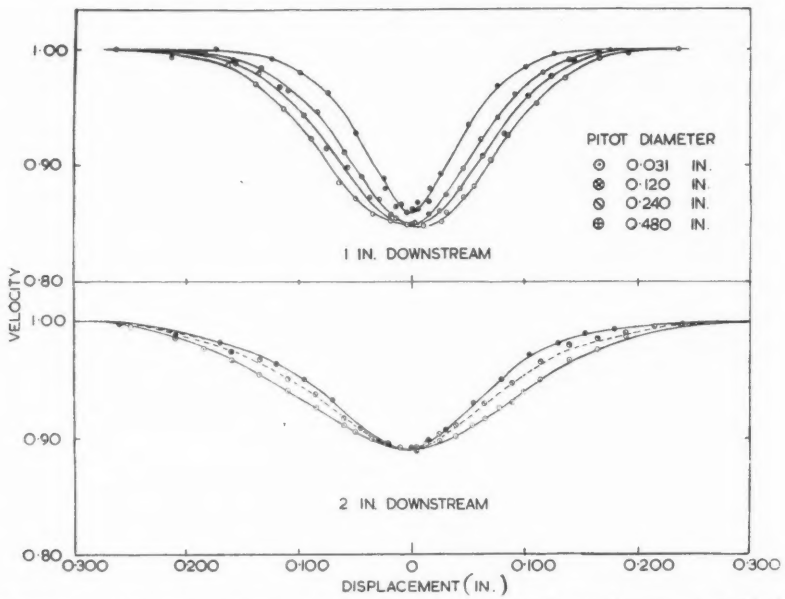

Figure 1. Wake velocity profiles observed by geometrically similar Pitots behind the aerofoil model.

The manometer was a simple vertical U-tube made of 3 mm precision bore glass tubing. A small quantity of detergent was added to the manometer water to minimize the effect of surface tension variations. The level was read with a travelling microscope fitted with a graticule to facilitate observation of fluctuating readings. Careful calibration showed that readings consistent to 0·001 in. of water were possible, though the precision could be increased by using a higher power microscope. When the amplitude of the fluctuations exceeded 0·010 in. of water, spot readings were taken every five seconds for half a minute and averaged to give the mean pressure.

Typical results are shown in figures 1 to 3, where the dimensionless wake velocity $(p/p_0)^{1/2}$ is plotted against transverse displacement y. From graphs of this type it was not possible to obtain the displacement correction and the corresponding value of K until the undisturbed profile was known. This was obtained by extrapolation from the profile measured with the

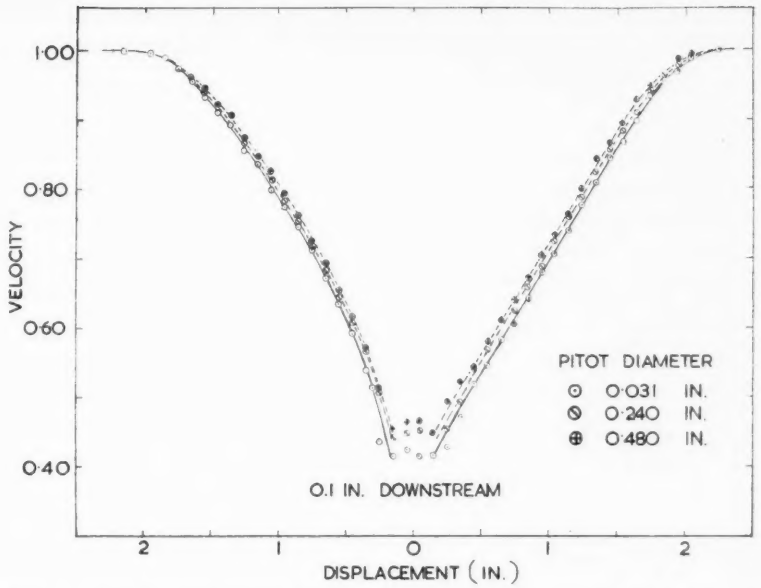

Figure 2. Wake velocity profiles observed by geometrically similar Pitots near the trailing edge of the axi-symmetric model.

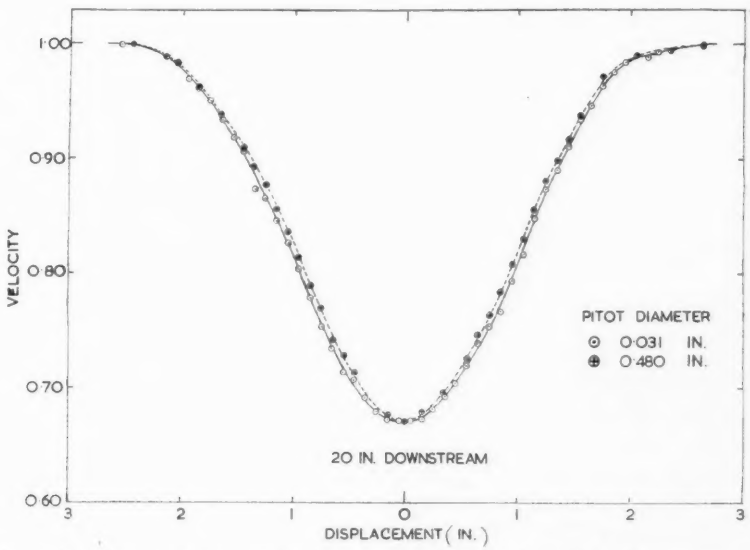

Figure 3. Wake velocity profiles observed several wake widths downstream of axi-symmetric model.

smallest tube. When K was small, the corrections for the smallest Pitot were negligible (less than 0·001 in. which was the limit of accuracy for measurements of y) compared with those for the largest tube, which were of the order of 0·05 in. Once the correction for low K was established, it was used to obtain the undisturbed velocity profile by extrapolation from that measured by the smallest Pitot. This prejudiced the accuracy of the results at high K values ($K > 0{\cdot}2$, say), but it was also difficult to obtain constant velocity gradients of sufficient width for measurements in this region.

The displacements observed have been plotted against the corresponding values of K in figure 4. This only includes those observations where the velocity gradient across the face of the tube was practically uniform. It can be seen from figure 4, particularly where $K < 0{\cdot}2$ and the accuracy is reasonably good, that the results show reasonable agreement with Hall's

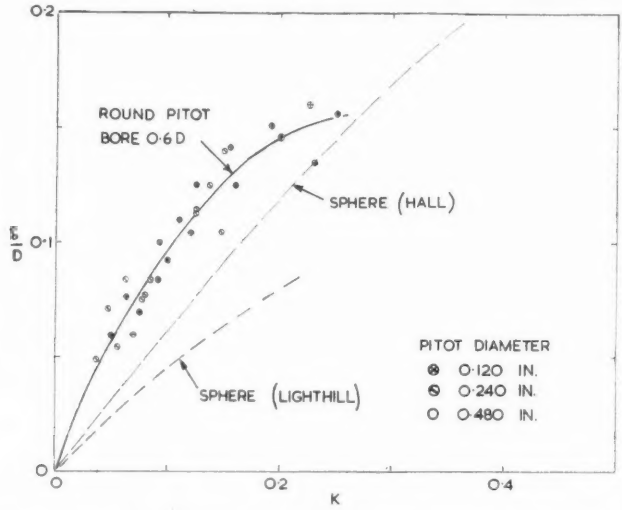

Figure 4. Pitot displacement corrections in two-dimensional uniform shear.

theoretical expression. The initial slope indicates a larger correction for a Pitot than for a sphere of the same diameter as Hall suggests. Lighthill (1957) has shown that the coefficient of $-K^3$ in Hall's expression (1) is much too small, which is in agreement with the results for flat-ended Pitots in figure 4. If Lighthill's expression is multiplied by two it fits these results.

Hall's theory applies to the displacement of the stagnation streamline in uniform shear flow. It might seem reasonable to suppose that an asymmetrical pressure distribution exists over the face of the tube corresponding to the incident flow. It is desirable therefore to check whether variations of the ratio of bore to diameter will alter the observed pressure. To this end a set of Pitots of constant diameter but varying bore were

tested, the results being shown in the upper part of figure 5. It can be seen that no significant difference was observed even though the ratio of bore to diameter was varied from 0·075 to 0·800. The observed pressure was, however, found to vary when the measurements were repeated close behind the trailing edge, as is demonstrated later in this paper.

In many instances (e.g. in supersonic flow) it is not possible to employ a Pitot small compared with the width of the wake. Results for traverses made with large Pitots, the largest spanning the wake, are included in figures 1 and 2. The observed displacements are less than those obtained by applying Hall's theory using the slope of the undisturbed profile at the centre of the Pitot. This is to be expected since Hall's theory applies to uniform shear and here both the sign and magnitude of the vorticity changes continuously across the face of the tube.

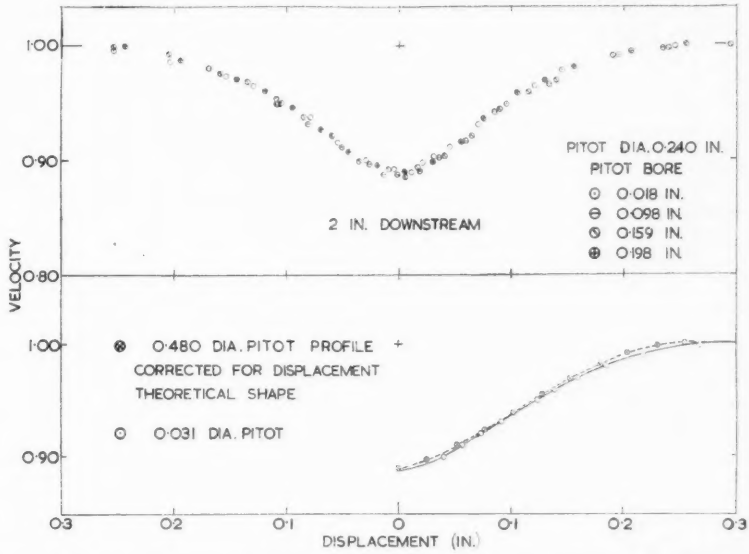

Figure 5. Effect of changing Pitot bore on observed wake velocity profile. The lower curve gives the corrected wake velocity profile.

It is, however, possible to obtain an approximate correction from a traverse with a large tube. The results in the lower part of figure 1 show that the corrections are zero at the centre of the wake. If the velocity in this position is taken as the minimum velocity, and if the maximum velocity is taken as unity, K being determined from these values, the corrections obtained are $\delta = 0{\cdot}031$ ($K = 0{\cdot}058$) compared with 0·033 observed with the large tube at the mean velocity. This correction is a little smaller than that observed, but not seriously so. It is well known that the shape of the velocity distribution in the wake obeys a universal law (Goldstein 1938, p. 581). If the velocity at the centre of the wake is known, and the width

of the wake is also known at the mean wake velocity, it is possible to establish the whole profile. The details of the process are given in the appendix to this paper, and the corrected profiles so obtained for the big Pitot are plotted in the lower part of figure 5. It can be seen that this empirical process can yield satisfactory results under favourable conditions.

3. Wake total-head measurements close to the trailing edge

The results obtained when traverses were made close to the trailing edge differed from those already described. It was found that the profiles did not coincide at the centre of the wake, where the displacement correction should be zero as in figure 1. This implies a total-head correction also exists, as was indicated by the results obtained by Young & Maas (1936). The results obtained just behind the symmetrical aerofoil were all similar to those plotted in figure 6. It can be seen here that the displacement is proportional to the Pitot diameter, although it differs on each side of the wake.

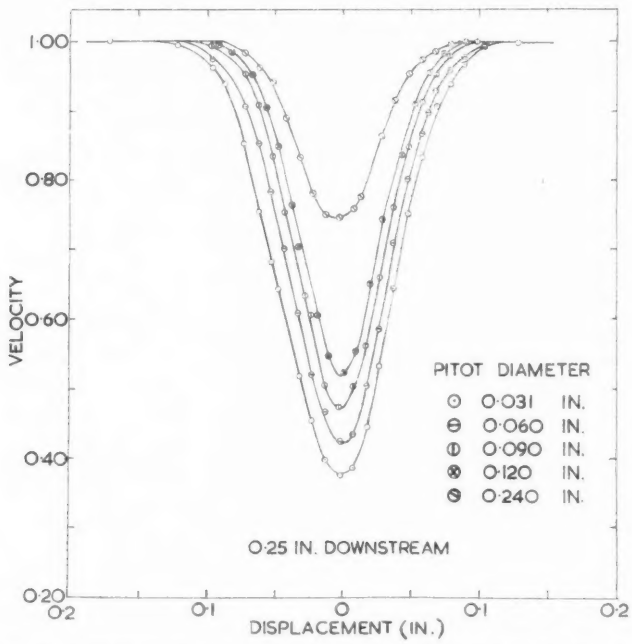

Figure 6. Wake velocity profiles recorded by geometrically similar Pitots near the trailing edge of aerofoil model.

Young & Maas obtained the correction by plotting the observed wake width at a given velocity versus the Pitot diameter. They obtained points lying approximately on straight lines of constant slope, the correction being equal to half this slope. Using their technique a displacement correction

equal to 0·24*D* was obtained for the results in figure 6. However, traverses 3/16 in. closer to the trailing edge yielded a correction equal to 0·28*D*, while traverses an equal distance downstream gave a correction of 0·16*D* when reduced by the same method.

The matter can be carried further. The momentum thickness calculated for each profile measured behind the aerofoil has been plotted against distance downstream from the trailing edge in figure 7. It can be seen that there is a tendency for the observed momentum thickness to rise sharply as the trailing edge is approached. If the correction were simply one of displacement towards the higher velocity one would expect the curve to drop as the trailing edge is approached, not rise. The effect could be explained by the existence of a velocity-head correction close to the trailing edge. A reason for its existence is not hard to find.

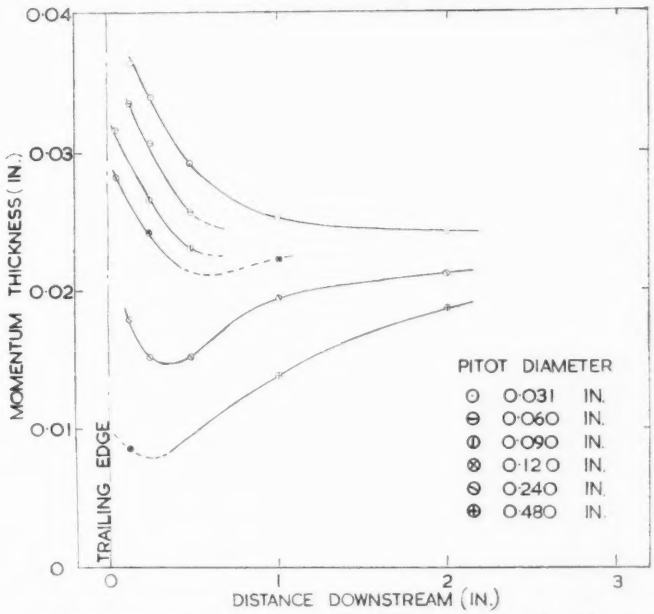

Figure 7. Momentum thickness calculated from uncorrected velocity profiles observed by geometrically similar Pitots in the aerofoil wake.

It is well known that a Pitot tube is very sensitive to yaw of more than a few degrees (Todd 1949). Not only is the mean direction of the flow inclined inwards near the trailing edges, but the flow direction oscillates rapidly about the trailing edge. This will produce large rapid variations in incident flow direction, and due to its directional characteristics the Pitot will record a pressure lower than the mean total head. Further downstream the fluctuations in the incident flow direction will be much smaller, and the Pitot will then record the mean total head.

It can be seen from figure 6 that this error in the total-head reading increases as the size of the Pitot is reduced. One would expect a Pitot close to the trailing edge would modify the flow there. The undisturbed flow is two-dimensional, but when a Pitot is introduced, the flow in its neighbourhood must be considered three-dimensional. In addition, the presence of a rigid body will introduce extra shear stresses if the flow direction departs from that of the body. This would modify the fluctuations in flow direction in the vicinity of the Pitot. The stabilizing of the flow would increase with the size of tube, with a corresponding reduction in the velocity-head error. The observations indicate that the reduction in the velocity-head error is roughly proportional to the diameter of the tube.

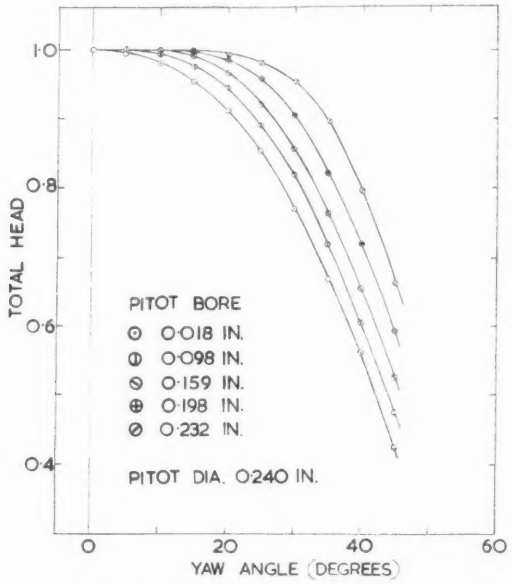

Figure 8. The effect of changing the bore of a yawed Pitot on its total head response.

This explanation of the results requires further confirmation. To this end, use may be made of the behaviour of yawed Pitot tubes. A series of Pitots of constant diameter but varying bore were tested in an empty tunnel at various angles of yaw. The results obtained are plotted in figure 8, which shows observed total head plotted against yaw angle. It can be seen that changes in bore produced substantial changes in total-head error. This seems reasonable as the forward stagnation point must be close to the leading corner of the Pitot and a pronounced pressure gradient must exist across the tapped face. Changes in bore will thus vary the observed pressure at any given yaw angle as the results indicate.

It has been shown earlier in figure 5 (upper part) that a series of Pitots of constant outside diameter but varying bore have the same displacement

correction in a stream of uniform vorticity. Furthermore, it seems reasonable to assume that their influence on the flow around them must be the same. The results of traverses made by a series of such Pitots are plotted in figure 9. In this case any difference between the profiles should be due to changes of total-head error of the form indicated in figure 8. The results indicate that substantial total-head errors do exist particularly at the centre and edges of the wake where the largest fluctuations are known to occur.

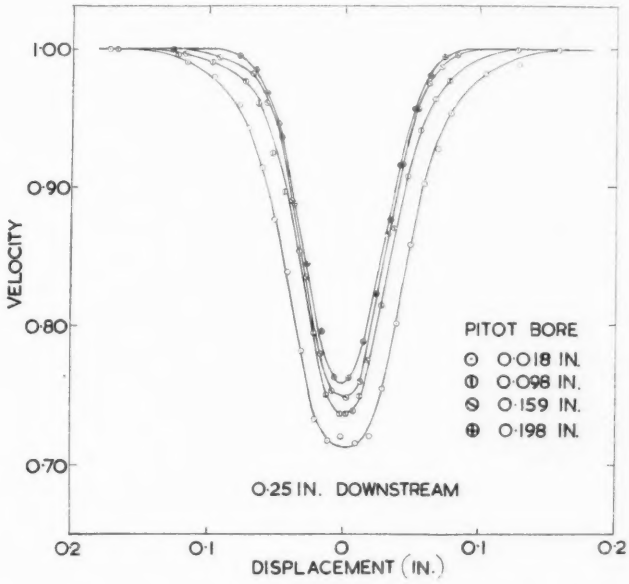

Figure 9. Wake velocity profiles displaying total head errors due to yaw.

A further experiment was performed to ensure the results in figure 9 were independent of the manometer system response. The 0·098 in. bore Pitot was fitted with a drilled plug to reduce its bore to 0·018 in. Traverses with the plug flush with the Pitot face reproduced the results obtained with the normal 0·018 in. Pitot, as would be expected. When the plug was pushed back, however, the behaviour approached that of an unplugged Pitot. The results are plotted in figure 10 and agree with those in figure 9. When the plug was displaced more than 0·050 in. the Pitot behaved as if it was unplugged. The dynamic response of the manometer system must have remained unchanged during these tests, demonstrating that the results in figure 9 were independent of the response.

It should be possible to obtain a profile corrected for velocity-head error corresponding to the results in figure 9, which are mean values. The results in figure 8 show how the correction varies with incident flow angle,

but it would be necessary to determine the distribution of incident flow angles with time before a mean correction could be calculated. An empirical correction can be estimated if it is assumed that the velocity-head error approaches zero as the Pitot wall thickness does so. This is true for small angles as shown in figure 8.

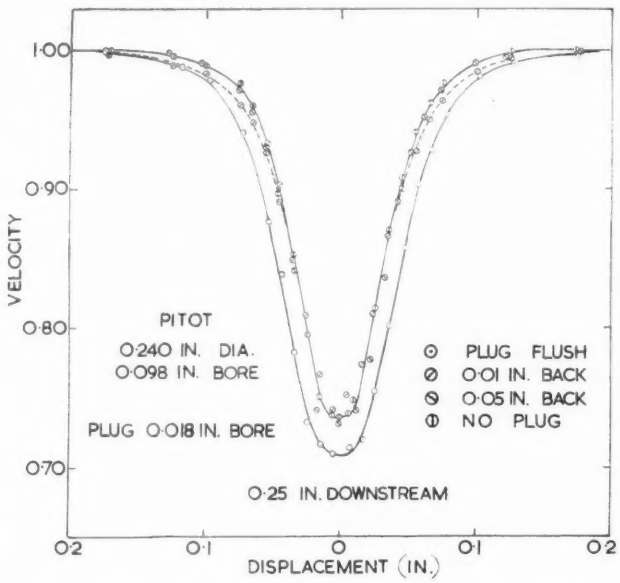

Figure 10. Wake velocity profiles observed with a manometer system of constant response obtained by fitting a sliding plug in the Pitot bore.

If this is done for the results in figure 9, the profile is very nearly that shown recorded with the largest bore Pitot, there being small corrections at the centre and edges of the wake. The profile so obtained must now be corrected for displacement error, and as the Pitot is large compared with the wake width the method outlined in the appendix is employed.

The profile finally corrected gives a momentum thickness of 0·025 in. (instead of the uncorrected value of 0·015 in.), which compares favourably with the values 0·025 in. and 0·0245 in. observed further down the wake using the smaller Pitot of 0·031 in. diameter.

The existence of a velocity-head error accounts for the discrepancy between Hall's results and those of Young & Maas. The presence of velocity-head corrections at the centre and edges of the wake, where the velocity gradient is small, explains why Young & Maas obtained large displacement corrections in this region.

4. Traverses in a turbulent boundary layer along a flat plate

In boundary layer flow it seems reasonable to expect that the results described above will be considerably modified by the presence of the wall. This will tend to reduce the displacement of the stagnation streamline as it will modify the flow around the Pitot. For the same reason one would expect that the random changes in flow direction will be much smaller. To illustrate this one may consider the extreme case of a Pitot in contact with a wall.

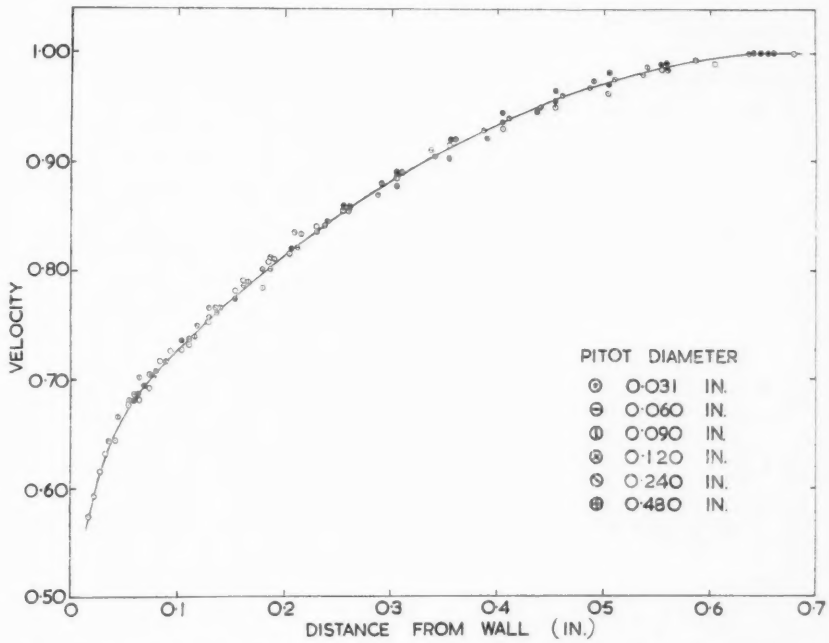

Figure 11. Comparison of the measurement of a turbulent boundary layer velocity profile by a series of geometrically similar Pitots.

Traverses made through the boundary layer near the trailing edge of a flat plate of 3 ft. chord at zero incidence confirmed the above suggestions. The results are plotted in figure 11, where it can be seen that no appreciable displacement or velocity-head error was observed, although the diameter of the largest Pitot was 16 times that of the smallest. This result was unexpected as it is reasonable to suppose some displacement would exist. A small displacement, 0·02 of the Pitot diameter, was recorded by the largest Pitot tube.

There is some evidence (Preston 1954) that corrections exist close to the wall for flat Pitots in a boundary layer. The results in figure 11 indicate that the correction for a round Pitot is negligible in this region, even when the

Pitot is touching the wall. Working with round Pitots, Macmillan (1957) observed displacements of the order of $0{\cdot}15D$ in a pipe, and of the same order in the boundary layer on a flat plate. His results also implied a total-head correction close to the wall which was expressed as a negative displacement. The absence of such corrections in the present results may be due to the higher response rate of the manometer system used.

Livesey (1956) obtained corrections for a flat-ended Pitot in a boundary layer that had been thickened considerably by a wire cloth screen. It is possible that the flow conditions in this case were more nearly those obtaining in a wake than those in a boundary layer. Livesey also reported that the corrections for a conical Pitot with a sharp lip were negligible indicating, that his other corrections were probably of the total-head type and not displacement corrections as he suggests. Assuming this is so the results in figure 4 can be applied to his measurements with the sharp-lipped Pitots. For his largest (0·7 in. diameter) Pitot at the centre of the velocity profile, we get $K = 0{\cdot}2$ giving a displacement of the order $0{\cdot}03D$ which is less than the scatter of the observations.

The results of both Livesey and Macmillan indicate that both types of corrections may be observed in a turbulent boundary layer. The conditions under which these corrections will occur have not been established.

5. Conclusions

The results indicate that the displacement of the effective centre of pressure recorded by a total-head tube in a wake obeys a relationship of the form put forward by Hall (1956) and by Lighthill (1957). This is expressed by equation (1), for a sphere in uniform shearing flow, and by the curve in figure 4 for a flat-ended round Pitot of conventional form.

When the Pitot is large compared with the dimensions of the wake, the displacement is reduced and may be determined approximately by the process outlined in the appendix.

In the region close behind a trailing edge, a velocity-head error also exists due to the characteristics of a yawed Pitot. Since this error is a function of the dynamic characteristics of the flow, it cannot be specified in terms of the Pitot geometry and the velocity gradient alone. It is possible to obtain a reasonably accurate corrected profile empirically, although the process is tedious. The results suggest that, for accurate drag measurements, it is best to make wake traverses well downstream of the trailing edge, and an advantage to use a Pitot with a sharp lip.

For a flat-ended round Pitot of conventional form and with bore 0·6 times the outer diameter, no corrections were observed in a turbulent boundary layer, even when the Pitot was touching the wall.

The majority of the experimental work was carried out in the Mechanical Engineering Department of the University of Adelaide.

Appendix

The estimation of displacement corrections for a Pitot large compared with the width of the wake

Schlichting (1930) has established that the velocity profile in a wake obeys the relation

$$\frac{U_0 - U}{U_0 - U_m} = \left[1 - \left(\frac{y}{y_0}\right)^{3/2}\right]^2, \tag{A 1}$$

where the notation is illustrated in figure 12.

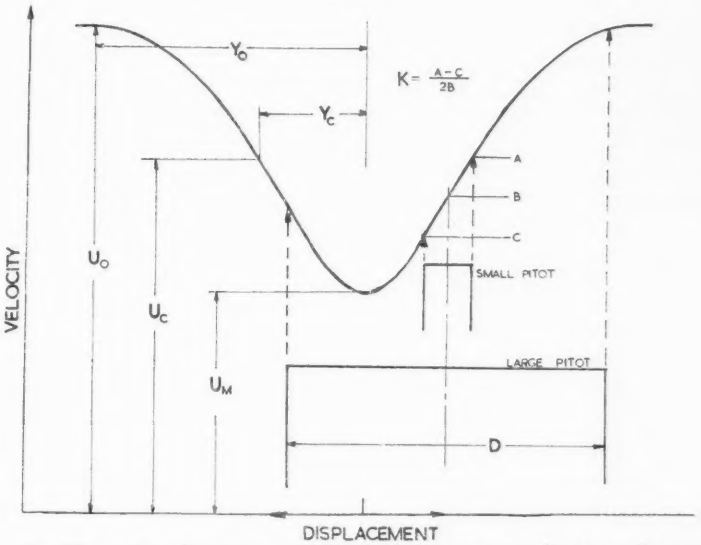

Figure 12. Illustration of notation used for displacement corrections to wake velocity profiles.

The value of U_m is given by the Pitot traverse regardless of the Pitot size, and y_0 can be found from (A 1) given the value of y corresponding to a known value of U. The most convenient for this purpose is y_c, corresponding to the mean wake velocity $U_c = \frac{1}{2}(U_0 + U_m)$, and (A 1) shows that $y_0 = 0{\cdot}441 y_c$.

The value of y_c must first be corrected for displacement. If the tube is small, the corrections can be determined from figure 4 using the appropriate value of K. When the Pitot diameter is of the same order of magnitude as the wake width, it has been shown experimentally that

$$K = \frac{U_0 - U_m}{2U_c}.$$

The corresponding value of δ/D may be read from figure 4.

Once y_0 is known, the whole profile may be calculated from (A 1). This profile will be in error near the edge of the wake, but it can be seen

from the lower part of figure 5 that otherwise the agreement is good. It is not suggested that this empirical procedure may be applied to a case where the Pitot diameter is very much larger than the wake width. Such a condition is unlikely to arise in practice; but, if so, it is not difficult to establish a suitable correction experimentally.

References

Goldstein, S. (Ed.) 1938 *Modern Developments in Fluid Dynamics*, Vol. 2. Oxford University Press.

Hall, I. M. 1956 *J. Fluid Mech.* **1**, 142.

Lighthill, M. J. 1957 *J. Fluid Mech.* **2**, 493.

Livesey, J. L. 1956 *J. Aero. Sci.* **23**, 949.

Macmillan, F. A. 1957 *Aero. Res. Counc., Lond., Rep. & Mem.* no. 3028.

Mawson, G. B. & Lilley, G. M. 1956 *College of Aeronautics, Cranfield, Rep.* no. 107.

Preston, J. H. 1954 *J. R. Aero. Soc.* **58**, 109.

Schlichting, H. 1930 *Ingen.-Arch.* **1**, 533.

Todd, K. W. 1949 *Proc. Instn Mech. Engrs, Lond.* **161**, 213.

Young, A. D. & Maas, J. N. 1936 *Aero. Res. Counc., Lond., Rep. & Mem.* no. 1770.

Flow in shock tubes with area change at the diaphragm section*

By R. A. ALPHER and D. R. WHITE
General Electric Research Laboratory, Schenectady, New York

(*Received* 27 *August* 1957)

SUMMARY

This paper describes theoretical and experimental studies of the effects on shock tube flows of a monotonic convergence at the diaphragm section. Systematic flow equations are developed for tubes of uniform bore and tubes having either a monotonic convergence or a convergence–divergence in the diaphragm section. Except across the shock front itself, isentropic processes and ideal-gas behaviour have been assumed. Simplified procedures are presented for predicting the ideal-flow parameters over a wide range of operating conditions, as well as for comparing straight and convergent tubes. Such comparisons made by other investigators are found to be incomplete or in error. The experiments described utilize a very simple device for altering the diaphragm section convergence and a multi-station measurement of shock velocity. The expected effect of convergence is verified over a wide range of Mach numbers. Even at Mach numbers where the processes of shock formation can no longer be ignored, it is found that the relative performance between a uniform and convergent tube is preserved.

INTRODUCTION

The basic shock tube is one of uniform cross-section throughout, in which the rapid removal of a diaphragm separating two gases at different pressures leads to the generation of a shock wave in the region of lower pressure. The regions initially at high and low pressure are designated as driver and driven sections respectively. It has now been well established experimentally that if all other initial conditions are equal, one will realize a stronger shock wave in a tube having in the diaphragm region an area reduction from driver to driven section than in a tube of uniform bore. So-called convergent shock-tube flows have been considered by Bannister & Mucklow (1948), Lukasiewicz (1952), Resler, Lin & Kantrowitz (1952), Wallace & Mitchell (1953), Wallace & Nassif (1954), Hooker & White (1955), and Alpher & White (1957). This last reference contains the theoretical work of this paper together with more extensive derivations and calculations.

* A preliminary account of this work was given at the 1957 Annual Meeting of the American Physical Society in New York City.

In this paper we shall develop a general idealized theory of shock-tube flows, valid for uniform, convergent, or convergent–divergent tubes, whether operated in the subsonic or supersonic cold-flow regimes. Experiments will be described which show the difference between uniform and convergent tubes to be as predicted over a wide range of Mach numbers, even though with increasing shock strength an increasing deviation from absolute predictions of the theory is noted.

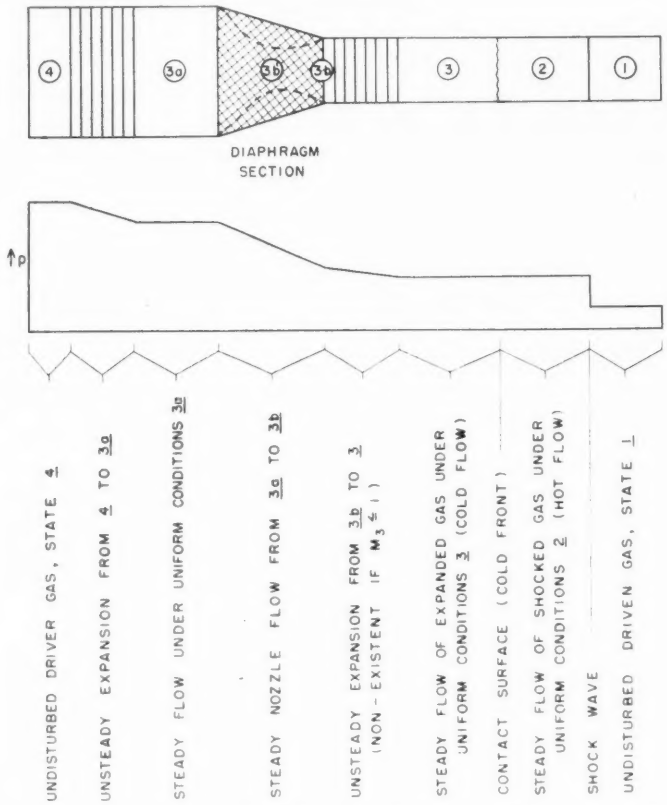
4
3a
3b
3b'
3
2
1
DIAPHRAGM SECTION
↑p
UNDISTURBED DRIVER GAS, STATE 4
UNSTEADY EXPANSION FROM 4 TO 3a
STEADY FLOW UNDER UNIFORM CONDITIONS 3a
STEADY NOZZLE FLOW FROM 3a TO 3b
UNSTEADY EXPANSION FROM 3b TO 3 (NON-EXISTENT IF M3 ≤ 1)
STEADY FLOW OF EXPANDED GAS UNDER UNIFORM CONDITIONS 3 (COLD FLOW)
CONTACT SURFACE (COLD FRONT)
STEADY FLOW OF SHOCKED GAS UNDER UNIFORM CONDITIONS 2 (HOT FLOW)
SHOCK WAVE
UNDISTURBED DRIVEN GAS, STATE 1

Figure 1. Schematic diagram of shock tube with convergent geometry at the diaphragm section. The dashed lines in the diaphragm section denote a convergent–divergent geometry with minimum area at $3b'$. The pressure distribution is, of course, only symbolic.

The model of the flow situation which has been employed is given in figure 1. After diaphragm removal, energy is extracted from the driver gas through an unsteady expansion from state 4 to state $3a$. The transition section presents three possibilities. If it is uniform, i.e. if it connects equal areas, states $3a$ and $3b$ coalesce and denote the state at the diaphragm location. If the cold flow is supersonic, this state is the point in an unsteady

expansion at which the Mach number becomes unity. If the transition is montotonically convergent, the flow from 3*a* to 3*b* is steady nozzle flow, and the convergent flow at 3*b* may be either subsonic or sonic. Following 3*b* one has either uniform flow in state 3 with $M_3 \leqslant 1$ or an unsteady supersonic expansion to state 3 with $M_3 > 1$. Finally, if the transition section is convergent–divergent, i.e. if 3*b*′ represents a minimum area, one has either a subsonic or supersonic nozzle between states 3*a* and 3*b*. In the supersonic case the exit flow at state 3*b* may be subjected to a further unsteady expansion to state 3. Boundary-layer effects, attenuation and the process of shock formation have not been considered. The driver gas is treated isentropically, and departures from ideality are not explicitly considered for the shocked gas. As will be seen, it is a simple matter to modify this presentation to include the real changes in the driven gas states.

Basic calculations involve determining, for initially given gases and thermodynamic states in the driver and driven sections (i.e. the pressures p_1 and p_4, sound velocities a_1 and a_4, and specific heat ratios γ_1 and γ_4) the resultant shock strength and the thermodynamic state of both the expanded and shocked gases.

Theory

Uniform shock tube

The situation in a uniform tube is sufficiently well known that it need have only brief mention. One wants to relate the initial pressure ratio across the diaphragm, $p_4/p_1 = z$, to the pressure ratio across the shock (i.e. the shock strength $p_2/p_1 = y$) or alternatively to the shock Mach number M_s. In the uniform tube there is a continuous unsteady expansion from state 4 to state 3. If $M_3 \geqslant 1$ one has sonic flow at the diaphragm location. The particle velocity imparted by an unsteady expansion from p_4 to p_3, where we note that $p = k\rho^\gamma$ and that $u_4 = 0$, can be written (see Liepman & Puckett (1947), p. 461)

$$u_3 = \int_{\rho_4}^{\rho_3} \left(\frac{dp}{d\rho}\right)^{1/2} \frac{d\rho}{\rho} = \frac{2a_4}{\gamma_4 - 1}\left[1 - \left(\frac{p_3}{p_4}\right)^{(\gamma_4-1)/2\gamma_4}\right]. \tag{1}$$

This velocity can be subsonic, sonic or supersonic in value. The flow or particle velocity behind the normal shock is determined from the shock Hugoniot; or, if treating the shocked gas as ideal gives an adequate approximation, then the Rankine–Hugoniot relations give

$$\frac{u_2}{a_1} = \frac{2^{1/2}(y-1)}{\{\gamma_1[(\gamma_1-1)+(\gamma_1+1)y]\}^{1/2}} = \frac{2}{\gamma_1+1}\frac{M_s^2-1}{M_s}. \tag{2}$$

We can combine (1) and (2) since at the interface between shocked and expanded gas we must have $u_3 = u_2$ and $p_3 = p_2$. Solving for z yields, for the uniform tube,

$$z = y\left(1 - \frac{a_1}{a_4}\frac{\gamma_1 - 1}{2}\frac{u_2}{a_1}\right)^{-2\gamma_4/(\gamma_4-1)}. \tag{3}$$

Tube with diaphragm section area change

Relationships between z and y or M_s for the tube with an area change in the diaphragm section are obtained as for the uniform tube. Referring again to figure 1, one proceeds as before to connect the shock front with the driving gas by matching pressure and flow velocity at the contact surface, except that now steady or unsteady processes, as the case may be, must be considered at the diaphragm section. Consider the general case of a convergent–divergent diaphragm section. When the shock-tube flow is established, the pressure ratio z may be expanded as follows (see figure 1):

$$z_c = \frac{p_4}{p_1} = \frac{p_4}{p_{3a}} \frac{p_{3a}}{p_{3b'}} \frac{p_{3b'}}{p_{3b}} \frac{p_{3b}}{p_3} \frac{p_3}{p_2} \frac{p_2}{p_1}. \tag{4}$$

Here the suffix c refers to the non-uniform tube, whereas suffix s will be used to refer to the uniform tube. The various pressure ratios in (4) can be interpreted directly. Thus p_4/p_{3a} is that ratio required to accelerate the driver gas by an unsteady expansion from rest to Mach number M_{3a}. The ratio $p_{3a}/p_{3b'}$ is that required to bring the driver gas by a steady expansion from M_{3a} to $M_{3b'}$. One can introduce the area ratio $A_4/A_{3b'}$ into $p_{3a}/p_{3b'}$ by using the condition of conservation of mass. Expansion from $3b'$ to $3b$ also will be a steady process, supersonic or subsonic according as the flow at $3b'$ has become sonic or not. (By our restriction to isentropic channel flow for the driver gas, we exclude that range of z which leads to an over-expansion for a convergent–divergent section.) In either event the ratio $P_{3b'}/P_{3b}$ is that required to bring the gas by a steady expansion from $M_{3b'}$ to M_{3b} through an area ratio $A_{3b'}/A_{3b}$. The ratio p_{3b}/p_3 is then that needed for an unsteady expansion from M_{3b} to M_3. At the contact surface, $p_3 = p_2$, and p_2/p_1 is defined as the shock strength y. Equation (4) can therefore be written as

$$z_c = \left\{\left[1 + \frac{\gamma_4 - 1}{2} M_{3a}\right]\left[\frac{2+(\gamma_4-1)M_{3b}^2}{2+(\gamma_4-1)M_{3a}^2}\right]^{1/2}\left[\frac{2+(\gamma_4-1)M_3}{2+(\gamma_4-1)M_{3b}}\right]\right\}^{2\gamma_4/(\gamma_4-1)} y. \tag{5}$$

Since this relation involves M_3, M_{3a} and M_{3b} as well as z_c and y, we require additional relationships. One of these involves the overall area ratio in the transition section, which can be written as follows, regardless of whether $M_{3b'}$ is subsonic or sonic or whether $3b'$ is a section of minimum area or an undistinguished section in a monotonic convergence:

$$\frac{A_4}{A_1} = \frac{M_{3b}}{M_{3a}}\left[\frac{2+(\gamma_4-1)M_{3a}^2}{2+(\gamma_4-1)M_{3b}^2}\right]^{(\gamma_4+1)/2(\gamma_4-1)}. \tag{6}$$

The second relation we require connects M_s with M_3, M_{3a} and M_{3b}. One expands M_3 in the same way as z_c in (4); thus

$$M_3 = \frac{u_3}{a_3} = \frac{u_2}{a_3} = \frac{u_2}{a_1}\Big/\frac{a_3}{a_1} = \frac{u_2}{a_1}\Big/\left(\frac{a_3}{a_{3b}}\frac{a_{3b}}{a_{3a}}\frac{a_{3a}}{a_4}\frac{a_4}{a_1}\right). \tag{7}$$

Substituting for the sound velocity ratios, we obtain

$$M_3 = \left[\frac{a_1}{u_2}\frac{a_4}{a_1} g^{(\gamma_4-1)/2\gamma_4} - \frac{\gamma_4 - 1}{2}\right]^{-1}, \tag{8}$$

where the quantity g, which we call an 'equivalence' factor (see next section), was first used by Resler, Lin & Kantrowitz (1952). It is defined as

$$g = \left\{\left[\frac{2+(\gamma_4-1)M_{3a}^2}{2+(\gamma_4-1)M_{3b}^2}\right]^{1/2}\left[\frac{2+(\gamma_4-1)M_{3b}}{2+(\gamma_4-1)M_{3a}}\right]\right\}^{2\gamma_4/(\gamma_4-1)}. \tag{9}$$

Using g, one can rewrite (5) as

$$z_c = \frac{y}{g}\left[1+\frac{\gamma_4-1}{2}M_3\right]^{2\gamma_4/(\gamma_4-1)} = \frac{y}{g}\left[1-\frac{u_2}{a_1}\frac{a_1}{a_4}\frac{\gamma_4+1}{2}g^{-(\gamma_4-1)/2\gamma_4}\right]^{-2\gamma_4/(\gamma_4-1)}. \tag{10}$$

Equations (6) to (10) enable the calculation of shock-tube flows with a convergent or convergent–divergent diaphragm section, in the case of subsonic, sonic or supersonic cold flow. The results for a uniform tube are recovered by noting that with $A_4/A_1 = 1$, one has $M_{3a} = M_{3b}$ with $g = 1$.

For subsonic cold flow (the assumption of isentropy excludes a transition to subsonic flow through a shock), the transition section is a subsonic nozzle with $M_{3b} = M_3$, $p_{3b} = p_3$ and $a_{3b} = a_3$. Equations (6), (8) and (9) reduce to three simultaneous equations in g, M_3 and M_{3a}, which can be solved by iteration with an *ab initio* choice of a_4, a_1 and M_s. In this subsonic case, only the ratio A_4/A_1 enters, and the existence of a minimum section $A_{3b'}$ is irrelevant.

For supersonic cold flow, $M_3 \geqslant 1$, one must have $M_{3b'} = 1$ (or $M_{3b} = 1$ if the section is monotonically convergent so that $A_{3b} = A_1$ is the minimum area). The usual relationships between area ratio and Mach number in supersonic nozzles apply, as used in obtaining (5), to give M_{3a} and M_{3b}. From these M_3, g, and z_c follow.

Computation of shock-tube parameters

The procedure used in developing the shock-tube equations suggests a rather simple graphical means of solving the equations for a given tube. The reader will recall that the shocked gas and the driver gas are connected by matching pressure and velocity across the contact surface. The graphical material can be divided into that pertaining to the driver and that to the driven gases, the one being independent of the other except as matched at the contact surface. The advantages of this are made clear in the following.

The shocked gas may be characterized by a plot of either shock strength y or shock Mach number versus u_2/a_1, where u_2 is the flow velocity imparted by the shock. Such curves may be computed from (2) for ideal gases, but require a knowledge of the shock Hugoniot if the shock strength is sufficient to merit this (see, for example, Döring 1949, Alpher 1957, or Lighthill 1957).

The driver gas is brought into the calculation in the following way. A statement of A_4/A_1, γ_4 and a_4 determines the equivalence factor g as a function of $u_3/a_4 = u_2/a_4$. Plots of g *vs* $(u_2/a_1)(a_1/a_4)$ are given in figure 2 for $\gamma_4 = 5/3$ and in figure 3 for $\gamma_4 = 7/5$ for both subsonic and supersonic cold flow. It may be noted that for $M_3 < 1$ these plots apply either to a monotonically convergent or a convergent–divergent transition section,

while for $M_3 > 1$ they hold only for the monotonically convergent section, since in this latter case $M_{3'}$ (see (9)) is taken as unity. Figure 4 is a plot of g *vs* γ_4 for various values of A_4/A_1 in the case $M_3 \geqslant 1$. Again the plot holds for monotonic convergence, since $M_{3'}$ is taken as unity. Such a plot is of use with combustion drivers, in which helium or hydrogen plus the products of hydrogen–oxygen combustion give an intermediate γ_4 value.

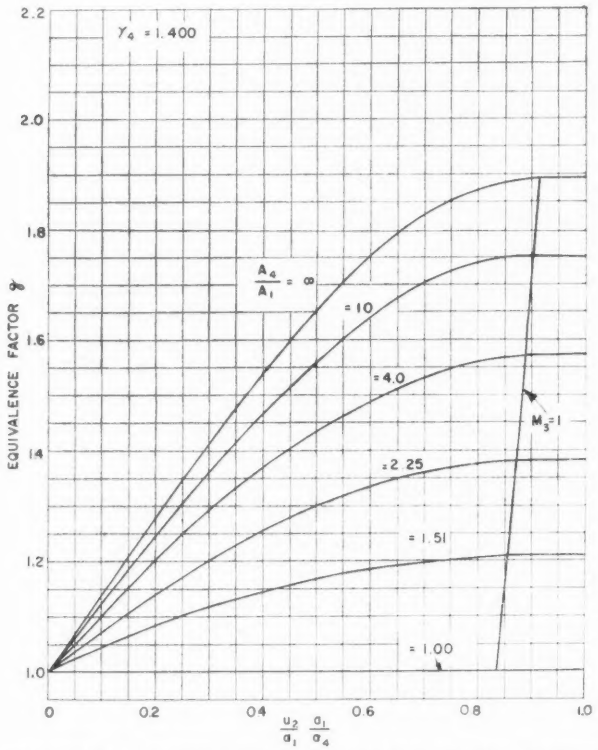

Figure 2. The equivalence factor g *vs* $(u_2/a_1)(a_1/a_4)$ for a selection of area ratios, with $\gamma_4 = 1{\cdot}4$. The connecting line at the right of the curves is the locus of g values for which the cold flow is sonic ($M_3 = 1$). For larger values of $(u_2/a_1)(a_1/a_4)$ corresponding to $M_3 > 1$, g is constant and equal to the values on this sonic line.

The usual calculation to be performed for a shock tube is the determination of the diaphragm pressure ratio z required to produce a shock of given strength y. One is given γ_1, γ_4, a_1, a_4, A_4/A_1 and y. From y the flow velocity u_2/a_1 is computed. The appropriate equivalence factor is then read from figures 2, 3 or 4. Finally from figure 5 (which is a plot of equation (10)) one reads gz/y, whence z is determined. It may be noted that the quantity z/y is the ratio of pressures through which the driver gas expands. When one has at hand a tube with fixed A_4/A_1, then curves

of z/y *vs* u_2/a_4 may be prepared which incorporate the appropriate equivalence factor. Such curves are particularly useful when various gases are to be used or when high temperature shock Hugoniots are to be taken into account.

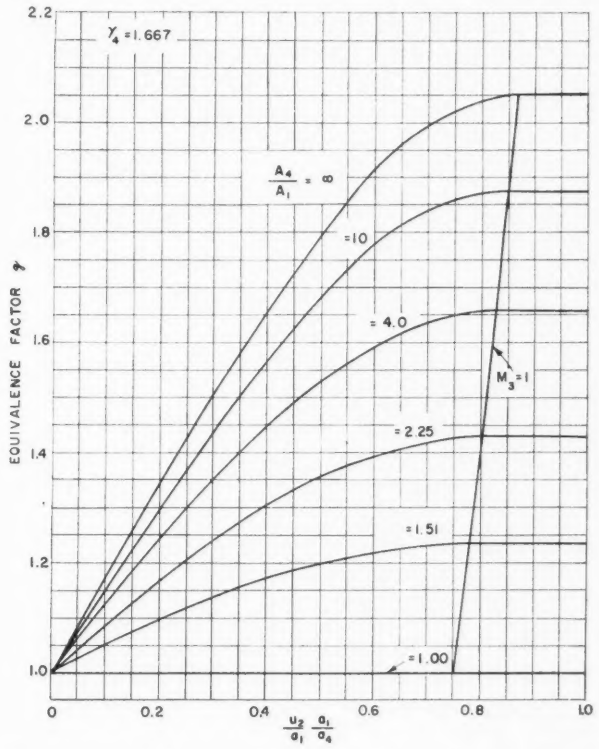

Figure 3. The equivalence factor g *vs* $(u_2/a_1)(a_1/a_4)$ for a selection of area ratios with $\gamma_4 = 1{\cdot}667$. The connecting line at the right of the curves has the same meaning as in figure 2.

To illustrate the results of such calculations, we have prepared figure 6, which gives the diaphragm pressure ratio required to produce given shock Mach numbers for helium driving into ideal argon (electronic excitation and ionization are negligible up to $M \doteqdot 10$ in argon) for several area ratios. An ideal y *vs* M_s curve is included for reference.

'Gain' factors

Although the use of a convergent transition section may have such advantages as smoothing out flow irregularities associated with combustion driving, as well as locating the diaphragm where it will not choke the flow if it does not open completely, the main reason for using such sections is that they provide an easy way of getting a stronger shock, other things

being equal. It is therefore pertinent to consider various measures of the 'gain' to be realized with a convergent tube as compared with a uniform tube. One such measure is the ratio $G_M = z_s/z_c$, where z_s and z_c are the respective values for a uniform and a convergent tube in which the same Mach number is achieved, all other things being equal. The simplest way of obtaining G_M, other than computing it from (3) and (10), is to read off z for the given A_4/A_1, and for $A_4/A_1 = 1$ for a given M_s, from a plot such as figure 6; the ratio in then computed between these z values. As may be readily shown from the analytical expression, the factor G_M becomes infinite, as does z_s, when M_s is increased without limit.

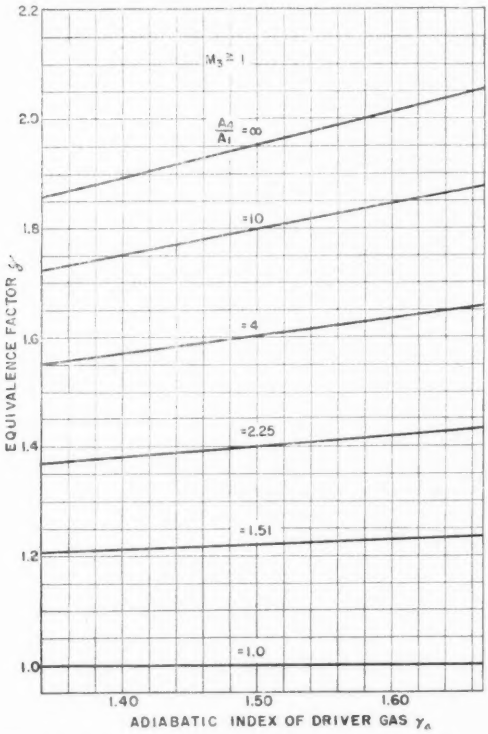

Figure 4. Limiting value of the equivalence factor g, corresponding to sonic or supersonic cold flow, *vs* γ_4 for various convergence area ratios in a monotonically converging tube.

A second measure of gain, G_z, may be defined as the ratio of the shock Mach number achieved in a convergent section tube to that in a uniform tube for the same diaphragm pressure ratio, all other things being equal. Analytic expression of such a factor is not possible, but values of G_z are readily obtained from plots such as figure 6 by reading the values of M_s for the given A_4/A_1 and for $A_4/A_1 = 1$ at a given z. It is not difficult to

show that for ideal gas behaviour G_z approaches a limiting value $g^{(\gamma_4-1)/2\gamma_4}$ as z increases without limit. These limiting values are implicit in table 1, which will be explained immediately below. Examination of equations (3), (8), and (10) indicates that the diaphragm pressure ratio and the cold flow Mach number both become infinite at a finite value of u_2. Hence, under ideal conditions (as represented by equation (2)), there is a maximum shock strength attainable in a given tube. Table 1 gives maximum values of the shock Mach number (i.e. the values for $p_4/p_1 \to \infty$) for various values of A_4/A_1, both for the temperature ratio $T_4/T_1 = 1$ and for $T_4/T_1 = 2$.

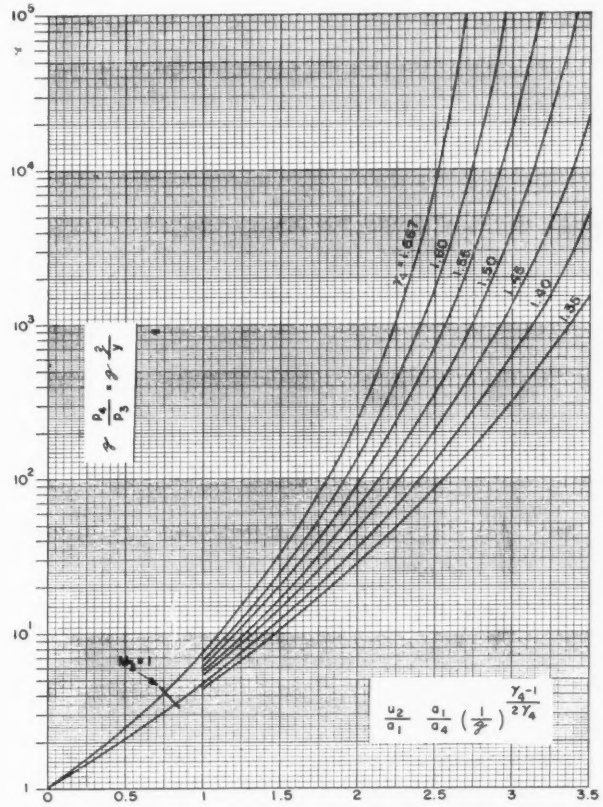

Figure 5. Curves for computing shock-tube performance. The point at which the cold flow becomes sonic is indicated.

Table 1 points out quite strikingly that the Mach number gain resulting from the use of a convergent transition section is not particularly large. The advantage of increasing sound velocity in the driver should be noted.

Comparisons of performance in convergent and straight tubes have been made by Lukasiewicz (1952), Resler, Lin & Kantrowitz (1952), and Yoler (1954) (see Alpher & White 1957 for a more detailed discussion

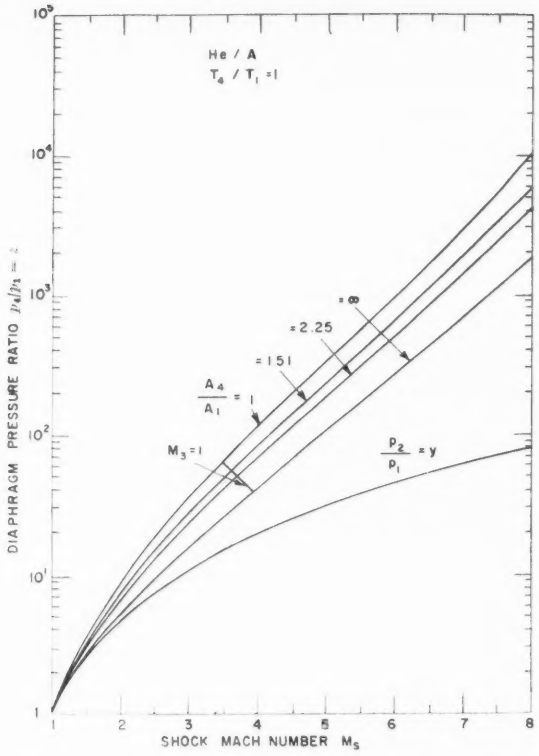

Figure 6. Diaphragm pressure ratio *vs* shock Mach number, for helium driving into argon at the same temperature. A plot of shock strength p_2/p_1 *vs* shock Mach number is included for reference.

	Driver-driven gas combination	$A_4/A_1 = 1$	1·51	2·25	∞
$T_4/T_1 = 1$	N_2/N_2	6·18	6·34	6·47	6·76
	N_2/A	7·48	7·69	7·84	8·20
	He/N_2	10·9	11·3	11·6	12·5
	He/A	12·8	13·3	13·7	14·7
	H_2/N_2	22·6	23·2	23·6	24·7
	H_2/A	27·5	28·3	28·8	30·1
$T_4/T_1 = 2$	He/N_2	14·8	15·4	15·9	17·1
	He/A	18·0	18·8	19·3	20·8
	H_2/N_2	31·9	32·8	33·4	34·9
	H_2/A	38·9	40·0	40·7	42·6

Table 1. Maximum values of shock Mach number M_s for $z = p_4/p_1 \to \infty$.

of their work). Lukasiewicz obtains limiting values of the equivalence factor g for $A_4/A_1 \to \infty$, but erroneously restricts them as holding only for equal cold flow Mach numbers M_3 in straight and convergent tubes. His work also suggests as a measure of gain the ratio of values of z in straight and convergent tubes required to achieve a given value of M_3. This does not appear to be a particularly useful measure since shocks of different strength will result. Resler, Lin & Kantrowitz discuss relative performance of the two situations from two viewpoints. First, one may regard the equivalence factor g as the 'gain in effective pressure' on driving a shock by using a steady flow (convergent) rather than an unsteady flow (uniform) transition section at the diaphragm. Second, they point out that a tube with a convergent section is 'equivalent' to a straight tube having an initial pressure ratio gz_c and an initial sound speed ratio $(a_4/a_1)g^{(\gamma_4-1)/2\gamma_4}$ (see equation (10)). Their discussion of these matters is quite brief and limited to the case of supersonic cold flow. Finally Yoler has used the equivalence factor g as though it were the gain factor G_M, which invalidates some of the data reduction and conclusions in his work.

Experimental work

Described below are some experiments with a shock tube in which the area ratio A_4/A_1 across the diaphragm section was alternatively 1·0 or 1·51. They show that the shock enhancement due to a convergent diaphragm section is satisfactorily predicted by the preceding analysis. Measured quantities were the initial pressures p_4 and p_1, and the shock velocity as a function of distance from the diaphragm. The shock tube had a driven section $3\frac{1}{4}$ in. square in cross-section and 40 ft. long. The driver was circular in cross-section, with a 4·5 in. inside diameter, and is 6·5 ft. long. Driver gases were helium and hydrogen, while driven gases were air, nitrogen, and argon. The most extensive data were obtained with helium/air, and only these will be reported here since the experiments with other gas combinations merely corroborated these results. In all tests the driver pressure was slowly raised until the diaphragm ruptured. The diaphragms were clamped at the driver end of the transition section, and were generally of 0·010 to 0·030 in. thickness stainless steel scored in a cross, one-third to a half of the thickness being removed by the scoring tool. Driver pressures were in the range of 100 to 800 lb./in.^{2} and were measured with a calibrated Bourdon gauge. Driven section pressures were measured with a manometer for $p_1 > 50$ mm of mercury, a Wallace and Tiernan absolute pressure indicator for 50 mm $> p_1 > 2$ mm, or a McLeod gauge for $p_1 < 2$ mm.

Since the processes of shock formation and attenuation cause the shock velocity to change with distance from the diaphragm, instrumentation was devised to enable measurement of the shock velocity as a function of position in the tube, and hence to determine the maximum shock strength wherever it occurred relative to the diaphragm. The arrival of the shock at an instrument station along the tube was detected by a thin-film heat detector

of the sputtered platinum type (Rabinowicz, Jessey & Bartsch 1956). To permit a number of such signals from different stations to be coupled to a recording system, it was desirable to lock out signals subsequent to the first from each station, and also to make the duration of this first signal very short. The heat detector output was amplified and fed to a 6D4 thyratron (the more commonly used 2D21 thyratron was found to be unsuitable due to its having firing delays of from 8 to 20 microseconds for weaker signals). The outputs from six of these thyratrons were fed through individual decoupling diodes to a blocking-oscillator type of pulse generator. Hence, through two such circuits, brief pulses were generated corresponding to shock arrivals at up to twelve stations spaced along the tube at 32·6 in. intervals. A vertical raster pattern was formed on the screen of a cathode-ray oscilloscope by connecting to the y-input a crystal-controlled sawtooth voltage generator of 100 microseconds period, the x-deflection being actuated by the oscilloscope's time base with a much longer period of about 10 milliseconds. In this manner about 500 cm of sweep at a writing speed of 20 microseconds/cm were obtained for a single sweep of the oscilloscope's time base. Time markers at 10 microsecond intervals were applied through intensity modulation of the oscilloscope. The amplified and shaped (i.e. shortened and freed from extraneous signals following the initial one) pulses originating from the heat gauges were applied directly to the x-plates of the oscilloscope, and so caused horizontal breaks in the vertical raster. The oscilloscope was triggered by the output from a barium–titanate transducer, which was fixed in the wall of the shock tube near the diaphragm and was sensitive to mechanical vibrations of the tube as the diaphragm broke. The shock velocity at different positions in the tube could readily be deduced from a photographic record of the raster, on which time intervals could be measured with a possible error of about a microsecond.

The shock tube as constructed had an area ratio $A_4/A_1 = 1{\cdot}51$. For these experiments an area ratio of unity was obtained by inserting down the centre of the driver a wooden dowel which terminated short of the diaphragm. This resulted in quite dissimilar cross-sections in the driver and driven parts of the tube, but permitted use of the same diaphragms as before the modification, so that the mechanics of the rupturing diaphragm was not a variable in the comparison.

In general a rapid acceleration of the shock to a maximum velocity was noted relatively near the diaphragm, followed by a gradual deceleration as the shock proceeded down the tube. Since the treatment in the present paper takes no account of shock formation and attenuation processes, the maximum shock velocity observed was judged to be that most suitable for comparison with the theoretical results. Since this observed value is actually the average over a significant interval, it is in general slightly smaller than the actual peak velocity.

The data are shown in figure 7. Note that the experimental shocks in each case are somewhat weaker than the theoretical predictions, but that the

shock enhancement due to a convergent transition section is in excellent agreement with theory.

Our experiments have been continued to the study of stronger shocks than those described here; and with the present shock tube the indications are that, for diaphragm pressure ratios above about 1000 with hydrogen

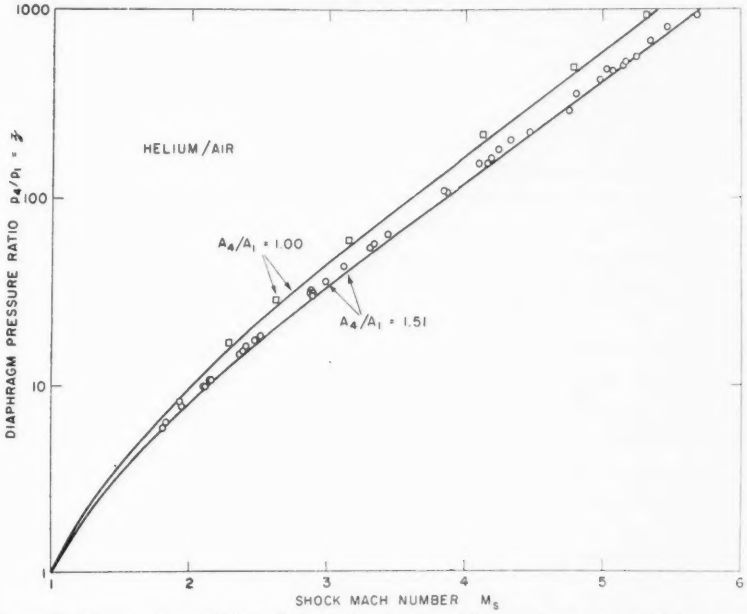

Figure 7. Comparison of ideal shock-tube theory with experiment for a $3\frac{1}{4}$ in. square shock tube to demonstrate the effect of a convergence at the diaphragm section.

or helium as the driver gas, the performance of the tube can no longer be depicted by an ideal theory. Shocks stronger than predicted by ideal theory are observed, and the maximum shock velocity in an experiment can occur quite far from the diaphragm. To explain such observations, one must consider the finite time for diaphragm rupture, mixing effects in the contact zone, shocked gas non-ideality, and wall attenuation effects. Nevertheless, even with these stronger shocks, the enhancement due to convergence appears to be predicted fairly accurately by ideal theory.

References

Alpher, R. A. 1957 The Saha equation and the adiabatic exponent in shock wave calculations, *J. Fluid Mech.* **2,** 123.

Alpher, R. A. & White, D. R. 1957 Ideal theory of shock tubes with area change near diaphragm, *General Electric Research Laboratory, Schenectady, New York, Report* no. 57–RL–1664.

Bannister, F. K. & Mucklow, G. F. 1948 Wave action following sudden release of compressed gas from a cylinder, *Proc. Instn Mech. Engrs.* **159,** 269.

Döring, W. 1949 Die Geschwindigkeit und Struktur von intensiven Stosswellen in Gasen, *Ann. d. Phys.* **6,** 133.

Hooker, W. J. & White, D. R. 1955 Design considerations for shock tubes generating hypersonic flow ($M > 6$), *General Electric Research Laboratory, Schenectady, New York, Chemistry Research Department Mem. Rep.* no. C–55–120.

Liepmann, H. W. & Puckett, A. E. 1947 *Introduction to Aerodynamics of a Compressible Fluid.* New York : Wiley.

Lighthill, M. J. 1957 Dynamics of a dissociating gas, Part I, equilibrium flow, *J. Fluid Mech.* **2,** 1.

Lukasiewicz, L. 1952 Shock tube theory and application, *National Aeronautical Establishment, Ottawa, Report* no. 15.

Rabinowicz, J., Jessey, M. E. & Bartsch, C. A. 1956 Resistance thermometer for transient high-temperature studies, *J. Appl. Phys.* **27,** 97.

Resler, E. L., Lin, S. C. & Kantrowitz, A. 1952 The production of high temperature gases in shock tubes, *J. Appl. Phys.* **23,** 1390.

Wallace, F. J. & Mitchell, R. W. S. 1953 Wave action following the sudden release of air through an engine port system, *Proc. Instn Mech. Engrs.* (B) **1B,** 8 & 343.

Wallace, F. J. and Nassif, M. H. 1954 Air flow in naturally aspirated two stroke engines, *Proc. Instn Mech. Engrs.* **168,** 515.

Yoler, Y. A. 1954 Hypersonic shock tube, *California Institute of Technology, Guggenheim Aeronautical Laboratory, Hypersonic Wind Tunnel Project, Mem.* no. 18.

The effects of a sound wave on the compressible boundary layer on a flat plate

By C. R. ILLINGWORTH
Department of Mathematics, University of Manchester

(*Received* 19 *September* 1957)

SUMMARY

The boundary layer on a hot flat plate which is fixed at zero incidence in a slow stream carrying a progressive sound wave is investigated. Formulae are obtained for the skin friction and the heat transfer in the extreme cases when the frequency is very low and very high. In addition, different methods of simplifying the boundary layer equations in unsteady compressible flow are briefly compared.

1. INTRODUCTION

During the last few years there has been a revival of interest in the theory of unsteady laminar boundary-layer flows. The solution for the initial growth of the boundary layer on a body started from rest has long been known, but the recent work has been concerned with the later stages of such a motion and with the boundary layers associated with fluctuating external flows. One of the first contributions to these new developments was made by Moore (1951), who considered the compressible boundary layer on a heat-insulated flat plate moving with variable velocity in a uniform medium. Moore's work has since been supplemented by that of Ostrach (1955) who treats the same problem for an isothermal flat plate. Both these papers are relevant to the boundary layer on a missile whose velocity changes continually during flight.

Another important contribution, dealing with unsteady incompressible boundary layers, has been made by Lighthill (1954). He investigates the boundary layer in plane flow over a fixed cylinder of arbitrary cross-section when the free stream is fluctuating with small amplitude about a steady mean value. For incompressible flow, this problem is mathematically the same as if the cylinder were moving with the same fluctuating velocity in a uniform medium at rest. For this reason, Moore's and Ostrach's results when interpreted for incompressible fluctuating flow link up with Lighthill's predictions concerning a flat plate.

Lighthill mentioned the Rijke tube among the possible fields of application of the theory of fluctuating boundary layers, and it was, in fact, the phenomenon of the Rijke tube that suggested the work described in this paper. Rayleigh (1894) describes how such a tube may be set up. He quotes the case of a tube 5 ft. long and $4\frac{3}{4}$ in. in diameter, open at both ends and held vertically. When a fine wire gauze stretching across the tube about 1 ft. from the bottom was made red hot by a flame, and then the

flame was suddenly removed, almost immediately a sound of considerable power was emitted which lasted for several seconds. In the tube there is a stream of air composed of two components, namely the fairly slow convection current up the tube combined with the longitudinal motion associated with standing sound waves. The energy of the sound waves is derived from the varying transfer of heat from the gauze to the surrounding air, and this changes with the fluctuations in the speed of the air current past the gauze. In the Rijke tube, therefore, we have an example of a hot obstacle in a fluctuating air stream. It is true that the Reynolds number for the flow past the fine wires of the gauze described by Rayleigh is below the range of Reynolds numbers for which boundary-layer theory is valid, and therefore the theory which follows really applies to an obstacle of larger longitudinal dimensions than the gauze.

The principal aim of the present paper is to investigate the effect of high wall temperature on the skin friction and heat transfer on a flat plate fixed in a stream carrying sound waves. In addition, we shall take some account of the effects of the fluctuations in density and temperature that accompany the sound waves in the external stream. (In Lighthill's theory, for incompressible flow, the obstacle may be warm, but not hot, and the density and temperature are constant in the external flow.) Our investigation is closely related to, but not equivalent to, Moore's work on a moving plate. For if, in Moore's problem, we change from axes fixed in the medium to axes fixed in the plate, so as to give the appearance of a plate at rest in a moving medium, we thereby introduce an apparent pressure gradient $-\rho\, dU/dt$ in the boundary layer, where ρ is the density and $U(t)$ is the velocity of the plate. On the other hand, the pressure gradient for a fixed plate in a stream $U(t)$ which fluctuates slightly and has a uniform mean density ρ_∞ is $-\rho_\infty\, dU/dt$. The two pressure gradients are different unless $\rho = \rho_\infty$. Thus it is only for incompressible fluids that Moore's and Ostrach's results provide the answers to our present problem.

2. Equations of motion

We shall consider the boundary layer on a cylindrical obstacle fixed in an unsteady stream. An example of such a stream occurs when sound waves are propagated downstream in steady flow past the obstacle, and this particular flow when the obstacle is a flat plate will be investigated in some detail in § 3. The flow is supposed to be perpendicular to the axis of the fixed cylinder, and so only two space coordinates are involved, x measured along the surface of the cylinder from the leading edge, and y measured perpendicular to the surface. The boundary-layer equations then are

ideal gas
c_p = Const.
P = Const
$k = \frac{c_p \mu}{\rho}$

$$\frac{\partial \rho}{\partial t} + \frac{\partial(\rho u)}{\partial x} + \frac{\partial(\rho v)}{\partial y} = 0, \tag{1}$$

$$\rho\left(\frac{\partial u}{\partial t} + u\frac{\partial u}{\partial x} + v\frac{\partial u}{\partial y}\right) = -\frac{\partial p_1}{\partial x} + \frac{\partial}{\partial y}\left(\mu\frac{\partial u}{\partial y}\right), \tag{2}$$

$$\rho\left(\frac{\partial I}{\partial t} + u\frac{\partial I}{\partial x} + v\frac{\partial I}{\partial y}\right) - \left(\frac{\partial p_1}{\partial t} + u\frac{\partial p_1}{\partial x}\right) = \frac{1}{P}\frac{\partial}{\partial y}\left(\mu\frac{\partial I}{\partial y}\right) + \mu\left(\frac{\partial u}{\partial y}\right)^2, \tag{3}$$

where u and v are the velocity components in the x and y directions, ρ, I and μ are the density, specific enthalpy and viscosity respectively, and P is the Prandtl number, supposed to be constant. The suffix 1 refers to the external stream at the edge of the boundary layer and the external velocity u_1, density ρ_1, pressure p_1 and enthalpy I_1, which are all functions of t and x in general, obey the equations

$$\frac{\partial \rho_1}{\partial t} + \frac{\partial(\rho_1 u_1)}{\partial x} = 0, \tag{4}$$

$$\rho_1\left(\frac{\partial u_1}{\partial t} + u_1 \frac{\partial u_1}{\partial x}\right) = -\frac{\partial p_1}{\partial x}, \tag{5}$$

$$\rho_1\left(\frac{\partial I_1}{\partial t} + u_1 \frac{\partial I_1}{\partial x}\right) - \left(\frac{\partial p_1}{\partial t} + u_1 \frac{\partial p_1}{\partial x}\right) = 0. \tag{6}$$

The last equation expresses the fact that the entropy of each fluid elemen in the external stream is conserved, but in the example considered in § 3 we shall use the even stronger condition that the external stream is homentropic. To these equations must be added the equation of state

$$p = \frac{\gamma - 1}{\gamma} \rho I, \tag{7}$$

valid for a gas with constant specific heats, and the equation

$$\rho I = \rho_1 I_1, \tag{8}$$

which, in conjunction with (7), expresses the fact that the pressure p does not change across the boundary layer at any station.

It is convenient now to follow Moore's method of analysis. This is an extension of the Howarth (1948) transformation to unsteady boundary layers. First, the y-coordinate is replaced by Y, where

$$Y(t, x, y) = \frac{1}{\rho_\infty} \int_0^y \rho(t, x, s)\, ds \tag{9}$$

in which the suffix ∞ refers to some standard state of the fluid. Later we shall identify this state with the mean state of the free stream. Next, Moore introduces a function ψ satisfying

$$u = \frac{\rho_\infty}{\rho} \frac{\partial \psi}{\partial y} = \frac{\partial \psi}{\partial Y}, \tag{10}$$

which closely corresponds to the stream function in steady plane flow. (For example, mass flux is measured by $\rho_\infty \psi$.) Then, the equation of continuity (1) is satisfied if

$$v = -\frac{\rho_\infty}{\rho}\left(\frac{\partial \psi}{\partial x} + \frac{\partial Y}{\partial t}\right), \tag{11}$$

and, with t, x, Y as the independent variables, (2) and (3) are immediately transformed into

$$\left(\frac{\partial}{\partial t} + \frac{\partial \psi}{\partial Y}\frac{\partial}{\partial x} - \frac{\partial \psi}{\partial x}\frac{\partial}{\partial Y}\right)\frac{\partial \psi}{\partial Y} = -\frac{1}{\rho_1}\frac{\partial p_1}{\partial x}\frac{I}{I_1} + \frac{1}{\rho_\infty^2}\frac{\partial}{\partial Y}\left(\mu\rho\frac{\partial^2 \psi}{\partial Y^2}\right), \tag{12}$$

$$\left(\frac{\partial}{\partial t}+\frac{\partial\psi}{\partial Y}\frac{\partial}{\partial x}-\frac{\partial\psi}{\partial x}\frac{\partial}{\partial Y}\right)I-\frac{1}{\rho_1}\left(\frac{\partial p_1}{\partial t}+\frac{\partial\psi}{\partial Y}\frac{\partial p_1}{\partial x}\right)\frac{I}{I_1}$$
$$=\frac{1}{\rho_\infty^2}\left[\frac{1}{P}\frac{\partial}{\partial Y}\left(\mu\rho\frac{\partial I}{\partial Y}\right)+\mu\rho\left(\frac{\partial^2\psi}{\partial Y^2}\right)^2\right]. \quad (13)$$

These equations may be simplified further by making the special assumption that the viscosity varies as the temperature T across each station in the boundary layer. According to this,

$$\mu=\mu_w T/T_w, \quad (14)$$

where the viscosity at the wall μ_w may be related to the wall temperature T_w by Sutherland's law

$$\frac{\mu_w}{\mu_\infty}=\left(\frac{T_w}{T_\infty}\right)^{3/2}\frac{T_\infty+T_s}{T_w+T_s}, \quad (15)$$

where T_s is a characteristic temperature of the fluid, 114° K for air. The formula (14) which was discussed by Chapman & Rubesin (1949), is a good approximation to the true viscosity–temperature relation (Sutherland's law) near the wall, all along the boundary layer. Of course it is less accurate in the outer part of the boundary layer, where it would be better to use $\mu=\mu_1 T/T_1$, but errors in the viscosity and conductivity there are mitigated by the smallness of the velocity and temperature derivatives. Equations (14) and (15) together imply that

$$\mu=C\mu_\infty I/I_\infty, \quad (16)$$

where

$$C=\chi^{1/2}\frac{T_\infty+T_s}{\chi T_\infty+T_s}, \quad (17)$$

in which $\chi=T_w/T_\infty$. It now follows, with the help of (7) and (8), that

$$\mu\rho=\mu^*\rho_\infty, \quad (18)$$

where

$$\mu^*=C\frac{p_1}{p_\infty}\mu_\infty. \quad (19)$$

When $\mu\rho$ is replaced by $\mu^*\rho_\infty$, according to (18), the boundary layer equations take the simplified form

$$\left(\frac{\partial}{\partial t}+\frac{\partial\psi}{\partial Y}\frac{\partial}{\partial x}-\frac{\partial\psi}{\partial x}\frac{\partial}{\partial Y}\right)\frac{\partial\psi}{\partial Y}=-\frac{1}{\rho_1}\frac{\partial p_1}{\partial x}\frac{I}{I_1}+C\nu_\infty\frac{p_1}{p_\infty}\frac{\partial^3\psi}{\partial Y^3}, \quad (20)$$

$$\left(\frac{\partial}{\partial t}+\frac{\partial\psi}{\partial Y}\frac{\partial}{\partial x}-\frac{\partial\psi}{\partial x}\frac{\partial}{\partial Y}\right)I-\frac{1}{\rho_1}\left(\frac{\partial p_1}{\partial t}+\frac{\partial\psi}{\partial Y}\frac{\partial p_1}{\partial x}\right)\frac{I}{I_1}$$
$$=C\nu_\infty\frac{p_1}{p_\infty}\left[\frac{1}{P}\frac{\partial^2 I}{\partial Y^2}+\left(\frac{\partial^2\psi}{\partial Y^2}\right)^2\right]. \quad (21)$$

These are simultaneous differential equations for the mass-flux function ψ and the enthalpy I, which are the two quantities we have to determine.

3. Flat plate fixed in a low speed fluctuating stream

We have already mentioned the flow in the Rijke tube. In order to gain some information about the behaviour of the boundary layer on the obstacle in this kind of flow, we shall examine the boundary layer on a hot

flat plate which is fixed at zero incidence in a low speed stream containing a progressive sound wave. We choose a flat plate as the obstacle rather than a circular cylinder, which would be more representative of the wires in the gauze, because the external flow past it is simpler. A flat plate at zero incidence does not, in a first approximation to the boundary-layer problem, affect the incident stream. With a circular cylinder, unless we restricted attention to wavelengths of sound much greater than the radius of the cylinder, we should have to include the effects of the scattering of the sound wave in the velocity external to the boundary layer. (Of course, in the Rijke tube, the sound waves are in fact much longer than the dimensions of the obstacle.) With a flat plate there is no scattering whatever the frequency of the sound waves.

If the stream past the plate has a mean velocity U_∞, and if there is a sound wave of frequency ω moving downstream in it, the resultant velocity may be written, in complex form, as

$$u_1(t, x) = U_\infty\left[1 + \epsilon \exp\left(i\omega t - \frac{M}{M+1} is\right)\right], \tag{22}$$

in which $\epsilon \ll 1$. Here, M is the Mach number of the mean flow and s is the frequency parameter $\omega x/U_\infty$. The corresponding pressure and temperature are given by

$$p_1(t, x) = p_\infty\left[1 + \gamma M\epsilon \exp\left(i\omega t - \frac{M}{M+1} is\right)\right], \tag{23}$$

$$T_1(t, x) = T_\infty\left[1 + (\gamma - 1)M\epsilon \exp\left(i\omega t - \frac{M}{M+1} is\right)\right]. \tag{24}$$

These expressions are valid for all values of M and ω; the only approximation that they involve is that ϵ^2 and higher powers of ϵ should be negligible.

We shall confine attention to the case when M is small, partly because this is appropriate to the low speed stream in the Rijke tube and partly because the solution of the boundary layer equations, especially for the temperature, is thereby shortened. In the extreme case $M = 0$, which applies to an incompressible external stream, the speed of sound then being infinite, (22) becomes

$$u_1(t, x) = U_\infty(1 + \epsilon e^{i\omega t}), \tag{25}$$

and the corresponding pressure, density, and temperature, are constants with the values p_∞, ρ_∞ and T_∞ respectively. Thus, by setting $M = 0$, the progressive nature of the sound wave is obliterated, and the problem is reduced to that of the compressible boundary layer on a flat plate in an incompressible stream whose velocity is fluctuating in magnitude. This problem for a fluid that is incompressible in the boundary layer as well as in the external stream has been discussed by Lighthill (1954) for a cylindrical obstacle of arbitrary cross-section, and by Gibellato (1955) for a flat plate. By taking $M = 0$ in the following theory we shall be able to show how large temperature differences modify their results.

The simplification to the boundary-layer solution that is possible when M is small is brought about by neglecting the dissipation in the energy equation (21). This is a crucial step that sets a limit to the magnitude of M. For the discarded dissipation is $O(M^2)$, while the terms retained are $O(\chi-1)$, where $\chi = T_w/T_\infty$, and we shall assume that χ is $O(1)$. For a red-hot wire, χ would be in the region of 2. We are therefore committed to neglecting any term whose weight is $O(M^2)$ compared with those retained.

It follows that the external stream may be expressed as

$$u_1(t,x) = U_\infty(1+E), \tag{26}$$

$$p_1(t,x) = p_\infty(1+\gamma ME), \tag{27}$$

$$T_1(t,x) = T_\infty[1+(\gamma-1)ME], \tag{28}$$

where $E = \epsilon \exp(i\omega t - Mis)$. This stream, like the one from which it has been derived, is homentropic, and so $\rho_1 dI_1 = dp_1$. Consequently, with dissipation neglected, the energy equation (21) takes the simpler form

$$\left(\frac{\partial}{\partial t} + \frac{\partial\psi}{\partial Y}\frac{\partial}{\partial x} - \frac{\partial\psi}{\partial x}\frac{\partial}{\partial Y}\right)\frac{I}{I_1} = \frac{C\nu_\infty}{P}\frac{p_1}{p_\infty}\frac{\partial^2}{\partial Y^2}\left(\frac{I}{I_1}\right). \tag{29}$$

In solving equations (20) and (29) it will be convenient to separate the cases of low and high frequency. The frequency parameter s is equal to kx/M, where k is the wave number. In the Rijke tube the quantity kx, being of the order of the ratio of the diameter of the wire to the length of the tube, is small, but since we are considering M to be also small it is quite possible for s to be large. More precisely, we shall examine the cases of small and large values of s in turn.

Case of low frequency

When s is small, the external stream is given by

$$u_1(t,x) = U_\infty[1+(1-Mis)\epsilon e^{i\omega t}], \tag{30}$$

$$p_1(t,x) = p_\infty[1+\gamma M\epsilon e^{i\omega t}], \tag{31}$$

$$T_1(t,x) = T_\infty[1+(\gamma-1)M\epsilon e^{i\omega t}], \tag{32}$$

when terms involving M^2 are neglected. Care is required in evaluating terms like $(-1/\rho_1)\partial p_1/\partial x$ in equation (20). This is equal to

$$\frac{\partial u_1}{\partial t} + u_1\frac{\partial u_1}{\partial x} = \frac{U_\infty^2}{x}[(1-M)is - M(is)^2]\epsilon e^{i\omega t}$$

according to (26), and does not vanish as (31) would suggest. The appropriate form of the function ψ in the solution for small s is

$$\psi = (CU_\infty\nu_\infty x)^{1/2}\left[F(\eta) + \epsilon e^{i\omega t}\sum_{n=0}^{\infty}(is)^n f_n(\eta)\right], \tag{33}$$

where $\eta = [U_\infty/(C\nu_\infty x)]^{1/2}Y$. It follows that

$$\frac{\partial\psi}{\partial Y} = u = U_\infty\left[F'(\eta) + \epsilon e^{i\omega t}\sum_{n=0}^{\infty}(is)^n f_n'(\eta)\right], \tag{34}$$

and

$$-\frac{\partial\psi}{\partial x} = \tfrac{1}{2}(CU_\infty \nu_\infty/x)^{1/2} \times \times\left[\eta F'(\eta) - F(\eta) + \epsilon e^{i\omega t}\sum_{n=0}^{\infty}(is)^n\{\eta f_n'(\eta) - (2n+1)f_n(\eta)\}\right], \quad (35)$$

where the dashes denote differentiation with respect to η. The temperature may be written in the form

$$T/T_1 = \chi - (\chi-1)G(\eta) + \epsilon e^{i\omega t}\sum_{n=0}^{\infty}(is)^n g_n(\eta). \quad (36)$$

The boundary conditions require that

$$\left.\begin{aligned} &F(0) = F'(0) = 0, && F'(\infty) = 1;\\ &G(0) = 0, && G(\infty) = 1;\\ &f_0(0) = f_0'(0) = 0, && f_0'(\infty) = 1;\\ &f_1(0) = f_1'(0) = 0, && f_1'(\infty) = -M;\\ &f_n(0) = f_n'(0) = 0, && f_n'(\infty) = 0 \quad (n \geqslant 2);\\ &g_0(0) = -(\gamma-1)M\chi, && g_0(\infty) = 0;\\ &g_n(0) = 0, && g_n(\infty) = 0 \quad (n \geqslant 1). \end{aligned}\right\} \quad (37)$$

When the expressions (34), (35) and (36) are substituted into (20) we obtain, from the term independent of ϵ, Blasius's equation

$$F''' + \tfrac{1}{2}FF'' = 0. \quad (38)$$

The Blasius function F is tabulated for instance by Schlichting (1955), and the numerical values required in the present problem were taken from that source. Considering next the terms involving ϵ (ϵ^2 is of course neglected), we obtain from the terms independent of s

$$f_0''' + \tfrac{1}{2}Ff_0'' + \tfrac{1}{2}F''f_0 = -\gamma MF''' = \tfrac{1}{2}\gamma MFF'', \quad (39)$$

and, from the terms with the factor s,

$$D_1 f_1 = f_0' - (1-M)[\chi - (\chi-1)G], \quad (40)$$

where D_1 denotes the operator

$$\frac{d^3}{d\eta^3} + \tfrac{1}{2}F\frac{d^2}{d\eta^2} - F'\frac{d}{d\eta} + \tfrac{3}{2}F''.$$

Similarly, equation (29) yields the equations

$$\frac{1}{P}G'' + \tfrac{1}{2}FG' = 0, \quad (41)$$

$$\frac{1}{P}g_0'' + \tfrac{1}{2}Fg_0' = (\chi-1)\left[\tfrac{1}{2}G'f_0 + \frac{\gamma M}{P}G''\right] = \tfrac{1}{2}(\chi-1)G'(f_0 - \gamma MF), \quad (42)$$

and

$$D_2 g_1 = \tfrac{3}{2}(\chi-1)G'f_1 + g_0, \quad (43)$$

where D_2 denotes the operator

$$\frac{1}{P}\frac{d^2}{d\eta^2} + \tfrac{1}{2}F\frac{d}{d\eta} - F'.$$

The required solution of (41) is

$$G = \int_0^\eta [F''(s)]^P\, ds \Big/ \int_0^\infty [F''(s)]^P\, ds, \quad (44)$$

and this function is tabulated in table 1 for $P = 0{\cdot}72$, which has been taken as a representative value of the Prandtl number for air. Now, equations (39) and (42) would still survive if ω were zero, when the external velocity would be $U_\infty(1+\epsilon)$. In fact, f_0 and g_0 represent the perturbations in the steady flow solution when the parameters U_∞ and ν_∞ that occur in the steady solution are changed to $U_\infty(1+\epsilon)$ and $\nu_\infty(1+\gamma M\epsilon)$ respectively. This last expression arises from the fact that the factor $C\nu_\infty p_1/p_\infty$ in (20) and (29), which is $C\nu_x$ when the flow is steady, takes the value $C\nu_\infty(1+\gamma M\epsilon)$ in the quasi-steady case ($\omega = 0$). Thus

$$(CU_\infty \nu_\infty x)^{\frac{1}{2}} f_0 = \left[U_\infty \frac{\partial}{\partial U_\infty} + \gamma M \nu_\infty \frac{\partial}{\partial \nu_\infty} \right] [(CU_\infty \nu_\infty x)^{\frac{1}{2}} F(\eta)],$$

whence

$$f_0 = \tfrac{1}{2}(F + \eta F') + \tfrac{1}{2}\gamma M(F - \eta F'). \tag{45}$$

Similarly,

$$\begin{aligned} g_0 &= -(\gamma-1)M\chi(1-G) + \left[U_\infty \frac{\partial}{\partial U_\infty} + \gamma M \nu_\infty \frac{\partial}{\partial \nu_\infty} \right] [\chi - (\chi-1)G(\eta)] \\ &= -(\gamma-1)M\chi(1-G) - \tfrac{1}{2}(\chi-1)(1-\gamma M)\eta G', \end{aligned} \tag{46}$$

in which the first term arises because g_0 and $\chi - (\chi-1)G$ have to satisfy different boundary conditions.

The solution of (40) may be written as

$$\begin{aligned} f_1 = -f_{11} + \chi f_{12} - M\Big[\tfrac{1}{4}\gamma \Big(\eta - \frac{F'}{F''(0)} \Big) + \tfrac{1}{4}(1-\tfrac{1}{4}\gamma)F + \tfrac{3}{4}(1-\tfrac{1}{4}\gamma)\eta F' - \\ - \tfrac{1}{4}\gamma f_{11} + (\chi - 1 + \tfrac{1}{4}\gamma) f_{12} + (1-\tfrac{1}{4}\gamma) f_{13} \Big], \end{aligned} \tag{47}$$

where f_{11}, f_{12} and f_{13} are the solutions of

$$D_1 f_{11} = G - (\tfrac{1}{2}\eta F'' + F'), \tag{48}$$

$$D_1 f_{12} = G - 1, \tag{49}$$

$$D_1 f_{13} = F'^2 - 1, \tag{50}$$

subject to the boundary conditions $f_{1n}(0) = f'_{1n}(0) = f'_{1n}(\infty) = 0$ for $n = 1, 2, 3$. These three differential equations are solved by first finding the solution of the homogeneous differential equation

$$D_1 f_{10} = 0,$$

subject to $f_{10}(0) = f'_{10}(0) = 0$, $f''_{10}(0) = 1$. Then, to find f_{11} for example, the particular integral $\bar{f}_{11}$, of (48) that satisfies $\bar{f}_{11}(0) = \bar{f}'_{11}(0) = \bar{f}''_{11}(0) = 0$ is next determined, and the required function is given by

$$f_{11} = \bar{f}_{11} - \frac{\bar{f}'_{11}(\infty)}{f'_{10}(\infty)} f_{10}. \tag{51}$$

The functions f_{1n} ($n = 0, 1, 2, 3$) are tabulated in table 1.

Finally, the solution of (43) may be written as

$$g_1 = (\chi-1)(g_{11}-\chi g_{12}) + M[\chi(\gamma-1)g_{13} + (\chi-1)\{\tfrac{3}{4}(1-\tfrac{1}{4}\gamma)\eta G' - \tfrac{1}{4}\gamma g_{11} + \\ + (\chi-1+\tfrac{1}{4}\gamma)g_{12} + \tfrac{3}{2}(1-\tfrac{1}{4}\gamma)g_{14} - \tfrac{3}{8}(\gamma/F''(0))g_{15}\}], \quad (52)$$

where g_{11}, g_{12}, g_{13}, g_{14} and g_{15} are the solutions of

$$D_2\, g_{11} = -\tfrac{1}{2}(3f_{11}+\eta)G', \quad (53)$$

$$D_2\, g_{12} = -\tfrac{3}{2}f_{12}G', \quad (54)$$

$$D_2\, g_{13} = G-1, \quad (55)$$

$$D_2\, g_{14} = -f_{13}G', \quad (56)$$

$$D_2\, g_{15} = -F'G', \quad (57)$$

subject to the boundary conditions $g_{1n}(0) = g_{1n}(\infty) = 0$ for $n = 1, 2, 3, 4, 5$. The solutions of these are found, as for the corresponding f equations, by first determining the solution of

$$D_2\, g_{10} = 0 \quad (58)$$

subject to $g_{10}(0) = 0$, $g'_{10}(0) = 1$, and then combining it in turn with the particular integrals of (53)–(57) for which $g_{1n}(0) = g'_{1n}(0) = 0$. The functions g_{1n} ($n = 0, 1, \ldots, 5$) so determined are tabulated in table 2.

The skin friction is

$$\tau_w(t,x) = \frac{\mu_w\rho_w}{\rho_\infty}\left(\frac{U_\infty}{C\nu_\infty x}\right)^{1/2}\left(\frac{\partial u}{\partial\eta}\right)_{\eta=0} = \rho_\infty U_\infty^2\left(\frac{C\nu_\infty}{U_\infty x}\right)^{1/2}\frac{p_1}{p_\infty}\times \\ \times\left[F''(0) + \epsilon e^{i\omega t}\sum_{n=0}^{\infty}(is)^n f''_n(0)\right], \quad (59)$$

and if $(\tau_w)_s$ denotes the skin friction for steady flow, viz.

$$(\tau_w)_s = 0{\cdot}332\rho_\infty U_\infty^2\left(\frac{C\nu_\infty}{U_\infty x}\right)^{1/2},$$

it follows that

$$\frac{\tau_w}{(\tau_w)_s} = 1 + \epsilon e^{i\omega t}[1{\cdot}5 + (3{\cdot}661\chi - 1{\cdot}105)is + \\ + M\{0{\cdot}7 - (3{\cdot}661\chi + 1{\cdot}228)is\}], \quad (60)$$

for $\gamma = 1{\cdot}4$, provided that s is small enough for s^2 and higher powers to be negligible.

Similarly, the heat transfer from the plate to the air is

$$q_w(t,x) = -\frac{\mu_w\rho_w}{P\rho_\infty}\left(\frac{U_\infty}{C\nu_\infty x}\right)^{1/2}\left(\frac{\partial I}{\partial\eta}\right)_{\eta=0} \\ = \frac{1}{P}\rho_\infty\left(\frac{CU_\infty\nu_\infty}{x}\right)^{1/2}\frac{p_1}{p_\infty}I_1\left[(\chi-1)G'(0) - \epsilon e^{i\omega t}\sum_{n=0}^{\infty}(is)^n g'_n(0)\right], \quad (61)$$

and if $(q_w)_s$ is the heat transfer in steady flow, viz.

$$(q_w)_s = 0{\cdot}296\,\frac{1}{P}\,\rho_\infty\left(\frac{CU_\infty\nu_\infty}{x}\right)^{1/2}(I_w - I_\infty),$$

η	G	G'	f_{10}	f'_{10}	f''_{10}	f_{11}	f'_{11}
0	0	0·2956	0	0	1	0	0
0·2	0·0591	0·2956	0·020	0·200	1·000	0·007	0·073
0·4	0·1182	0·2953	0·080	0·400	1·000	0·029	0·145
0·6	0·1772	0·2944	0·180	0·600	1·000	0·065	0·213
0·8	0·2359	0·2927	0·320	0·800	1·000	0·114	0·276
1·0	0·2942	0·2898	0·500	1·000	1·001	0·175	0·334
1·2	0·3518	0·2857	0·720	1·200	1·002	0·247	0·383
1·4	0·4084	0·2800	0·980	1·401	1·006	0·328	0·424
1·6	0·4636	0·2726	1·281	1·603	1·013	0·416	0·454
1·8	0·5173	0·2635	1·622	1·807	1·025	0·509	0·474
2·0	0·5689	0·2525	2·003	2·013	1·045	0·605	0·483
2·2	0·6182	0·2398	2·427	2·225	1·077	0·701	0·481
2·4	0·6648	0·2256	2·894	2·445	1·123	0·796	0·468
2·6	0·7083	0·2100	3·406	2·676	1·188	0·888	0·447
2·8	0·7487	0·1933	3·966	2·922	1·274	0·974	0·418
3·0	0·7856	0·1758	4·576	3·187	1·385	1·055	0·383
3·2	0·8190	0·1580	5·242	3·478	1·523	1·127	0·344
3·4	0·8488	0·1403	5·969	3·798	1·688	1·192	0·302
3·6	0·8751	0·1229	6·764	4·155	1·881	1·248	0·261
3·8	0·8980	0·1062	7·634	4·552	2·098	1·296	0·220
4·0	0·9177	0·0906	8·588	4·995	2·338	1·337	0·182
4·2	0·9343	0·0762	9·635	5·489	2·597	1·370	0·148
4·4	0·9482	0·0632	10·787	6·035	2·870	1·396	0·118
4·6	0·9597	0·0517	12·053	6·637	3·154	1·417	0·092
4·8	0·9690	0·0417	13·445	7·297	3·443	1·433	0·070
5·0	0·9765	0·0332	14·976	8·015	3·735	1·445	0·052
5·2	0·9824	0·0260	16·655	8·791	4·026	1·454	0·038
5·4	0·9870	0·0201	18·496	9·625	4·314	1·461	0·028
5·6	0·9905	0·0153	20·509	10·516	4·597	1·465	0·019
5·8	0·9932	0·0115	22·706	11·463	4·875	1·469	0·013
6·0	0·9952	0·0085	25·098	12·466	5·147	1·471	0·009
6·2	0·9966	0·0062	27·696	13·522	5·414	1·472	0·006
6·4	0·9977	0·0045	30·510	14·631	5·676	1·473	0·004
6·6	0·9984	0·0032	33·552	15·792	5·934	1·474	0·002
6·8	0·9990	0·0022	36·830	17·004	6·189	1·474	0·002
7·0	0·9993	0·0015	40·357	18·267	6·440	1·475	0·001
7·2	0·9996	0·0010	44·140	19·580	6·690	1·475	0·000
7·4	0·9997	0·0007	48·192	20·943	6·938	1·475	0·000
7·6	0·9998	0·0004	52·521	22·355	7·185	1·475	0·000
7·8	0·9999	0·0003	57·137	23·817	7·431	1·475	0·000
8·0	1·0000	0·0002	62·051	25·327	7·676	1·475	0·000

Table 1.

η	f''_{11}	f_{12}	f'_{12}	f''_{12}	f_{13}	f'_{13}	f''_{13}
0	**0·3671**	0	0	**1·2159**	0	0	**1·4599**
0·2	0·363	0·023	0·224	1·022	0·028	0·272	1·260
0·4	0·351	0·087	0·410	0·840	0·106	0·504	1·062
0·6	0·331	0·185	0·560	0·669	0·227	0·697	0·868
0·8	0·303	0·309	0·678	0·510	0·382	0·852	0·679
1·0	0·268	0·454	0·765	0·364	0·565	0·969	0·497
1·2	0·226	0·613	0·824	0·229	0·768	1·051	0·325
1·4	0·178	0·782	0·858	0·107	0·984	1·100	0·164
1·6	0·126	0·955	0·868	−0·002	1·206	1·118	0·018
1·8	0·072	1·128	0·858	−0·097	1·429	1·108	−0·113
2·0	0·017	1·297	0·830	−0·179	1·647	1·074	−0·225
2·2	−0·036	1·459	0·787	−0·245	1·857	1·019	−0·318
2·4	−0·085	1·611	0·733	−0·296	2·054	0·948	−0·389
2·6	−0·127	1·751	0·670	−0·331	2·235	0·865	−0·438
2·8	−0·162	1·878	0·601	−0·352	2·399	0·774	−0·466
3·0	−0·187	1·992	0·530	−0·358	2·545	0·680	−0·474
3·2	−0·203	2·090	0·459	−0·352	2·671	0·586	−0·464
3·4	−0·209	2·175	0·390	−0·335	2·779	0·495	−0·440
3·6	−0·207	2·247	0·326	−0·309	2·870	0·411	−0·404
3·8	−0·197	2·306	0·267	−0·278	2·944	0·334	−0·361
4·0	−0·182	2·354	0·214	−0·244	3·004	0·267	−0·314
4·2	−0·162	2·392	0·169	−0·208	3·052	0·208	−0·266
4·4	−0·141	2·422	0·131	−0·174	3·088	0·160	−0·220
4·6	−0·119	2·445	0·100	−0·141	3·116	0·120	−0·177
4·8	−0·098	2·462	0·074	−0·112	3·137	0·089	−0·139
5·0	−0·079	2·475	0·054	−0·087	3·152	0·064	−0·107
5·2	−0·062	2·484	0·039	−0·066	3·163	0·046	−0·080
5·4	−0·047	2·491	0·028	−0·050	3·170	0·032	−0·059
5·6	−0·035	2·496	0·019	−0·036	3·176	0·022	−0·042
5·8	−0·026	2·499	0·013	−0·026	3·179	0·014	−0·030
6·0	−0·018	2·501	0·008	−0·018	3·182	0·010	−0·020
6·2	−0·013	2·502	0·006	−0·012	3·183	0·006	−0·014
6·4	−0·009	2·503	0·003	−0·008	3·184	0·004	−0·009
6·6	−0·006	2·503	0·002	−0·006	3·185	0·002	−0·006
6·8	−0·004	2·504	0·001	−0·004	3·185	0·001	−0·004
7·0	−0·002	2·504	0·001	−0·002	3·186	0·001	−0·002
7·2	−0·002	2·504	0·000	−0·002	3·186	0·000	−0·001
7·4	−0·001	2·504	0·000	−0·001	3·186	0·000	−0·001
7·6	−0·001	2·504	0·000	−0·000	3·186	0·000	−0·000
7·8	−0·000	2·504	0·000	−0·000	3·186	0·000	−0·000
8·0	−0·000	2·504	0·000	−0·000	3·186	0·000	−0·000

Table 1 (*cont.*).

η	g_{10}	g'_{10}	g_{11}	g'_{11}	g_{12}	g'_{12}
0	0	1	0	0·2689	0	0·2484
0·2	0·200	1·000	0·054	0·267	0·050	0·248
0·4	0·400	1·004	0·106	0·260	0·099	0·246
0·6	0·602	1·013	0·157	0·249	0·148	0·239
0·8	0·806	1·031	0·206	0·233	0·194	0·228
1·0	1·015	1·060	0·250	0·213	0·238	0·212
1·2	1·231	1·103	0·290	0·188	0·279	0·189
1·4	1·457	1·162	0·326	0·160	0·314	0·161
1·6	1·697	1·241	0·354	0·128	0·343	0·129
1·8	1·955	1·340	0·376	0·093	0·365	0·092
2·0	2·234	1·462	0·391	0·057	0·380	0·054
2·2	2·541	1·609	0·399	0·021	0·386	0·015
2·4	2·880	1·780	0·400	−0·015	0·386	−0·022
2·6	3·255	1·977	0·393	−0·049	0·378	−0·057
2·8	3·672	2·199	0·380	−0·079	0·363	−0·088
3·0	4·136	2·445	0·362	−0·105	0·343	−0·113
3·2	4·652	2·714	0·339	−0·126	0·318	−0·133
3·4	5·223	3·005	0·312	−0·141	0·290	−0·146
3·6	5·855	3·314	0·283	−0·150	0·261	−0·152
3·8	6·550	3·640	0·252	−0·154	0·230	−0·154
4·0	7·312	3·980	0·222	−0·152	0·200	−0·149
4·2	8·143	4·330	0·192	−0·147	0·170	−0·141
4·4	9·045	4·689	0·163	−0·138	0·143	−0·130
4·6	10·019	5·053	0·137	−0·126	0·118	−0·117
4·8	11·066	5·422	0·113	−0·113	0·096	−0·103
5·0	12·187	5·792	0·092	−0·099	0·077	−0·088
5·2	13·383	6·163	0·073	−0·085	0·061	−0·075
5·4	14·653	6·534	0·058	−0·071	0·047	−0·062
5·6	15·996	6·903	0·045	−0·059	0·036	−0·050
5·8	17·414	7·272	0·034	−0·048	0·027	−0·040
6·0	18·905	7·638	0·026	−0·038	0·020	−0·031
6·2	20·469	8·003	0·019	−0·030	0·015	−0·024
6·4	22·106	8·367	0·014	−0·023	0·010	−0·018
6·6	23·816	8·730	0·010	−0·017	0·007	−0·014
6·8	25·598	9·091	0·007	−0·013	0·005	−0·010
7·0	27·452	9·452	0·005	−0·009	0·003	−0·007
7·2	29·378	9·812	0·003	−0·007	0·002	−0·005
7·4	31·377	10·171	0·002	−0·005	0·001	−0·004
7·6	33·447	10·530	0·001	−0·003	0·001	−0·002
7·8	35·589	10·889	0·000	−0·002	0·000	−0·002
8·0	37·802	11·247	0·000	−0·002	0·000	−0·001

Table 2.

η	g_{13}	g'_{13}	g_{14}	g'_{14}	g_{15}	g'_{15}
0	0	0·7079	0	0·2093	0	0·0956
0·2	0·128	0·568	0·042	0·209	0·019	0·094
0·4	0·228	0·439	0·084	0·207	0·038	0·090
0·6	0·304	0·322	0·124	0·202	0·055	0·084
0·8	0·358	0·217	0·164	0·193	0·071	0·076
1·0	0·392	0·126	0·201	0·179	0·085	0·066
1·2	0·409	0·048	0·235	0·161	0·097	0·055
1·4	0·412	−0·016	0·265	0·137	0·107	0·043
1·6	0·404	−0·067	0·290	0·110	0·114	0·030
1·8	0·386	−0·107	0·309	0·080	0·119	0·018
2·0	0·362	−0·135	0·322	0·047	0·122	0·005
2·2	0·333	−0·153	0·328	0·014	0·122	−0·006
2·4	0·301	−0·163	0·327	−0·018	0·119	−0·017
2·6	0·268	−0·165	0·321	−0·048	0·115	−0·026
2·8	0·235	−0·162	0·309	−0·074	0·109	−0·034
3·0	0·204	−0·154	0·292	−0·096	0·102	−0·040
3·2	0·174	−0·143	0·271	−0·112	0·093	−0·044
3·4	0·147	−0·130	0·247	−0·124	0·084	−0·046
3·6	0·122	−0·116	0·222	−0·130	0·075	−0·047
3·8	0·100	−0·102	0·196	−0·130	0·065	−0·046
4·0	0·081	−0·088	0·170	−0·127	0·056	−0·044
4·2	0·065	−0·074	0·145	−0·120	0·048	−0·041
4·4	0·051	−0·062	0·122	−0·111	0·040	−0·037
4·6	0·040	−0·051	0·101	−0·100	0·033	−0·033
4·8	0·031	−0·041	0·082	−0·088	0·027	−0·029
5·0	0·024	−0·033	0·066	−0·075	0·021	−0·025
5·2	0·018	−0·026	0·052	−0·063	0·017	−0·021
5·4	0·013	−0·020	0·040	−0·052	0·013	−0·017
5·6	0·010	−0·015	0·031	−0·042	0·010	−0·014
5·8	0·007	−0·011	0·023	−0·034	0·008	−0·011
6·0	0·005	−0·008	0·017	−0·026	0·006	−0·008
6·2	0·003	−0·006	0·012	−0·020	0·004	−0·006
6·4	0·002	−0·004	0·009	−0·015	0·003	−0·005
6·6	0·002	−0·003	0·006	−0·011	0·002	−0·004
6·8	0·001	−0·002	0·004	−0·008	0·002	−0·003
7·0	0·001	−0·002	0·003	−0·006	0·001	−0·002
7·2	0·001	−0·001	0·002	−0·004	0·001	−0·001
7·4	0·000	−0·001	0·001	−0·003	0·000	−0·001
7·6	0·000	−0·000	0·001	−0·002	0·000	−0·001
7·8	0·000	−0·000	0·000	−0·002	0·000	−0·000
8·0	0·000	−0·000	0·000	−0·001	0·000	−0·000

Table 2 (*cont.*).

it follows that

$$\frac{q_w}{(q_w)_s} = 1 + \epsilon e^{i\omega t}\left[0{\cdot}5 + (0{\cdot}840\chi - 0{\cdot}910)is + \right.$$
$$\left. + \frac{M}{\chi - 1}\{0{\cdot}7\chi - 1{\cdot}1 - (0{\cdot}840\chi^2 - 0{\cdot}080\chi + 0{\cdot}198)is\}\right], \quad (62)$$

for $\gamma = 1{\cdot}4$, again provided that s^2 and higher powers are negligible.

Case of high frequency

When the frequency parameter s is large, it is appropriate to expand in inverse powers of s. If $\alpha = (is)^{-1/2}$ and $\beta = (i\omega/C\nu_\infty)^{1/2}Y$, it follows that $\eta = \alpha\beta$, and we may write, instead of (33),

$$\psi = U_\infty \left(\frac{C\nu_\infty}{i\omega}\right)^{1/2}\left[\frac{1}{\alpha}F(\alpha\beta) + E\sum_{n=0}^{\infty}\alpha^n h_n(\beta)\right]. \quad (63)$$

Then,

$$\frac{\partial\psi}{\partial Y} = u = U_\infty\left[F'(\alpha\beta) + E\sum_{n=0}^{\infty}\alpha^n h_n'(\beta)\right], \quad (64)$$

and

$$-\frac{\partial\psi}{\partial x} = \tfrac{1}{2}(i\omega C\nu_\infty)^{1/2}\left[\alpha^2\beta F'(\alpha\beta) - \alpha F(\alpha\beta) + E\sum_{n=0}^{\infty}(n\alpha^2 + 2M)\alpha^n h_n(\beta)\right]. \quad (65)$$

Corresponding to (36) we write

$$T/T_1 = \chi - (\chi - 1)G(\alpha\beta) + E\sum_{n=0}^{\infty}\alpha^n k_n(\beta). \quad (66)$$

For small α,

$$F(\alpha\beta) = \tfrac{1}{2}F''(0)\alpha^2\beta^2 + O(\alpha^5),$$

and

$$G(\alpha\beta) = G'(0)\alpha\beta + O(\alpha^4),$$

provided β is not too large. With the help of these approximations, we obtain, by substituting in (20) and considering successive powers of α, the following differential equations

$$h_0''' - h_0' = -\chi(1 - M),$$
$$h_0''' - h_1' = (\chi - 1)(1 - M)G'(0)\beta + MF''(0)(h_0 - \beta h_0'),$$
$$h_2''' - h_2' = MF''(0)(h_1 - \beta h_1'),$$
$$h_3''' - h_3' = \tfrac{1}{2}F''(0)(\tfrac{1}{2}\beta^2 h_0'' - \beta h_0') + MF''(0)(h_2 - \beta h_2').$$

In the complementary function of each differential equation, the term involving e^β must be suppressed because it has the wrong behaviour for large β, and therefore there are only two constants of integration. These are determined by the boundary conditions $h_n(0) = h_n'(0) = 0$. The appropriate solutions are

$$h_0 = (1 - M)\chi(\beta + e^{-\beta} - 1),$$
$$h_1 = -\tfrac{1}{2}(\chi - 1)G'(0)\beta^2 + M[\tfrac{1}{2}(\chi - 1)G'(0)\beta^2 + \chi F''(0)\{\beta + \tfrac{1}{4}e^{-\beta}(9 + 5\beta + \beta^2) - \tfrac{9}{4}\}],$$
$$h_2 = -M(\chi - 1)F''(0)G'(0)(\beta + \tfrac{1}{6}\beta^3 + e^{-\beta} - 1),$$
$$h_3 = \tfrac{1}{16}(1 - M)\chi F''(0)[4\beta^2 + e^{-\beta}(13 + 13\beta + 5\beta^2 + \tfrac{2}{3}\beta^3) - 13].$$

Similarly by substituting in (29) we obtain the differential equations

$$P^{-1}k_0'' - k_0 = 0,$$

$$P^{-1}k_1'' - k_1 = -M[F'''(0)\beta k_0 + (\chi-1)G'(0)h_0],$$

$$P^{-1}k_2'' - k_2 = -M[F'''(0)\beta k_1 + (\chi-1)G'(0)h_1],$$

$$P^{-1}k_3'' - k_3 = \tfrac{1}{4}F'''(0)\beta^2 k_0' + \tfrac{1}{2}(\chi-1)G'(0)\beta h_0' - M[F'''(0)\beta k_2 + (\chi-1)G'(0)h_2].$$

The appropriate solutions, for moderate β, are

$$k_0 = -M(\gamma-1)\chi e^{-\beta\sqrt{P}},$$

$$k_1 = M\chi(\chi-1)G'(0)\left[\beta + \frac{e^{-\beta\sqrt{P}} - Pe^{-\beta}}{1-P} - 1\right],$$

$$k_2 = M(\chi-1)^2[G'(0)]^2\left[\frac{1}{P}(e^{-\beta\sqrt{P}}-1) - \tfrac{1}{2}\beta^2\right],$$

$$k_3 = \tfrac{1}{2}\chi(\chi-1)G'(0)\left[-\beta + \frac{2P}{(1-P)^2}e^{-\beta\sqrt{P}} - \left\{\frac{P}{1-P}\beta + \frac{2P}{(1-P)^2}\right\}e^{-\beta}\right] -$$
$$- M\left[\tfrac{1}{2}\chi(\chi-1)G'(0)\left\{-\beta + \frac{2P}{(1-P)^2}e^{-\beta\sqrt{P}} - \left(\frac{P}{1-P}\beta + \right.\right.\right.$$
$$\left.\left.\left. + \frac{2P}{(1-P)^2}\right)e^{-\beta}\right\} + \tfrac{1}{16}(\gamma-1)\chi F'''(0)(\beta + P^{1/2}\beta^2 + \tfrac{2}{3}P\beta^3)e^{-\beta\sqrt{P}}\right],$$

the term $e^{\beta\sqrt{P}}$ in the complementary functions having been discarded in each case, and the solutions having been made to satisfy the boundary conditions

$$k_0(0) = -M(\gamma-1)\chi, \qquad k_n(0) = 0 \quad (n \geqslant 1).$$

It now follows that for large frequencies (α small)

$$\tau_w(t,x) = \frac{\mu_w\rho_w}{\rho_\infty}\left(\frac{i\omega}{C\nu_\infty}\right)^{1/2}\left(\frac{\partial u}{\partial\beta}\right)_{\beta=0}$$
$$= \rho_\infty U_\infty^2\left(\frac{C\nu_\infty}{U_\infty x}\right)^{1/2}\frac{p_1}{p_\infty}\left[F''(0) + E\sum_{n=0}^{\infty}\alpha^{n-1}h_n''(0)\right],$$

and so

$$\frac{\tau_w}{(\tau_w)_s} = 1 + E[3{\cdot}011\chi(is)^{1/2} - 0{\cdot}8903(\chi-1) + 0{\cdot}3125\chi(is)^{-1} +$$
$$+ M\{-3{\cdot}011\chi(is)^{1/2} + 1{\cdot}140\chi + 0{\cdot}5097 - 0{\cdot}2956(\chi-1)(is)^{-1/2} -$$
$$- 0{\cdot}3125\chi(is)^{-1}\}], \quad (67)$$

provided the cube and higher powers of $s^{-1/2}$ are neglected.

Similarly the heat transfer from the plate is

$$q_w(t,x) = -\frac{\mu_w\rho_w}{P\rho_\infty}\left(\frac{i\omega}{C\nu_\infty}\right)^{1/2}\left(\frac{\partial I}{\partial\beta}\right)_{\beta=0}$$
$$= \frac{1}{P}\rho_\infty\left(\frac{CU_\infty\nu_\infty}{x}\right)^{1/2}\frac{p_1}{p_\infty}I_1\left[(\chi-1)G'(0) - E\sum_{n=0}^{\infty}\alpha^{n-1}k_n'(0)\right],$$

and so

$$\frac{q_w}{(q_w)_s} = 1 + E\Big[0{\cdot}3945\chi(is)^{-1} + \frac{M}{\chi-1}\{-1{\cdot}148\chi(is)^{1/2} - 0{\cdot}5410\chi^2 + \\ + 2{\cdot}3410\chi - 1{\cdot}8 + 0{\cdot}3484(\chi-1)^2(is)^{-1/2} - (0{\cdot}3945\chi^2 - \\ - 0{\cdot}4226\chi)(is)^{-1}\}\Big] \quad (68)$$

for $P = 0{\cdot}72$, with the cube and higher powers of $s^{-1/2}$ neglected.

If, in order to compare the formulae for small and large frequency, we write

$$\frac{\tau_w}{(\tau_w)_s} = 1 + \epsilon e^{i(\omega t - Ms)}(A + iB),$$

and

$$\frac{q_w}{(q_w)_s} = 1 + \epsilon e^{i(\omega t - Ms)}(C + iD),$$

where A, B, C and D are real, then

$$\left.\begin{aligned} A &= 1{\cdot}5 + 0{\cdot}7M && \text{(small } s\text{)} \\ &= 2{\cdot}129s^{1/2} - 0{\cdot}8903(\chi-1) + M[-2{\cdot}129s^{1/2} + 1{\cdot}1403\chi + \\ &\qquad + 0{\cdot}5097 - 0{\cdot}2090(\chi-1)s^{-1/2}] && \text{(large } s\text{),} \end{aligned}\right\} \quad (69)$$

$$\left.\begin{aligned} B &= (3{\cdot}661\chi - 1{\cdot}105)s - M(3{\cdot}661\chi - 0{\cdot}272)s && \text{(small } s\text{)} \\ &= 2{\cdot}129s^{1/2} - 0{\cdot}3125s^{-1} + M[-2{\cdot}129s^{1/2} + \\ &\qquad + 0{\cdot}2090(\chi-1)s^{-1/2} + 0{\cdot}3125s^{-1}] && \text{(large } s\text{),} \end{aligned}\right\} \quad (70)$$

$$\left.\begin{aligned} C &= 0{\cdot}5 + M\frac{0{\cdot}7\chi - 1{\cdot}1}{\chi-1} && \text{(small } s\text{)} \\ &= M\left[\frac{-0{\cdot}8117\chi}{\chi-1}s^{1/2} + 1{\cdot}8 - 0{\cdot}5410\chi + 0{\cdot}2464(\chi-1)s^{-1/2}\right] && \text{(large } s\text{),} \end{aligned}\right\} \quad (71)$$

$$\left.\begin{aligned} D &= (0{\cdot}840\chi - 0{\cdot}910)s - \frac{M}{\chi-1}(0{\cdot}840\chi^2 - 0{\cdot}080\chi + 0{\cdot}198)s && \text{(small } s\text{)} \\ &= -0{\cdot}3945\chi s^{-1} + M\left[\frac{-0{\cdot}8117\chi}{\chi-1}s^{1/2} - 0{\cdot}2464(\chi-1)s^{-1/2} + \right. \\ &\qquad \left. + \frac{0{\cdot}3945\chi^2 - 0{\cdot}4225\chi}{\chi-1}s^{-1}\right] && \text{(large } s\text{).} \end{aligned}\right\} \quad (72)$$

The angles $\tan^{-1}(B/A)$ and $\tan^{-1}(D/C)$ are the amounts by which the phases of the skin friction and the heat transfer respectively are in advance of the mainstream fluctuation.

In the important special case $M = 0$,

$$\left.\begin{aligned} \frac{\tau_w}{(\tau_w)_s} &= 1 + \epsilon e^{i\omega t}[1{\cdot}5 + i(3{\cdot}661\chi - 1{\cdot}105)s] && \text{(small } s\text{)} \\ &= 1 + \epsilon e^{i\omega t}[2{\cdot}129s^{1/2} - 0{\cdot}8903(\chi-1) + \\ &\qquad + i(2{\cdot}129s^{1/2} - 0{\cdot}3125s^{-1})] && \text{(large } s\text{).} \end{aligned}\right\} \quad (73)$$

When further the flow is completely incompressible, $\chi = 1$, as we have

already mentioned, and we then obtain

$$\left.\begin{aligned}\frac{\tau_w}{(\tau_w)_s} &= 1+\epsilon e^{i\omega t}(1{\cdot}5+2{\cdot}556is) \qquad \text{(small } s\text{)}\\ &= 1+\epsilon e^{i\omega t}[2{\cdot}129s^{1/2}+i(2{\cdot}129s^{1/2}-0{\cdot}3125s^{-1})] \quad \text{(large } s\text{).}\end{aligned}\right\} \tag{74}$$

(We may notice here that Moore (1951) gives 2·555 as the coefficient of is in the formula for small s.) The formulae given by Lighthill for the skin friction in this case are

$$\left.\begin{aligned}\frac{\tau_w}{(\tau_w)_s} &= 1+\epsilon e^{i\omega t}(1{\cdot}5+\tfrac{51}{20}is) \qquad \text{(small } s\text{)}\\ &= 1+\epsilon e^{i\omega t}[2{\cdot}062s^{1/2}+i(2{\cdot}062s^{1/2})] \qquad \text{(large } s\text{).}\end{aligned}\right\} \tag{75}$$

The good agreement between (74) and (75), and particularly the fact that the coefficients of is for low frequencies are practically equal, strongly supports the use of the Pohlhausen approximate method by Lighthill in this problem. Lighthill also showed that the whole range of values of the frequency might reasonably well be covered by using (75) only. For at

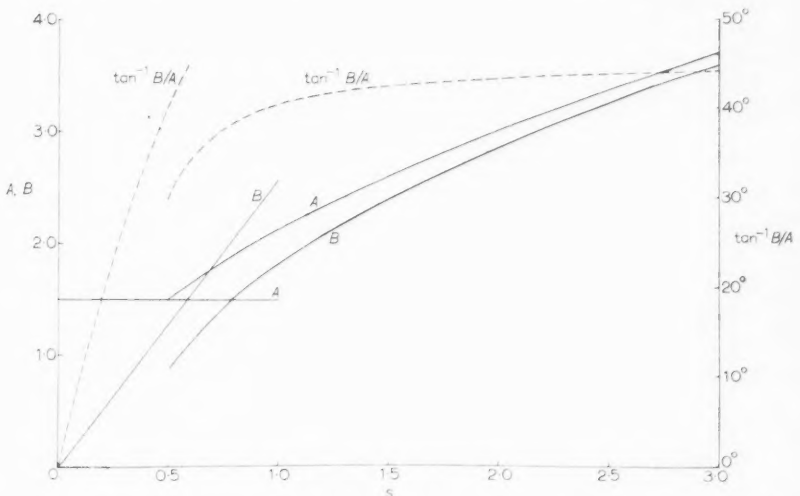

Figure 1. Variation of A, B, and $\tan^{-1}(B/A)$ with frequency parameter s when $M = 0$ and $\chi = 1$.

the place $s = s_0$ where the values of $\tan^{-1}(B/A)$ are equal in the two parts of (75), the values of $(A^2+B^2)^{1/2}$ agree, and so it is reasonable to assume that the two parts of (75) apply to the respective ranges $s < s_0$ and $s > s_0$. This point is illustrated in figure 1, where the quantities A, B and $\tan^{-1}(B/A)$ as given by (74), rather than (75), are plotted for various values of s. For if the term involving s^{-1} in (74) is discarded, so as to bring the formula into line with (75), the B-curve for large s will coincide with the given A-curve for large s. Then, $A = B$ for both large and small s at

$s = s_0 = 0{\cdot}59$ and here the two A-curves are close together. Figure 2, based on (73), shows the same information for $\chi = 2$ as figure 1 does for $\chi = 1$. However, for $\chi = 2$, the whole range of values of s does not appear to be as well represented as it was for $\chi = 1$ simply by the formulae for small and large s. To make a strict comparison with the previous discussion, we should retain only the terms involving $s^{1/2}$ in the part of (73) referring to large s. Then, the A- and B-curves for large s would coincide with the A-curve for large s in figure 1, and we should have $A = B$ for both small and large s at $s = s_0 = 0{\cdot}24$. Here the values of A would be 1·5 for small s and 1·043 for large s (from the A-curve on figure 1). This involves a much larger discrepancy than the case $\chi = 1$, where the corresponding numbers are 1·5 and 1·64 respectively. In fact, figure 2 suggests that the formulae (73) will not be adequate to cover all values of the frequency for an arbitrary value of χ.

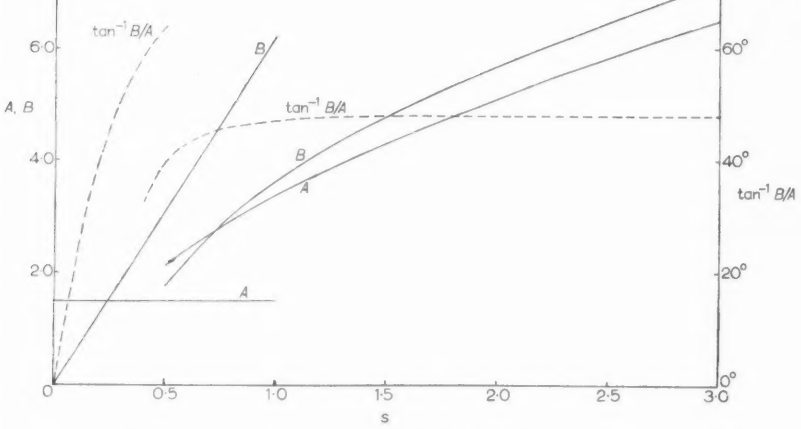

Figure 2. Variation of A, B, and $\tan^{-1}(B/A)$ with frequency parameter s when $M = 0$ and $\chi = 2$.

The quantity $\tan^{-1}(B/A)$ is of course the phase advance of the skin friction relative to the main stream. As (69) and (70) show, this has the asymptotic value $\frac{1}{4}\pi$ for large frequencies whatever the values of χ and M (small). For any specified small value of s, on the other hand, the phase advance is increased by increasing the value of χ, that is, by increasing the temperature of the plate and therefore reducing the inertia of the gas near the surface.

As regards the heat transfer from the wall, it can be seen from (71) and (72) that the phase advance for small frequency is small and negative in the incompressible case ($\chi = 1$) as Lighthill found. In fact, for the case $M = 0$,

$\chi = 1$, Lighthill's work gives

$$\frac{q_w}{(q_w)_s} = 1 + \epsilon e^{i\omega t}(0{\cdot}5 - 0{\cdot}03is) \quad \text{for small } s,$$

whereas the present calculations give the same formula with the coefficient 0·03 replaced by 0·070. (Ostrach's (1955) value is 0·069 to the present order of accuracy.) The Pohlhausen method has in fact predicted this coefficient reasonably well, giving the correct sign and a small quantity of the correct order of magnitude. As χ is increased, the phase advance increases (becoming positive at $\chi = 1{\cdot}08$), as it does for the skin friction. Since, for large values of s, C and D are 0 in the case $M = 0$ provided that terms smaller than $s^{1/2}$ are neglected, the heat transfer does not lend itself to a graphical representation corresponding to figures 1 and 2.

Appendix

A note on transformations of the compressible boundary-layer equations for unsteady flow

The analysis of § 2 shows that the Howarth transformation as extended by Moore provides a very useful method of treating the boundary-layer equations for unsteady compressible flow. Now, in the theory of steady boundary layers, besides the Howarth transformation there are the von Mises and the Crocco transformations. All these transformations hinge upon the replacement of the coordinate y perpendicular to the wall by a convenient alternative variable. The Howarth transformation uses $\frac{1}{\rho_\infty}\int_0^y \rho\, dy$ instead of y, as we have already seen; the von Mises transformation uses the stream function, which exists in steady plane flow, and the Crocco transformation uses the velocity component u. These have all been described by Howarth (1953). The Crocco transformation has been mainly employed in studying the steady boundary layer on a flat plate, whilst the other two transformations, besides their application to the flat plate, have both been used to show that a compressible boundary layer with a non-zero pressure gradient in certain circumstances may be given in terms of the solution of an associated incompressible boundary-layer flow. It is therefore of some interest to examine whether the von Mises and the Crocco transformations can also be conveniently extended to the case of unsteady boundary-layer flow.

The von Mises equations

In the von Mises transformation for unsteady flow, the new variables are t, x and ψ, where ψ is the mass flux function defined by the equation

$$\frac{\rho u}{\rho_\infty} = \frac{\partial \psi}{\partial y}.$$

In terms of the new variables

$$\rho u = \rho_\infty \left(\frac{\partial y}{\partial \psi}\right)^{-1} \quad \text{and} \quad \rho v = \int_0^\psi \left(\frac{\partial y}{\partial t}\frac{\partial \rho}{\partial \psi} - \frac{\rho_\infty}{\rho u}\frac{\partial \rho}{\partial t}\right) d\psi + \rho u \frac{\partial y}{\partial x}. \qquad (76)$$

It is easy to show that the momentum equation (2) becomes

$$\frac{\partial u}{\partial t}+u\frac{\partial u}{\partial \psi}\int_0^{\psi}\frac{1}{u^2}\frac{\partial u}{\partial t}\,d\psi+u\frac{\partial u}{\partial x}=-\frac{1}{\rho_1}\frac{\partial p_1}{\partial x}\frac{I}{I_1}+\frac{u}{\rho_\infty^2}\frac{\partial}{\partial \psi}\left(\mu\rho u\frac{\partial u}{\partial \psi}\right), \tag{77}$$

in which the first two terms on the left-hand side may be replaced by

$$u\frac{\partial}{\partial \psi}\left(u\int_0^{\psi}\frac{1}{u^2}\frac{\partial u}{\partial t}\,d\psi\right),$$

and that the energy equation (3) becomes

$$\frac{\partial I}{\partial t}+u\frac{\partial I}{\partial \psi}\int_0^{\psi}\frac{1}{u^2}\frac{\partial u}{\partial t}\,d\psi+u\frac{\partial I}{\partial x}-\frac{1}{\rho_1}\left(\frac{\partial p_1}{\partial t}+u\frac{\partial p_1}{\partial x}\right)\frac{I}{I_1}$$
$$=\frac{1}{P\rho_\infty^2}u\frac{\partial}{\partial \psi}\left(\mu\rho u\frac{\partial I}{\partial \psi}\right)+\frac{\mu\rho u^2}{\rho_\infty^2}\left(\frac{\partial u}{\partial \psi}\right)^2. \tag{78}$$

Of course these von Mises equations have little practical value if they are in all circumstances more difficult to solve than the corresponding equations (12) and (13) that result from the Howarth transformation. It is scarcely possible to assert that they will be more difficult without a detailed study of some special cases, but it will perhaps be worth while to notice how unsteadiness of the flow increases the difficulties of solution in one or two simple cases of steady flow that have been investigated by means of the von Mises transformation. To take an easy example, consider steady flow past a flat plate for which the momentum equation in the von Mises form is

$$\frac{\partial u}{\partial x}=\frac{1}{\rho_\infty^2}\frac{\partial}{\partial \psi}\left(\mu\rho u\frac{\partial u}{\partial \psi}\right). \tag{79}$$

This equation was solved by von Kármán & Tsien (1938) under the assumptions that $\mu=\mu_s(T/T_s)^n$ with $n=0{\cdot}76$, $P=1$, and that there is no heat transfer at the plate. The last two conditions ensure that $I+\frac{1}{2}u^2=I_s+\frac{1}{2}U_s^2$, where the suffix s refers to the uniform main stream, and the first condition shows that $\mu\rho=\mu_s\rho_s(I/I_s)^{n-1}$, so that $\mu\rho$ is a function of u only, given by

$$\mu\rho=\mu_s\rho_s\left[1+\frac{U_s^2}{2I_s}\left(1-\frac{u^2}{U_s^2}\right)\right]^{n-1}. \tag{80}$$

Thus, (79) reduces to a *second* order differential equation for the single dependent variable u. If the expression (80) is substituted in equation (12), a *third* order equation for ψ results, and so there is something to be said for preferring the von Mises momentum equation in this problem.

In the field of unsteady flow a relatively simple problem of the same type concerns a flat plate in a constant stream when the temperature of the plate is a function of time. Then there are no pressure gradients and the von Mises momentum equation reduces to

$$\frac{\partial}{\partial \psi}\left(u\int_0^{\psi}\frac{1}{u^2}\frac{\partial u}{\partial t}\,d\psi\right)+\frac{\partial u}{\partial x}=\frac{1}{\rho_s^2}\frac{\partial}{\partial \psi}\left(\mu\rho u\frac{\partial u}{\partial \psi}\right). \tag{81}$$

Even if we assume that $P=1$, it is no longer possible to write

$$I+\tfrac{1}{2}u^2=I_s+\tfrac{1}{2}U_s^2.$$

now that there is heat transfer at the plate, and so $\mu\rho$ cannot be expressed in terms of u only, as in equation (80).

However, if, instead of assuming that $\mu \propto T^n$, we adopt the approximation referred to in § 2 and write

$$\mu\rho = C\mu_\infty \rho_\infty$$

where C, given by (17), is a known function of t only, equation (81) is a differential equation involving only the one dependent variable u. Thus, by altering the assumed viscosity temperature law, we have kept to a problem of the Kármán–Tsien type, namely, the solution of a second-order partial differential equation for u, as far as the momentum equation is concerned. Of course it still remains to solve the energy equation (78), for information about the temperature (and density) in the boundary layer.

Actually, if we use the rather formal viscosity–temperature law $\mu \propto T$, so that $\mu\rho = \mu_\infty \rho_\infty$, this problem can be simplified still further. For the velocity u then loses its explicit dependence on t, and the momentum equation is

$$\frac{\partial u}{\partial x} = \nu_\infty \frac{\partial}{\partial \psi}\left(u \frac{\partial u}{\partial \psi}\right).$$

Thus $u(x, \psi)$ is simply the velocity (expressed in von Mises coordinates) for steady incompressible flow past a flat plate. The temperature would then be given by solving the energy equation

$$\frac{\partial I}{\partial t} + u\frac{\partial I}{\partial x} = \frac{\nu_\infty}{P} u \frac{\partial}{\partial \psi}\left(u \frac{\partial I}{\partial \psi}\right) + \nu_\infty u^2 \left(\frac{\partial u}{\partial \psi}\right)^2.$$

The Crocco equations

In the Crocco transformation the new variables are t, x and z, where z is the non-dimensional velocity distribution function given by

$$z = u(t, x, y)/u_1(t, x). \tag{82}$$

When u_1 is a constant this is precisely the transformation that Crocco used to investigate the steady boundary layer on a flat plate. Following Crocco, we eliminate ρv between the transformed equations of continuity and momentum, and introduce the shearing stress

$$\tau = \mu \frac{\partial u}{\partial y} = \mu u_1 \left(\frac{\partial y}{\partial z}\right)^{-1}$$

as a dependent variable in place of u. In this way, (1) and (2) lead to the equation

$$\frac{\partial u_1}{\partial t} z \frac{\partial}{\partial z}\left(\frac{\mu\rho}{\tau}\right) - u_1 \frac{\partial}{\partial t}\left(\frac{\mu\rho}{\tau}\right) + u_1 \frac{\partial u_1}{\partial x} z^2 \frac{\partial}{\partial z}\left(\frac{\mu\rho}{\tau}\right) - u_1^2 z \frac{\partial}{\partial x}\left(\frac{\mu\rho}{\tau}\right)$$
$$= -\frac{1}{\rho_1}\frac{\partial p_1}{\partial x}\frac{\partial}{\partial z}\left(\frac{\mu\rho}{\tau}\frac{I}{I_1}\right) + \frac{1}{u_1}\frac{\partial^2 \tau}{\partial z^2}. \tag{83}$$

Similarly, by transforming (2) and (3) and eliminating ρv between them

we obtain

$$\mu\rho\left(u_1\frac{\partial I}{\partial t}-\frac{\partial u_1}{\partial t}z\frac{\partial I}{\partial z}-u_1\frac{\partial u_1}{\partial x}z^2\frac{\partial I}{\partial z}+u_1^2z\frac{\partial I}{\partial x}\right)-$$
$$-\mu\rho\frac{I}{I_1}\left(\frac{u_1}{\rho_1}\frac{\partial p_1}{\partial t}+\frac{1}{\rho_1}\frac{\partial p_1}{\partial x}\frac{\partial I}{\partial z}+u_1^2\frac{1}{\rho_1}\frac{\partial p_1}{\partial x}z\right)+\frac{1}{u_1}\tau\frac{\partial\tau}{\partial z}\frac{\partial I}{\partial z}$$
$$=\frac{1}{Pu_1}\tau\frac{\partial}{\partial z}\left(\tau\frac{\partial I}{\partial z}\right)+u_1\tau^2. \quad (84)$$

The boundary conditions that go with these equations concern the values of τ and I at the wall, $z=0$, and at the outer edge of the boundary layer $z=1$. Equation (2) shows that $\partial\tau/\partial y=\partial p_1/\partial x$ at the wall, and so

$$\tau\frac{\partial\tau}{\partial z}=\mu_w u_1\frac{\partial p_1}{\partial x}\quad\text{at } z=0. \quad (85)$$

Since the shearing stress vanishes at the outer edge of the boundary layer

$$\tau=0\quad\text{at } z=1. \quad (86)$$

We shall suppose that either the wall temperature (enthalpy I_w) or the heat flux, q_w, from the wall is specified. It follows that I must satisfy either

$$I=I_w\quad\text{or}\quad(\tau\partial I/\partial z)=-Pu_1q_w\quad\text{at } z=0. \quad (87)$$

Finally, the condition

$$I=I_1\quad\text{at } z=1 \quad (88)$$

completes the list of four boundary conditions.

Equations (83) and (84) are quite complicated, especially because of the large number of terms on the left-hand side in each case. In this respect they are much worse than either the Howarth–Moore equations (12) and (13) or the von Mises equations (77) and (78). However, it would be feasible to use them in some circumstances. Some preliminary work showed that it would have been practicable to obtain the results of § 3 by solving these equations, but the simpler calculations involved in starting from the Howarth–Moore equations turned out to be preferable. One advantage of the Crocco equations is that the momentum equation is of the second order, but one of the complications encountered in the work just mentioned arose from the frequently occurring term $\mu\rho/\tau$. It will be recalled that in § 3, τ was expressed as a power series, and the reciprocal of such a series, arising in $\mu\rho/\tau$, is another series with complicated coefficients. Of course these difficulties would also be present if the Crocco equations were applied to a steady boundary layer with a non-uniform main stream. So far as the author is aware, even this has not been done.

The Crocco equations are considerably shortened by assuming that the external stream is uniform. In fact for the simple problem, mentioned above, of a flat plate with a varying temperature and with $\mu\rho=\mu_\infty\rho_\infty$, they would reduce to

$$\frac{\partial^2\tau}{\partial z^2}+\mu_\infty\rho_\infty U_\infty^3 z\frac{\partial}{\partial x}\left(\frac{1}{\tau}\right)=0, \quad (89)$$

$$\frac{1}{P}\tau\frac{\partial}{\partial z}\left(\tau\frac{\partial I}{\partial z}\right)+\mu_\infty\rho_\infty U_\infty^3\left(\frac{1}{U_\infty}\frac{\partial I}{\partial t}+z\frac{\partial I}{\partial x}\right)+\tau\frac{\partial\tau}{\partial z}\frac{\partial I}{\partial z}-U_\infty^2\tau^2=0. \quad (90)$$

The solution of (89) for τ is known from the work of Crocco for the case of steady flow, and the problem therefore reduces to solving (90) for I.

In conclusion, the small amount of evidence from the problem considered in this paper suggests that the Howarth–Moore transformation is the simplest to apply of the three available transformations in unsteady compressible boundary-layer theory.

References

Chapman, D. R. & Rubesin, M. W. 1949 *J. Aero. Sci.* **16,** 547.

Gibellato, S. 1955 *Atti Accad. Sci. Torino Cl. Sci. Fis Mat. Nat.* **89,** 180.

Howarth, L. 1948 *Proc. Roy. Soc.* A, **194,** 16.

Howarth, L. (Ed.) 1953 *Modern Developments in Fluid Dynamics. High Speed Flow.* Oxford : Clarendon Press.

Kármán, T. von & Tsien, H. S. 1938 *J. Aero. Sci.* **5,** 227.

Lighthill, M. J. 1954 *Proc. Roy. Soc.* A, **224,** 1.

Moore, F. K. 1951 *Nat. Adv. Comm. Aero., Wash., Tech. Note* no. 2471.

Ostrach, S. 1955 *Nat. Adv. Comm. Aero., Wash., Tech. Note* no. 3569.

Rayleigh, Lord 1894 *The Theory of Sound,* 2nd Ed. London : Macmillan.

Schlichting, H. 1955 *Boundary Layer Theory.* London : Pergamon Press.

Non-linear interactions in a viscous heat-conducting compressible gas

By BOA-TEH CHU* and LESLIE S. G. KOVÁSZNAY
The Johns Hopkins University, Baltimore, Maryland

(*Received* 27 *May* 1957 *and in revised form* 26 *September* 1957)

SUMMARY

The linearized equations of motion show that in a viscous heat-conducting compressible medium three modes of fluctuations exist, each one of which is a familiar type of disturbance. The vorticity mode occurs in an incompressible turbulent flow, the entropy mode is familiar as temperature fluctuations in low speed turbulent heat transfer problems, and the sound mode is the subject of conventional acoustics. A consistent higher order perturbation theory is presented with the only restrictions being that the Prandtl number is $\frac{3}{4}$ and the viscosity and heat conductivity are monotonic functions of the temperature alone. The theory is based on expansion of the disturbance fields in powers of an amplitude parameter α. The non-linearity of the full Navier–Stokes equations can be interpreted as interaction between the three basic modes; in order to help physical insight the interactions are classed as ' mass-like ', ' force-like ', and ' heat-like ' effects.

Besides the amplitude parameter α there is another subsidiary non-dimensional parameter ϵ which indicates the relative importance of viscosity and heat conduction effects as compared to the inertial effects, ϵ is proportional to the ratio of the molecular mean free path and the characteristic length of the flow pattern (Knudsen number). The main contribution of the paper is the outline of a consistent successive approximation for an arbitrary order in α and the presentation of explicit formulae for the second order (bilateral) interactions.

A special case of rather general significance is treated in more detail. This is when all three basic modes have intensities and length scales of the same orders of magnitude and in addition to α the parameter ϵ is also small; the second-order interactions are then relatively few and easily identifiable and are shown in table 1.

The present analysis also sheds some light on the ' zero order ' approximation which treats the vorticity and entropy disturbances as a ' frozen pattern ' and the sound field as propagating non-dissipative waves. The interpretation of hot-wire measurements relies heavily on these simplified models and the present paper lends some support to these current hot-wire practices.

* Now at Brown University, Providence, Rhode Island.

1. Introduction

In fluid mechanics the non-linearity of the governing equations manifests itself in several ways. Some of the non-linear effects are described by various special names, for instance, the continuous generation of vorticity in the phenomenon called turbulence, the gradual steepening of the slope of compression waves, the generation of aerodynamic sound, acoustic streaming, scattering of sound waves by turbulence, etc. The question arises of whether all types of non-linear phenomena governed by the compressible Navier–Stokes equations have been uncovered or whether there are still others that have escaped attention. This can be answered only by a systematic study of the equations.

There is another important question; by varying some overall parameter (e.g. the Mach number of the mean flow, the length scale of the fluctuation, etc.) the relative importance of the various non-linear effects may vary. A typical problem is the change in the nature of turbulence as the Mach number of the primary flow increases. In actual experimentation the measured quantities must be interpreted within a theoretical framework even if it serves only to guide our thinking. The measurement of fluctuating quantities in a turbulent flow has been extended to high speed flows (Kovásznay 1953) and the present approach was strongly motivated by the desire to generalize the crude but simple concepts that were obtained from the linearized problem.

Both at low speeds and at high speeds, the hot-wire measurements are carried out keeping the probe at a fixed location and the records are obtained as fluctuations in time and all statistical averaging is performed in the time domain. These time records at low speeds are often regarded as approximate instantaneous space traverses by virtue of Taylor's hypothesis that the flow pattern is carried with the main flow and changes only relatively slowly. In high speed flow the simple linearized theory of the compressible case indicated that there are three fluctuation modes and for two of them (vorticity and entropy modes) this simple motion of 'frozen pattern' can be immediately extended. We may call these 'parabolic' modes as they obey parabolic differential equations. The third mode, the pressure or sound mode, obeys a hyperbolic differential equation and can be interpreted as a system of acoustic waves travelling with respect to the main flow.

The linearized theory does not indicate any interaction among the modes as long as the domain of interest is far from solid boundaries and it may be valid as long as the fluctuations are weak. When the intensity of fluctuation ceases to be small, the flow can still be conveniently interpreted as built up by superposition of the three basic modes of fluctuation. However, in addition to those originally accounted for, there are also fluctuations produced by the interaction of the basic modes. A systematic study of these interactions is expected to cover all the possible non-linear phenomena.

The analysis presented here does not attempt to 'solve' compressible heat conducting viscous flow problems in the sense of an initial value or boundary value problem. It attempts rather to serve as a guide to assess all the non-linear interactions in a consistent framework in which experimental information (of the usual incomplete nature) can be understood.

2. Fundamental equations

The fundamental system of differential equations governing the motion of a viscous, heat-conducting, compressible medium consists of the continuity, momentum and energy equations. If p, ρ, T, E, $\mathbf{v}$, μ and κ denote respectively the pressure, density, temperature, entropy, velocity, coefficients of viscosity and heat conduction, the fundamental equations assume the following form:

$$\frac{\partial \rho}{\partial t} + \operatorname{div} \rho \mathbf{v} = m, \tag{2.1}$$

$$\rho \frac{D\mathbf{v}}{Dt} = -\operatorname{grad} p - \tfrac{2}{3} \operatorname{grad}(\mu \operatorname{div} \mathbf{v}) + \operatorname{div}[\mu \operatorname{def} \mathbf{v}] + \rho \mathbf{f}, \tag{2.2}$$

$$\frac{p}{R} \frac{DE}{Dt} = \operatorname{div}[\kappa \operatorname{grad} T] + \mu[\tfrac{1}{2}(\operatorname{def} \mathbf{v}) : (\operatorname{def} \mathbf{v}) - \tfrac{2}{3}(\operatorname{div} \mathbf{v})^2] + Q, \tag{2.3}$$

where D/Dt is Stokes material derivative and def $\mathbf{v}$ is the rate of deformation tensor. (If the components of the velocity $\mathbf{v}$, referred to axes $Ox_1 x_2 x_3$, are v_1, v_2, v_3, then def $\mathbf{v}$ is the second order tensor whose ij-th component is $(\partial v_i/\partial x_j + \partial v_j/\partial x_i)$ and (def $\mathbf{v}$) : (def $\mathbf{v}$) denotes the double tensor product $\sum\sum (\partial v_i/\partial x_j + \partial v_j/\partial x_i)^2$.) In the equations, m denotes the rate of mass production (or injection) per unit volume, $\mathbf{f}$ denotes the body force per unit mass and Q denotes the rate of heat addition per unit volume.

The coefficients of viscosity μ and heat conduction κ are assumed to be known monotonic functions of the temperature, i.e. $\mu = \mu(T)$ and $\kappa = \kappa(T)$.

For a perfect gas, the variables p, ρ, T and E are related by the equations of state

$$p = \rho R T \tag{2.4}$$

or

$$E - E_r = C_v \log\left(\frac{p}{p_r}\right)\left(\frac{\rho_r}{\rho}\right)^{\gamma}, \tag{2.5}$$

where $\gamma = C_p/C_v$, C_p being the specific heat at constant pressure and C_v that at constant volume. The subscript r designates some standard reference state.

If m, $\mathbf{f}$, Q are known functions of x_i and t, the above five equations, together with the boundary conditions, are expected to be sufficient to determine the five unknowns p, ρ, T, E and $\mathbf{v}$. We shall be ultimately interested in the case $m = 0$, $\mathbf{f} = 0$, and $Q = 0$, but in the scheme of successive approximations the effect of the lower order terms on the higher

ones will be expressed most conveniently through these apparent 'external' forcing functions.

Let us consider a four-dimensional space-time domain G, the size of which is determined by several considerations discussed in the ensuing paragraphs. Let

$$V = \int\int d\boldsymbol{\xi} d\tau$$

denote the four-dimensional volume of G where $d\boldsymbol{\xi}$ stands for the volume element $d\xi_1\, d\xi_2\, d\xi_3$ and $d\tau$ for the element of time. We define the mean values of the pressure and entropy in G by

$$p_0 = \frac{1}{V}\int\int_G p(\boldsymbol{\xi}, \tau)\, d\boldsymbol{\xi} d\tau, \tag{2.6}$$

$$E_0 = \frac{1}{V}\int\int_G E(\boldsymbol{\xi}, \tau)\, d\boldsymbol{\xi} d\tau, \tag{2.7}$$

and define ρ_0, T_0, μ_0, κ_0 by the equations*

$$p_0 = \rho_0 R T_0, \tag{2.8}$$

$$E_0 = E_r + C_v \log\left(\frac{p_0}{p_r}\right)\left(\frac{\rho_r}{\rho_0}\right)^{\gamma}, \tag{2.9}$$

$$\mu_0 = \mu(T_0), \qquad \kappa_0 = \kappa(T_0). \tag{2.10}$$

Finally, the coordinate system is chosen so that

$$\mathbf{v}_0 = \frac{1}{V}\int\int_G \mathbf{v}(\boldsymbol{\xi}, \tau)\, d\xi d\tau = 0, \tag{2.11}$$

that is, the coordinate system moves with the mean velocity of the fluid.

It should be noted that the mean values p_0, E_0, etc., depend upon the size of the space-time domain G. Consequently the fluctuations $p - p_0$, $E - E_0$, etc., as well as the 'intensity' of the fluctuations, $(p - p_0)/p_0$, $(E - E_0)/E_0$, etc., also depend on the size of G. If we assume that p, E and all other flow variables are continuous functions of the space and time coordinates, then the 'intensity' of the fluctuations in G can be made arbitrarily small by limiting our consideration to a sufficiently small space-time domain G. Let α be a non-dimensional parameter characterizing the intensity of the disturbance. For example, we may take α as the maximum of $|p - p_0|/|p_0|$, $|v/a_0|$ etc., where a_0 is the velocity of sound of the mean state.

We now assume that in a sufficiently small space-time domain G, the pressure, density, temperature, entropy, p, ρ, T etc., can be expanded as power series in α. This is the first condition which limits the extent of the domain G. The actual size of G is determined by the values of the spatial and temporal gradients of the fluctuations relative to our coordinate system.

* Note that ρ_0, T_0, etc. are not defined in the same manner as p_0 and E_0 mainly to simplify the algebra. The ultimate physical conclusions are not affected by the manner in which ρ_0, etc. are defined.

For low speed turbulence Lin's (1953) analysis indicates that the ratio of the temporal gradients to the spatial gradients may be small (compared with the mean velocity), in fact of the order of the velocity fluctuations themselves. The domain G would then be elongated along the time axis as can also be suspected from equations (6.5). For very small fluctuations, such as during final period of decay of grid turbulence, G may be quite sizeable.

We write

$$p = p_0 + p^{(1)} + p^{(2)} + \ldots, \tag{2.12 a}$$

$$\rho = \rho_0 + \rho^{(1)} + \rho^{(2)} + \ldots, \tag{2.12 b}$$

where $p^{(1)}$, $\rho^{(1)}$ are of order α, and $p^{(n)}$, $\rho^{(n)}$ are of order α^n.

Substituting (2.12) into the fundamental system of equations (2.1) to (2.5) inclusive and collecting terms of the same order in α, we find

$$\frac{\partial \rho^{(n)}}{\partial t} + \rho_0 \nabla . \mathbf{v}^{(n)} = F_1^{(n)}, \tag{2.13 a}$$

$$\rho_0 \frac{\partial \mathbf{v}^{(n)}}{\partial t} + \nabla p^{(n)} - \mu_0 \nabla^2 \mathbf{v}^{(n)} - \tfrac{1}{3}\mu_0 \nabla(\nabla . \mathbf{v}^{(n)}) = \mathbf{F}_2^{(n)}, \tag{2.13 b}$$

$$\frac{p_0}{R} \frac{\partial E^{(n)}}{\partial t} - \kappa_0 \nabla^2 T^{(n)} = F_3^{(n)}, \tag{2.13 c}$$

$$\frac{p^{(n)}}{p_0} - \frac{\rho^{(n)}}{\rho_0} - \frac{T^{(n)}}{T_0} = F_4^{(n)}, \tag{2.13 d}$$

$$\frac{E^{(n)}}{R} - \frac{\gamma}{\gamma - 1} \frac{T^{(n)}}{T_0} + \frac{p^{(n)}}{p_0} = F_5^{(n)}. \tag{2.13 e}$$

The functions $F_i^{(n)}$ for $n > 1$ represent the non-linearity of the original equations. For $n = 1$,

$$F_1^{(1)} = m, \qquad \mathbf{F}_2^{(1)} = \rho \mathbf{f}, \qquad F_3^{(1)} = Q, \qquad F_4^{(1)} = 0, \qquad F_5^{(1)} = 0.$$

For $n > 1$, the $F^{(n)}$ depend only on the $p^{(k)}$, $\rho^{(k)}$, etc., where $k \leqq n-1$. For example, $F_1^{(2)} = -\nabla . [\rho^{(1)} \mathbf{v}^{(1)}]$. The principal advantage of the scheme presented here is that the differential equations are the same for all values of n, only the 'inhomogeneous terms' are different, and in the scheme of successive approximation these are computed from the solutions of the lower order equations.

It is convenient now to eliminate two of the four thermodynamic variables and introduce non-dimensional quantities for the remaining two. We write

$$P^{(n)} = \frac{p^{(n)}}{\gamma p_0}, \tag{2.14}$$

$$S^{(n)} = \frac{E^{(n)}}{C_\mu}. \tag{2.15}$$

The speed of sound of the undisturbed medium is $a_0^2 = \gamma p_0 / \rho_0$. We assume further that the Prandtl number $(\mu C_\mu / \kappa) = \frac{3}{4}$, the sole purpose of this being to simplify the algebra.

The governing equations now become

$$\nabla . \mathbf{v}^{(n)} + \frac{\partial P^{(n)}}{\partial t} - \frac{\partial S^{(n)}}{\partial t} = \frac{m^{(n)}}{\rho_0}, \tag{2.16 a}$$

$$\frac{\partial \mathbf{v}^{(n)}}{\partial t} + a_0^2 \nabla P^{(n)} - \nu_0 \nabla^2 \mathbf{v}^{(n)} - \tfrac{1}{3}\nu_0 \nabla(\nabla . \mathbf{v}^{(n)}) = \mathbf{f}^{(n)}, \tag{2.16 b}$$

$$\frac{\partial S^{(n)}}{\partial t} - \tfrac{4}{3}\nu_0 \nabla^2 S^{(n)} - \tfrac{4}{3}(\gamma - 1)\nu_0 \nabla^2 P^{(n)} = \frac{Q^{(n)}}{\rho_0 C_p T_0}, \tag{2.16 c}$$

where $\nu_0 = \mu_0/\rho_0$ denotes the kinematic viscosity of the undisturbed medium and

$$m^{(1)} = m, \qquad \mathbf{f}^{(1)} = \mathbf{f}, \qquad Q^{(1)} = Q.$$

The higher order $m^{(n)}$, $\mathbf{f}^{(n)}$, $Q^{(n)}$ are functions of the lower order solutions For the particular case $n = 2$, we find

$$\frac{m^{(2)}}{\rho_0} = -\nabla[(P^{(1)} - S^{(1)})\mathbf{v}^{(1)}] + \frac{1}{2}\frac{\partial}{\partial t}[(\gamma - 1)(P^{(1)})^2 + (S^{(1)})^2 + P^{(1)}S^{(1)}], \tag{2.17 a}$$

$$\mathbf{f}^{(2)} = -(P^{(1)} - S^{(1)})\frac{\partial \mathbf{v}^{(1)}}{\partial t} - (\mathbf{v}^{(1)} . \nabla)\mathbf{v}^{(1)} - \tfrac{3}{2}\nabla\left[\frac{\mu^{(1)}}{\rho_0}(\nabla . \mathbf{v}^{(1)})\right] + \nabla . \left[\frac{\mu^{(1)}}{\rho_0} \operatorname{def} \mathbf{v}^{(1)}\right], \tag{2.17 b}$$

$$\frac{Q^{(2)}}{\rho_0 C_p T_0} = -\gamma P^{(1)}\frac{\partial S^{(1)}}{\partial t} - (\mathbf{v}^{(1)} . \nabla)S^{(1)} + \tfrac{4}{3}\nabla . \left[\frac{\mu^{(1)}}{\rho_0}\nabla\{S^{(1)} + (\gamma - 1)P^{(1)}\}\right] + \frac{\nu_0}{C_p T_0}[\tfrac{1}{2}(\operatorname{def} \mathbf{v}^{(1)}) : (\operatorname{def} \mathbf{v}^{(1)}) - \tfrac{2}{3}(\nabla . \mathbf{v}^{(1)})^2] - \frac{2}{3}\frac{\gamma - 1}{\gamma}\nu_0 \nabla^2\left[\gamma(P^{(1)})^2 - 2\gamma P^{(1)}S^{(1)} - \frac{\gamma}{\gamma - 1}(S^{(1)})^2\right]. \tag{2.17 c}$$

In these equations, $\mu^{(1)}/\rho_0$ is a function of $P^{(1)}$ and $S^{(1)}$, for, by Taylor's expansion,

$$\mu(T) = \mu_0 + \left(\frac{d\mu}{dT}\right)_{T=T_0}(T - T_0) + \frac{1}{2!}\left(\frac{d^2\mu}{dT^2}\right)_{T=T_0}(T - T_0)^2 + \ldots$$

$$= \mu_0 + T^{(1)}\left(\frac{d\mu}{dT}\right)_{T=T_0} + \left[T^{(2)}\left(\frac{d\mu}{dT}\right)_{T=T_0} + \frac{(T^{(1)})^2}{2}\left(\frac{d^2\mu}{dT^2}\right)_{T=T_0}\right] + \ldots,$$

so that $\mu^{(1)} = T^{(1)}(d\mu/dT)_{T=T_0}$, $\mu^{(2)} = T^{(2)}(d\mu/dT)_{T=T_0} + \frac{1}{2}(T^{(1)})^2(d^2\mu/dT^2)_{T=T_0}$, etc. If we define $\mu_0' = (d\mu/dT)_{T=T_0}$, then

$$\frac{\mu^{(1)}}{\rho_0} = \frac{\mu_0'}{\rho_0}T^{(1)} = \frac{\mu_0'}{\mu_0}\nu_0 T_0[S^{(1)} + (\gamma - 1)P^{(1)}].$$

A considerable simplification follows from the fact that the systems of equations (2.16) are identical in form for all values of n. The 'source functions' $m^{(1)}$, $\mathbf{f}^{(1)}$, $Q^{(1)}$ correspond to the actual rate of fluid injection, body force and rate of heat addition, if any, while $m^{(2)}$, $\mathbf{f}^{(2)}$, $Q^{(2)}$ are calculated from the solution of the first-order equations and represent only *apparent* rates of mass, momentum, and heat injection. This concept allows us to

study the behaviour of the fluid motion governed by (2.1) to (2.5) in two steps. Firstly, we treat the system (2.16) as if $m^{(n)}$, $\mathbf{f}^{(n)}$, $Q^{(n)}$ were known and secondly, examine the structure of the quantities $m^{(n)}$, $\mathbf{f}^{(n)}$, $Q^{(n)}$.

3. The three basic modes of fluctuations and their production

In a sufficiently small space-time domain G the intensity of the fluctuations in the flow field can be made arbitrarily small and terms of order α^2 and higher powers of α in (2.12) may be neglected. We shall take $n = 1$ in equation (2.16), temporarily suppress the superscript (1), and obtain for the first-order fluctuations

$$\nabla . \mathbf{v} + \frac{\partial P}{\partial t} - \frac{\partial S}{\partial t} = \frac{m}{\rho_0}, \tag{3.1 a}$$

$$\frac{\partial \mathbf{v}}{\partial t} + a_0^2 \nabla P - \nu_0 \nabla^2 \mathbf{v} - \tfrac{1}{3}\nu_0 \nabla(\nabla . \mathbf{v}) = \mathbf{f}, \tag{3.1 b}$$

$$\frac{\partial S}{\partial t} - \tfrac{4}{3}\nu_0 \nabla S - \tfrac{1}{3}(\gamma - 1)\nu_0 \nabla^2 P = \frac{Q}{\rho_0 C_p T_0}. \tag{3.1 c}$$

We can describe the kinematic field by two new independent variables, the vorticity $\boldsymbol{\Omega}$ and the specific dilatation rate q (the rate of volume increase per unit volume of the fluid) where

$$\boldsymbol{\Omega} = \nabla \times \mathbf{v}, \qquad q = \nabla . \mathbf{v}. \tag{3.2}$$

Taking the curl and divergence of (3.1 b), we have

$$\frac{\partial \boldsymbol{\Omega}}{\partial t} - \nu_0 \nabla^2 \boldsymbol{\Omega} = \nabla \times \mathbf{f}, \tag{3.1 b}'$$

$$\frac{\partial q}{\partial t} - \tfrac{4}{3}\nu_0 \nabla^2 q = -a_0^2 \nabla^2 P + \nabla . \mathbf{f}. \tag{3.1 b}''$$

The two equations (3.1 b)′ and (3.1 b)″ are equivalent to (3.1 b), since once $\boldsymbol{\Omega}$ and q are known, the velocity field can be calculated from (3.2) and the appropriate boundary conditions.

By a slight manipulation as indicated below, the system of equations (3.1 a), (3.1 b)′, (3.1 b)″ and (3.1 c) can be further combined into the following four equations:

$$\frac{\partial \boldsymbol{\Omega}}{\partial t} - \nu_0 \nabla^2 \boldsymbol{\Omega} = \nabla \times \mathbf{f}, \tag{3.3 a}$$

$$\frac{1}{a_0^2}\frac{\partial^2 P}{\partial t^2} - \nabla^2 P - \frac{4\gamma}{3}\frac{\nu_0}{a_0^2}\frac{\partial}{\partial t}(\nabla^2 P) = \frac{1}{a_0^2}\left[\left(\frac{\partial}{\partial t} - \tfrac{4}{3}\nu_0 \nabla^2\right)\frac{m}{\rho_0} - \nabla . \mathbf{f} + \frac{\partial}{\partial t}\left(\frac{Q}{\rho_0 C_p T_0}\right)\right], \tag{3.3 b}$$

$$\frac{\partial S}{\partial t} - \tfrac{1}{3}\nu_0 \nabla^2 S = \tfrac{4}{3}(\gamma - 1)\nu_0 \nabla^2 P + \frac{Q}{\rho_0 C_p T_0}, \tag{3.3 c}$$

$$q = -\frac{\partial P}{\partial t} + \frac{\partial S}{\partial t} + \frac{m}{\rho_0}. \tag{3.3 d}$$

Equation (3.3 a) is the same as (3.1 b); (3.3 c) is the same as (3.1 c); (3.3 d) is obtained by substituting (3.2) into (3.1 a); (3.3 b) is obtained by eliminating S and q from (3.1 b)″, (3.3 d) and (3.3 c).

The system of equations (3.2) and (3.3) can be conveniently split into three sub-systems as follows. Let us write

$$\boldsymbol{\Omega} = \boldsymbol{\Omega}_\Omega + \boldsymbol{\Omega}_p + \boldsymbol{\Omega}_s, \tag{3.4a}$$

$$P = P_\Omega + P_p + P_s, \tag{3.4b}$$

etc.; then

$$\frac{\partial \boldsymbol{\Omega}_\Omega}{\partial t} - \nu_0 \nabla^2 \boldsymbol{\Omega}_\Omega = \nabla \times \mathbf{f}, \tag{3.5a}$$

$$P_\Omega = 0, \qquad S_\Omega = 0, \qquad q_\Omega = 0, \tag{3.5b}$$

$$\nabla \times \mathbf{v}_\Omega = \boldsymbol{\Omega}_\Omega, \qquad \nabla . \mathbf{v}_\Omega = 0; \tag{3.5c}$$

$$\boldsymbol{\Omega}_p = 0, \tag{3.6a}$$

$$\frac{\partial^2 P_p}{\partial t^2} - a_0^2 \nabla^2 P_p - \tfrac{4}{3}\gamma \nu_0 \frac{\partial}{\partial t} \nabla^2 P_p = \left(\frac{\partial}{\partial t} - \tfrac{4}{3}\nu_0 \nabla^2\right) \frac{m}{\rho_0} - \nabla . \mathbf{f} + \frac{\partial}{\partial t} \frac{Q}{\rho_0 C_p T_0}, \tag{3.6b}$$

$$\frac{\partial S_p}{\partial t} - \tfrac{4}{3}\nu_0 \nabla^2 S_p = \tfrac{4}{3}(\gamma - 1)\nu_0 \nabla^2 P_p, \tag{3.6c}$$

$$q_p = -\frac{\partial P_p}{\partial t} + \frac{\partial S_p}{\partial t} + \frac{m}{\rho_0}, \tag{3.6d}$$

$$\nabla \times \mathbf{v}_p = 0, \qquad \nabla . \mathbf{v}_p = q_p; \tag{3.6e}$$

$$\boldsymbol{\Omega}_s = 0, \qquad P_s = 0, \tag{3.7a}$$

$$\frac{\partial S_s}{\partial t} - \tfrac{4}{3}\nu_0 \nabla^2 S_s = \frac{Q}{\rho_0 C_p T_0}, \tag{3.7b}$$

$$q_s = \frac{\partial S_s}{\partial t}, \tag{3.7c}$$

$$\nabla \times \mathbf{v}_s = 0, \qquad \nabla . \mathbf{v}_s = q_s. \tag{3.7d}$$

Of course, there are infinitely many ways in which we can split up the equations (3.2) and (3.4)*. However, the above choice is a convenient one since (3.5), (3.6) and (3.7) each represent individually familiar phenomena.

Thus (3.5) is identical with the equations describing the production, convection and dissipation of weak vorticity fluctuations in a viscous *incompressible* medium and will be called the *vorticity mode*. Such a flow field does not generate pressure fluctuations of the same order, since the latter is proportional to the square of the velocity fluctuation and hence is negligible when the vorticity fluctuation is weak. For a similar reason, there is no production of entropy fluctuation, since viscous dissipation is again a second-order quantity. Finally, the velocity field is solenoidal as it should be for an incompressible flow.

* It is possible to decompose the sound mode further into two types of physically distinct fluid motion: (1) that due to mass sources in an incompressible medium which is characterized by $P_q = 0$, $S_q = 0$, $\nabla . \mathbf{v}_q = q_q = m/\rho_0$, $\boldsymbol{\Omega}_q = \nabla \times \mathbf{v}_q = 0$; and (2) that associated with the propagation of pressure waves in a compressible medium which is characterized by (3.6 a), (3.6 b), (3.6 c), (3.6 e) and $q_p = -\partial P_p/\partial t + \partial S_p/\partial t$.

Equation (3.6) is identical with the equations describing the production, propagation and absorption of pressure waves in a viscous compressible heat-conductive medium, and will be called the *sound mode*. As a result of absorption, there will be entropy changes accompanying the pressure fluctuations. These entropy changes are denoted by S_μ in (3.6). The velocity field is irrotational as is expected for a sound field.

Finally, (3.7) can be recognized as the equations describing the production, convection and diffusion of hot spots in a heat-conducting fluid medium and will be called the *entropy mode*. Such a diffusion phenomenon does not generate pressure fluctuations and produces only a weak irrotational velocity field, necessary for the conservation of mass while the density varies.

The vorticity mode is the type of fluid motion most frequently encountered in the mechanics of viscous incompressible fluid. The sound mode is the type of fluid motion discussed in acoustics and in the theory of compressible fluids. The entropy mode has been the main subject of investigation in the theory of heat transfer in fluids. We thus see that the solution of (3.1) can always be thought of as consisting of the superposition of three basic modes of fluctuations that are familiar in branches of fluid mechanics. Naturally, not all the three modes of fluctuations will enter significantly into a particular problem, for example, in turbulent heat transfer problems and high-speed shear flows, the fluctuations consist principally of the vorticity and entropy modes.

We now assume that the space-time domain G does not contain any solid boundaries (this is the second condition which limits the size of G). In such a case, each of the three modes of fluctuations evolves as though the others were absent. Should G contain some solid boundaries, the last conclusion is no longer true, since the boundary conditions are imposed upon the resultant flow variables, such as the velocity vector $\mathbf{v}$ or temperature T, and not separately upon the individual modes (see, for example, Trilling (1955)).

Decomposition of a small disturbance into different modes of fluctuations has been made previously by several authors, Carrier & Carlson (1946), Lagerstrom, Cole & Trilling (1949), Cole & Wu (1952), Wu (1952), Kovásznay (1953). The terminology and classification adopted here follows closely that of Kovásznay. The modes of fluctuations are re-defined here to include the influence of body forces, mass and heat sources. The fluid dynamic effects produced by these agents will be the subject of discussion in the next section.

When the space-time domain G is not sufficiently small the intensity of fluctuation is not small and terms of the order of second and higher powers of α in (2.12) must be retained. Since equation (2.16) has the same form for $n = 1$ as for $n > 1$, the flow field can still be thought of as consisting of the three basic modes of fluctuations. Since the apparent source terms $m^{(n)}$, $\mathbf{f}^{(n)}$, $Q^{(n)}$, in (2.16) are functions of the fluctuations $P^{(k)}$, $S^{(k)}$, $\mathbf{v}^{(k)}$ where $k < n$, the terms $P^{(n)}$, $S^{(n)}$, $\mathbf{v}^{(n)}$ may be interpreted as the pressure, entropy and velocity fluctuations generated by the nth-order interactions of the three

modes of fluctuations. Of all these interactions the most important are the bilateral interactions of the three modes which contribute to the values of $P^{(2)}$, $S^{(2)}$ and $\mathbf{v}^{(2)}$.

The entire analysis is partly motivated by the interest in compressible flow turbulence and like phenomena. In those cases the fluctuation levels in the entire space-time domain are of the order of a few per cent of the corresponding mean values. The theory described here is valid for interactions of any order provided the process converges in G. Its application to the bilateral interactions of the various modes of fluctuations will be given in § 5 and § 6.

4. Effects of mass addition, body forces and heat sources

(1) *Effects of mass addition*

From equations (3.5), (3.6) and (3.7), we see that the effect of mass addition is to produce the *sound mode*. Closer examination of (3.6) reveals that the effects of mass addition are really two-fold. When the fluid is injected into the medium at a point or a region, it displaces the fluid that was originally there. Generally, the movement of the displaced fluid in turn generates pressure waves which propagate into the surrounding medium. However, mass addition with a spatio-temporal pattern obeying the diffusion equation does not cause pressure fluctuation, see (3.6 b). It induces an incompressible source flow, see (3.6 d), with a velocity potential ϕ_p obeying a Poisson-type equation

$$\nabla^2\phi_p = \frac{m}{\rho_0}. \tag{4.1}$$

(2) *Effects of body force*

Referring to (3.5), (3.6) and (3.7), we conclude that the effects produced by body forces are two-fold. They generate the vorticity mode and the sound mode. If the force field is decomposed into two component fields, an irrotational and solenoidal field, the irrotational force component produces the sound mode (cf. (3.6 b)) and cannot produce the vorticity mode (cf. (3.5 a)). On the other hand, the solenoidal component produces the vorticity mode and cannot produce the sound mode. Consequently, a harmonic force field (which is both irrotational and solenoidal) can produce neither vorticity fluctuations nor pressure fluctuations. Its only effect is to produce a harmonic velocity field given by (see (3.1 b))

$$\frac{\partial \mathbf{v}_H}{\partial t} = \mathbf{f}_H. \tag{4.2}$$

(3) *Effects of heat addition*

From (3.5), (3.6) and (3.7), we see that addition of heat to a medium generates the entropy mode and the sound mode. Physically this is clear for heat addition to a gas produces two effects. Firstly, it increases the temperature of the gas (and hence the entropy) and, secondly, it causes an

expansion of the heated fluid element. The first action is a more localized one and is described by the entropy mode. On the other hand, the expansion of the volume occupied by the heated fluid produces in the surrounding medium pressure waves, much like those generated by the inflation of a solid body. The action produced by the expansion of the heated fluid is thus described by the sound mode.

At the end of the preceding section, we showed that the fluctuations $P^{(n)}$, $S^{(n)}$, $Q^{(n)}$ can be interpreted as being generated by an apparent mass addition $m^{(n)}$, body force $\mathbf{f}^{(n)}$ and heat sources $Q^{(n)}$, resulting from the nth-order interaction of the various modes of fluctuations. The effects produced in the flow field by a particular type of interaction will then depend upon the manner in which the particular interaction affects the value of $m^{(n)}$, $\mathbf{f}^{(n)}$, $Q^{(n)}$. When the particular interaction gives rise predominantly to a contribution to $m^{(n)}$, we shall describe the effects produced as 'mass-like effects', and we shall speak of the interactions as having a 'mass-like action'. Likewise, we can speak of 'force-like effects', 'heat-like effects' or 'force-like actions' and 'heat-like actions'. Thus, for example, the bilateral vorticity–vorticity interaction will be shown to produce mainly a force-like effect, and a slight heat-like effect. A systematic study of the effects produced by bilateral interactions of the various modes of fluctuations is presented in the next section.

5. Effects of bilateral interactions of the various modes of fluctuations

General considerations

In § 3 we saw that the first-order system can be considered as the sum of three basic modes of fluctuations. Their contributions to the thermodynamic and kinematic variables are, from (3.4), (3.5), (3.6) and (3.7),

$$\boldsymbol{\Omega}^{(1)} = \boldsymbol{\Omega}_{\Omega}^{(1)}, \qquad P^{(1)} = P_p^{(1)}, \qquad S^{(1)} = S_p^{(1)} + S_s^{(1)}, \tag{5.1a}$$

$$\mathbf{v}^{(1)} = \mathbf{v}_{\Omega}^{(1)} + \mathbf{v}_p^{(1)} + \mathbf{v}_s^{(1)}. \tag{5.1b}$$

Substitution of (5.1) into (2.17) leads to the following expressions for the second-order source functions in terms of the separate first-order mode contributions as indicated by the double subscripts. (For example, $\mathbf{f}_{\Omega p}$ represents the apparent body force produced by the vorticity–sound interaction.)

$$m^{(2)} = \rho_0[m_{\Omega\Omega} + m_{pp} + m_{ss} + m_{\Omega p} + m_{ps} + m_{s\Omega}], \tag{5.2a}$$

$$\mathbf{f}^{(2)} = \mathbf{f}_{\Omega\Omega} + \mathbf{f}_{pp} + \mathbf{f}_{ss} + \mathbf{f}_{\Omega p} + \mathbf{f}_{ps} + \mathbf{f}_{s\Omega}, \tag{5.2b}$$

$$Q^{(2)} = \rho_0 C_p T_0[Q_{\Omega\Omega} + Q_{pp} + Q_{ss} + Q_{\Omega p} + Q_{ps} + Q_{s\Omega}]. \tag{5.2c}$$

The 18 interaction terms can be computed from equations (2.17) and a brief examination leads us immediately to the conclusion that bilateral interactions of the three basic modes produce in general fluctuations in all three modes. In this case we have all 18 second-order interaction terms as indicated by Kovásznay (1953).

It is a natural question to ask whether all these 18 terms are equally important. Naturally such questions can be answered only if more is stated about initial conditions and boundary conditions. In a concrete flow field these are imposed by grids, coolers, fans, etc. One mode can often be neglected and this immediately reduces the number of interaction terms by one-half.

In the next section an order of magnitude estimate of the non-linear interactions will be carried out for an important special example still having sufficient generality to illustrate the nature of these second-order interactions.

6. Bilateral interactions of the three basic modes of fluctuations

Let us assume that the particular region of flow is far away from the boundaries and all three modes of fluctuations are present. Each mode of fluctuations can be pictured as a superposition of a large (or infinite) number of Fourier components. Typical components for each of the three modes of fluctuations have been discussed by Kovásznay (1953), or can be found directly from (3.5), (3.6) and (3.7) with m, $\mathbf{f}$ and Q put equal to zero. These are summarized below.

(1) *The vorticity mode*

The typical component of the vorticity fluctuation is given by

$$\boldsymbol{\Omega}^{(1)} = \boldsymbol{\Omega}_0^{(1)} \exp[i\mathbf{k}_\Omega . \mathbf{x} - \nu_0 k_\Omega^2 t], \tag{6.1 a}$$

where $\boldsymbol{\Omega}_0^{(1)} . \mathbf{k}_\Omega = 0$ and $\boldsymbol{\Omega}_0^{(1)}$ is the complex amplitude fluctuation. $\mathbf{k}_\Omega$ is the wave-number vector, t denotes time and $\mathbf{x}$ the position vector. The corresponding velocity fluctuation is

$$\mathbf{v}_\Omega^{(1)} = i \frac{\mathbf{k}_\Omega \times \boldsymbol{\Omega}_0^{(1)}}{k_\Omega^2} \exp[i\mathbf{k}_\Omega . \mathbf{x} - \nu_0 k_\Omega^2 t]. \tag{6.1 b}$$

(2) *The sound mode*

The typical component of the pressure fluctuation is given by

$$P^{(1)} = P_0^{(1)} \exp[i\mathbf{k}_p . \mathbf{x} - ct], \tag{6.2 a}$$

where $P_0^{(1)}$ is the complex amplitude; $\mathbf{k}_p$, the wave-number vector, and c is the complex number

$$c = a_0 k_p \left(\frac{2\gamma}{3} \frac{\nu_0 k_p}{a_0} - i \left\{ 1 - \frac{4\gamma^2}{9} \left(\frac{\nu_0 k_p}{a} \right)^2 \right\}^{1/2} \right). \tag{6.2 b}$$

The real part of c gives the rate of damping while the imaginary part gives the frequency of oscillation. Note that the absolute magnitude of c is of the order of $a_0 k_p$, since in general $(\nu_0 k_p / a_0) \ll 1$. (See also the paragraph following equation (6.4).) The entropy generated as a result of the dissipation of the pressure waves is given by

$$S_y^{(1)} = \frac{\frac{4}{3}(\gamma - 1)\nu_0 k_p^2}{c - \frac{4}{3}\nu_0 k_p} P_0^{(1)} \exp[i\mathbf{k}_p . \mathbf{x} - ct]. \tag{6.2 c}$$

The velocity fluctuation associated with the sound mode is

$$\mathbf{v}_p^{(1)} = \frac{ia_0^2 k_p}{c - \frac{4}{3}\nu_0 k_p} P_0^{(1)} \exp[i\mathbf{k}_p \cdot \mathbf{x} - ct]. \tag{6.2 d}$$

(3) *The entropy mode*

The typical component of the entropy fluctuation associated with the entropy mode is

$$S_s^{(1)} = S_{s0}^{(1)} \exp[i\mathbf{k}_s \cdot \mathbf{x} - \tfrac{4}{3}\nu_0 k_s^2 t], \tag{6.3 a}$$

where $S_{s0}^{(1)}$ is the complex amplitude and $\mathbf{k}_s$ is the wave-number vector. The corresponding velocity fluctuation is

$$\mathbf{v}_s^{(1)} = i\tfrac{4}{3}\nu_0 \mathbf{k}_s S_{s0}^{(1)} \exp[i\mathbf{k}_s \cdot \mathbf{x} - \tfrac{4}{3}\nu_0 k_s^2 t]. \tag{6.3 b}$$

(4) *Relative orders of magnitude*

We are now ready to estimate the relative importance of the various interaction terms. By inspecting (5.3), (5.4) and (5.5) from the point of view of substitution of periodic solutions given by (6.1), (6.2) and (6.3), we can assert the following facts:

(*a*) Fluctuations in each mode may be characterized by two quantities, namely, an amplitude and a length scale.

(*b*) The medium has an intrinsic length scale, namely ν_0/a_0.

(*c*) In the interaction formulae, differentiation with respect to space coordinates does occur but integration does not; consequently, the terms containing derivatives decrease monotonically with decreasing wave-numbers (with increasing length scales).

We shall discuss the more complicated case where all three fluctuation modes have amplitude and scales, respectively, of the same order of magnitude. If one of the amplitudes or one of the wave-numbers is smaller than the other two, this can only simplify matters and never complicate them.

Whenever a quantity is differentiated with respect to the space coordinates, factors of k and k^2, etc., will appear. We shall assume that all three characteristic wave-numbers are of the same order of magnitude, i.e. k_Ω/k, k_p/k, k_s/k are each of order one, where k is the largest among k_Ω, k_p and k_s.

The amplitudes of the fluctuations have been characterized by the non-dimensional parameter α. The length scale of the fluctuations will be characterized by another non-dimensional parameter ϵ, defined as the ratio of the intrinsic scale of the medium ν_0/a_0 to the length scale of the disturbances k, that is,

$$\epsilon = \nu_0 k/a_0. \tag{6.4}$$

Clearly ϵ can be regarded as the Knudsen number of the disturbances, when it is small the inertial effects will dominate over heat conduction and viscous effects. The magnitude of ϵ can be estimated for atmospheric

conditions for which $\nu_0 = 0{\cdot}15\,\mathrm{cm^2\,sec^{-1}}$ and $a_0 = 30\,000\,\mathrm{cm\,sec^{-1}}$. The intrinsic length (which is simply proportional to the mean free path of the gas) is $\nu_0/a_0 = 0{\cdot}5 \times 10^{-5}$ cm. Even in the extreme case when the characteristic wavelength of the disturbance is as small as 1 mm, $\epsilon = 3{\cdot}14 \times 10^{-4}$.

The typical bilateral interaction term is of the order of α^2 and we shall consistently neglect terms of order α^3 and higher. If, however, $\epsilon \ll 1$ as is usually the case and especially if $\epsilon < \alpha$ we shall find bilateral interaction terms that are of the order $\alpha^2\epsilon$. (These usually represent higher derivatives associated with viscous or heat conduction terms.) We propose to neglect these terms as they will be smaller than the third-order interaction terms. Furthermore, if $\epsilon \ll \alpha$ we may even neglect the viscous and heat conduction terms in the first-order problem and obtain the simplest set of equations

$$\frac{\partial \boldsymbol{\Omega}^{(0)}}{\partial t} = 0, \tag{6.5 a}$$

$$\frac{\partial S^{(0)}}{\partial t} = 0, \tag{6.5 b}$$

$$\frac{\partial^2 \boldsymbol{P}^{(0)}}{\partial t^2} - \alpha_0^2 \nabla^2 \boldsymbol{P}^{(0)} = 0. \tag{6.5 c}$$

The superscript (0) emphasizes the difference between these equations and (3.5 a), (3.6 b) and (3.7 b).

This set of equations was presented by Kovásznay (1953) and represents a consistent 'zero order approximation' for weak fluctuation fields when the time interval of observation is short. The space domain of validity may or may not be also small depending on whether or not α increases with increasing space domain. (In homogeneous turbulence α may approach a limit for increasing domain.)

Equation (6.5 a) represents a 'frozen pattern' of vorticity (or solenoidal velocity) and when it is applied to homogeneous turbulence in a wind tunnel it predicts an unchanged flow pattern carried by the mean flow velocity as suggested by Taylor's hypothesis. Experimental verification of the frozen pattern concept by space-time correlation has been carried out in low speed flow for grid turbulence (Favre *et al.* 1954) and also the outer portion of the turbulent boundary layer (Favre *et al.* 1957).

Equation (6.5 b) indicates a 'frozen pattern' behaviour for temperature spots and was similarly used for evaluating hot-wire measurements in low-speed turbulent temperature fields. Equation (6.5 c) represents the well-known equations of sound propagation of the pressure field.

Equations (6.5) represent the most modest approximation for predicting the temporal behaviour of the three modes. Their value in interpreting hot-wire measurements in a high-speed flow is equal to that of Taylor's hypothesis as used for interpreting hot-wire measurements in low-speed turbulent flows.

We shall consider the amplitudes of the three modes to have orders of magnitude when the velocity fluctuations in the sound mode are comparable

to the velocity fluctuations in the vorticity mode and when the temperature fluctuations in the sound mode are comparable to the temperature fluctuations in the entropy mode, i.e. $|v_p^{(1)}| \approx |v_\Omega^{(1)}|$, $|T_p^{(1)}| \approx |T_s^{(1)}|$.

Space and time derivatives can be estimated from (6.1), (6.2) and (6.3) as follows. By choosing the reference space scale as k^{-1} and the reference time scale as $(a_0 k)^{-1}$ all the non-dimensional space derivatives will have the same order of magnitude as the quantity which is differentiated (except for factors k_Ω/k, k_p/k, k_s/k that were assumed earlier to be of order unity).

The orders of magnitude of the non-dimensional time derivatives differ depending upon the 'hyperbolic' (sound) or 'parabolic' (vorticity and entropy) character of the mode. For the sound mode the non-dimensional time derivative is of the same order as the space derivative (since the speed of sound was used as the reference velocity for forming non-dimensional quantities). For the vorticity and entropy modes, however, the non-dimensional time derivatives have order of magnitude $(k_\Omega/k)^2\epsilon$ or $(k_s/k)^2\epsilon$ times the quantities that differentiated. Indeed, differentiation of (6.1) with respect to t produces a factor $\nu_0 k_\Omega^2$ and non-dimensionalization of t by $(a_0 k)^{-1}$ results in the factor $(\nu_0 k_\Omega^2)/(a_0 k) = (k_\Omega/k)^2\epsilon$. Physically, this is clear for the rate of decay of the parabolic modes is an extremely slow process when their length scale is very large compared to the mean free path and when time is measured in units of the period of sound oscillation.

The above estimate for the order of magnitudes* of the various quantities associated with the sound mode can be summarized as follows:

$$\left.\begin{aligned} P^{(1)},\ \frac{v_p^{(1)}}{a_0},\ \frac{T_p^{(1)}}{T_0} &= O(\alpha), \qquad S_p^{(1)} = O\left(\frac{k_p}{k}\alpha\epsilon\right), \\ \frac{\partial P^{(1)}}{\partial x_i},\ \frac{\partial P^{(1)}}{\partial t},\ \frac{1}{a_0}\frac{\partial \mathbf{v}_p^{(1)}}{\partial x_i},\ \frac{1}{a_0}\frac{\partial v_p^{(1)}}{\partial t},\ \frac{1}{T_0}\frac{\partial T_p^{(1)}}{\partial x_i},\ &\frac{1}{T_0}\frac{\partial T_p^{(1)}}{\partial t} = O\left(\frac{k_p}{k^2}\alpha\right), \\ \frac{\partial S_p^{(1)}}{\partial x_i},\ &\frac{\partial S_p^{(1)}}{\partial t} = O\left(\frac{k_p^2}{k^2}\alpha\epsilon\right). \end{aligned}\right\} \tag{6.6}$$

According to our basic assumption in this section, the intensity of the vorticity mode must be such that $v_\Omega^{(1)}/a_0 = O(v_p^{(1)}/a_0) = O(\alpha)$. The order of the vorticity properly non-dimensionalized is then $\Omega^{(1)}/a_0 k_\Omega = O(\alpha)$.

The estimates concerning the vorticity mode can also be summarized simply as follows:

$$\left.\begin{aligned} \frac{\Omega^{(1)}}{a_0 k_\Omega} &= O\left(\frac{k_\Omega}{k}\alpha\right), & \frac{v_\Omega^{(1)}}{a_0} &= O(\alpha), \\ \frac{1}{a_0 k}\frac{\partial \boldsymbol{\Omega}_\Omega^{(1)}}{\partial x_i} &= O\left(\frac{k_\Omega^2}{k^2}\alpha\right), & \frac{1}{a_0}\frac{\partial \mathbf{v}_\Omega^{(1)}}{\partial x_i} &= O\left(\frac{k_\Omega}{k}\alpha\right), \\ \frac{1}{a_0 k}\frac{\partial \boldsymbol{\Omega}_\Omega^{(1)}}{\partial t} &= O\left(\frac{k_\Omega^3}{k^3}\alpha\epsilon\right), & \frac{1}{a_0}\frac{\partial \mathbf{v}_\Omega^{(1)}}{\partial t} &= O\left(\frac{k_\Omega^2}{k^2}\alpha\epsilon\right). \end{aligned}\right\} \tag{6.7}$$

* The terms k_p/k, etc., are retained to facilitate arguments in the sub-cases where one of the wave-numbers k_p, k_Ω and k_s is small.

Finally, in accordance with the basic assumption, the temperature fluctuation associated with the entropy mode must be $T_s^{(1)}/T_0 = O(T_p^{(1)}/T_0) = O(\alpha)$. Now from (2.18) and (3.7 a), $T_s^{(1)}/T_0 = S_s^{(1)}$. It follows that $S_s^{(1)} = O(\alpha)$, and from (6.3 b), we find

$$\frac{v_s^{(1)}}{a_0} = O\left(\frac{k_s}{k}\alpha\epsilon\right).$$

Consequently, the velocity associated with the entropy mode is usually a very small quantity. This is also clear from (3.7 c) and (3.7 d). Evidently this velocity is induced as a result of the diffusion of entropy spots, which is a rather slow process when time is measured in units of the period of sound oscillation of a comparable spatial scale.

The estimates for the order of magnitude of the various quantities associated with the entropy mode are now summarized*:

$$\left.\begin{aligned} S_s^{(1)},\ \frac{T_s^{(1)}}{T_0} &= O(\alpha), & \frac{v_s^{(1)}}{a_0} &= O\left(\frac{k_s}{k}\alpha\epsilon\right),\\ \frac{\partial S_s^{(1)}}{\partial x_i},\ \frac{1}{T_0}\frac{\partial T_s^{(1)}}{\partial x_i} &= O\left(\frac{k_s}{k}\alpha\epsilon\right), & \frac{1}{a_0}\frac{\partial \mathbf{v}_s^{(1)}}{\partial x_i} &= O\left(\frac{k_s^2}{k^2}\epsilon\alpha\right),\\ \frac{\partial S_s^{(1)}}{\partial t},\ \frac{1}{T_0}\frac{\partial T_s^{(1)}}{\partial t} &= O\left(\frac{k_s^2}{k^2}\alpha\epsilon\right), & \frac{1}{a_0}\frac{\partial \mathbf{v}_s^{(1)}}{\partial t} &= O\left(\frac{k_s^3}{k^3}\epsilon^2\alpha\right). \end{aligned}\right\} \tag{6.8}$$

By substituting the mode contributions in equations (2.17) the significant bilateral source terms can be readily obtained. Since only bilateral interactions of the first-order solutions are computed here we shall drop the superscript (1) in all subsequent equations. The bilateral source terms are

$$m_{\Omega\Omega} = 0, \tag{6.9 a}$$

$$m_{pp} = -\nabla.(P_p\,\mathbf{v}_p) + \frac{\gamma-1}{2}\frac{\partial}{\partial t}P_p^2 + O(\epsilon\alpha^2), \tag{6.9 b}$$

$$m_{ss} = O(\epsilon\alpha^2), \tag{6.9 c}$$

$$m_{\Omega p} = -\nabla.(P_p\,\mathbf{v}_\Omega) + O(\epsilon\alpha^2), \tag{6.9 d}$$

$$m_{ps} = \nabla.(S_s\,\mathbf{v}_p) + S_s\frac{\partial P_p}{\partial t} + O(\epsilon\alpha^2), \tag{6.9 e}$$

$$m_{s\Omega} = \nabla.(S_s\,\mathbf{v}_\Omega) + O(\epsilon\alpha^2); \tag{6.9 f}$$

$$\mathbf{f}_{\Omega\Omega} = -(\mathbf{v}_\Omega.\nabla)\mathbf{v}_\Omega, \tag{6.10 a}$$

$$\mathbf{f}_{pp} = -P_p\frac{\partial \mathbf{v}_p}{\partial t} - \tfrac{1}{2}\nabla(v_p^2) + O(\epsilon\alpha^2), \tag{6.10 b}$$

$$\mathbf{f}_{ss} = O(\epsilon\alpha^2), \tag{6.10 c}$$

$$\mathbf{f}_{p\Omega} = -[\nabla(\mathbf{v}_p.\mathbf{v}_\Omega) - \mathbf{v}_p\times\boldsymbol{\Omega}_\Omega] + O(\epsilon\alpha^2), \tag{6.10 d}$$

$$\mathbf{f}_{ps} = S_s\frac{\partial \mathbf{v}_p}{\partial t} + O(\epsilon\alpha^2), \tag{6.10 e}$$

$$\mathbf{f}_{s\Omega} = O(\epsilon\alpha^2). \tag{6.10 f}$$

* Here we assume that the quantity $\mu_0' T_0$ is of the same order of magnitude as μ_0. This is indeed the case for air if Sutherland's formula for viscosity is used, $(\mu_0'/\mu_0)T_0 = 1{\cdot}5 - T_0/(T_0+C)$ where $\mu_0' = (d\mu/dT)_{T=T_0}$ and $C = 140°$ K.

Finally, (5.5) can be simplified to

$$Q_{\Omega\Omega}, Q_{pp}, Q_{ss}, Q_{\Omega p} = O(\epsilon\alpha^2), \tag{6.11a}$$

$$Q_{ps} = -(\mathbf{v}_p.\nabla)S_s + O(\epsilon\alpha^2), \tag{6.11b}$$

$$Q_{s\Omega} = -(\mathbf{v}_\Omega.\nabla)S_s + O(\epsilon\alpha^2). \tag{6.11c}$$

The various types of interactions can now be described in greater detail.

Vorticity–vorticity interactions

According to (6.9a), (6.10a) and (6.11a) the bilateral vorticity–vorticity interaction produces mainly a force-like effect. In addition, there is a slight heat-like effect (of order ϵ smaller). The apparent body force is $-(\mathbf{v}_\Omega.\nabla)\mathbf{v}_\Omega$ or, in tensor notation,

$$[f_{\Omega\Omega}]_i = -v_{\Omega j}\frac{\partial}{\partial z_j}v_{\Omega i} = -\frac{\partial}{\partial x_j}[v_{\Omega i}v_{\Omega j}].$$

Since this force field is in general neither solenoidal nor irrotational, it generates both the vorticity mode and sound mode. The production of the vorticity fluctuation is of fundamental importance in the mechanics of turbulent motion. The production of sound by vorticity–vorticity interaction has been analysed in a general fashion by Lighthill (1952). Our result with regard to sound generation could have been anticipated from Lighthill's theory. However, speaking in terms of body force instead of stresses, this analysis brings out more clearly the fact that the solenoidal component of the force field plays no part in sound generation but is of basic importance in the energy transfer between different size eddies in the turbulent fluctuation field.

Sound–sound interaction

According to (6.9b), (6.10b) and (6.11a), bilateral interactions of sound modes produce primarily the mass-like and force-like effects. In addition there is a slight heat-like effect indicating that only weak entropy fluctuations are generated by sound–sound interactions. A typical example of sound–sound interaction is the 'steepening' of the finite amplitude compressive waves and it is well known that the deviation from the isentropic change through even a moderately weak shock wave is proportional only to the third power of the shock strength. This particular conclusion also suggests that the sound–sound interaction may lead to only a slight production of the vorticity fluctuations. From (6.10b), we have

$$\mathbf{f}_{pp} = -P\frac{\partial\mathbf{v}_p}{\partial t} - \tfrac{1}{2}\nabla v_p^2 + O(\epsilon\alpha^2).$$

Furthermore, the velocity induced by pressure waves propagating in a viscous compressible medium satisfies the equation

$$\frac{\partial\mathbf{v}_p}{\partial t} = -a_0^2\nabla P + {}_3\nu_0\nabla^2\mathbf{v}_p,$$

so that $\mathbf{f}_{pp}$ can be rewritten as

$$\mathbf{f}_{pp} = -\tfrac{1}{2}\nabla[a_0^2P^2 + v_p^2] + O(\epsilon\alpha^2).$$

Consequently, $\mathbf{f}_{pp}$ is principally an irrotational vector field, so that sound–sound interaction does produce only a slight vorticity fluctuation. There is, therefore, little possibility of altering the intensity of turbulent fluctuation in high speed flow through the random interaction of the pressure waves and, possibly, weak shock waves. We thus see that the main effect of sound–sound interaction is the production of the sound mode itself.

The net strength of the sound source, according to (3.3 b), (6.9 b), (6.10 b) and (6.11 a), is

$$\left(\frac{\partial}{\partial t} - \tfrac{4}{3}\nu_0\nabla^2\right)m_{pp} - \nabla.\mathbf{f}_{pp} + \frac{\partial Q_{pp}}{\partial t} = \nabla.[\mathbf{v}_p(\nabla.\mathbf{v}_p) + (\mathbf{v}_p.\nabla)\mathbf{v}_p + a_0^2\nabla(P_p^2)] + \\ + \frac{\gamma-1}{2}\frac{\partial^2}{\partial t^2}P_p^2 + O(\epsilon\alpha^2),$$

where use has been made of (3.6 d) and (3.6 e) (with $m = 0$). In tensor notation, the last result can be written simply as

$$\frac{\partial^2}{\partial x_i \partial x_j}(v_{pi}v_{pj} + a_0^2 P_p^2\delta_{ij}) + \frac{\gamma-1}{2}\frac{\partial^2}{\partial t^2}P_p^2 + O(\epsilon\alpha^2),$$

or alternatively

$$\frac{\partial^2}{\partial x_i \partial x_j}\left[v_{pi}v_{pj} + \frac{\gamma+1}{2}a_0^2 P_p^2\delta_{ij}\right] + (\gamma-1)\left[\left(\frac{\partial P_p}{\partial t}\right)^2 - a_0^2(\nabla P_p)^2\right] + O(\epsilon\alpha^2).$$

Assuming that the flow fluctuations at infinity are zero, the distribution of source strength, when integrated over the entire flow field, in general yields a resultant strength different from zero indicating that there is a net generation besides self-scattering. (A discussion of self-scattering was given by Westervelt (1957).)

Entropy–entropy interaction

Our analysis clearly shows that the entropy–entropy interaction, though a theoretical possibility, is practically insignificant. From (6.9 c), (6.10 c) and (6.11 a), it is seen that it produces only a slight mass-like and a slight heat-like effect (both of order of $\epsilon\alpha^2$), and an even smaller force-like effect (of order $\epsilon^2\alpha^2$).

Vorticity–sound interaction

According to (6.9 d), (6.10 d) and (6.11 a), the vorticity–sound interaction produces a mass-like and force-like effect. It has only a slight heat-like effect and hence produces only very slight entropy fluctuations (i.e. of order of $\epsilon\alpha^2$).

Since the force field in general is not an irrotational field, there will be vorticity production as a result of interaction. The source strength in the production of vorticity fluctuations is $\nabla\times(\mathbf{v}_p\times\boldsymbol{\Omega}_\Omega)$. This term includes the effect of both the stretching and expansion of vortex tubes and the convection of vorticity under the action of sound fluctuation. In the case

when a single shock wave is interacting with the turbulent flow, the theoretical calculation of Ribner (1954), which was explored experimentally by Kovásznay (1955), indicates that the effect is not very large, at least in that particular problem.

The vorticity–sound interaction also produces the sound mode. The resultant strength of the sound source as given by (3.7) can be simplified to

$$\left(\frac{\partial}{\partial t} - \tfrac{4}{3}\nu_0\nabla^2\right)m_{\Omega p} - \nabla.\,\mathbf{f}_{\Omega p} + \frac{\partial Q_{\Omega p}}{\partial t} = 2\nabla.\,[(\mathbf{v}_\Omega.\nabla)\mathbf{v}_p] + O(\epsilon\alpha^2).$$

In the last step of the derivation, use has been made of the relation

$$\frac{\partial P_p}{\partial t} = -\nabla.\,\mathbf{v}_p + O(\epsilon\alpha).$$

In tensor notation, the resultant source strength of the sound mode is simply $2\,\partial^2(\mathbf{v}_{\Omega i}\mathbf{v}_{pj})/\partial x_i\partial x_j$, a result which could have been anticipated from Lighthill's quadrupole radiation theory. Assuming that the flow fluctuations die down fast enough at infinity, integration of the source strength over the entire flow field yields no net contributions. Consequently, the sound mode produced by vorticity–sound interaction can be interpreted as the scattering of the incident sound wave by the vorticity fluctuations. Scattering of a shock wave by turbulent fluctuations has also been calculated by Ribner (1954).

Sound–entropy interaction

By (6.9 e), (6.10 e) and (6.11 b), the interaction of the sound and entropy modes produce all three basic modes of fluctuations.

Let us first examine the vorticity mode produced by the interaction. According to (3.3 a) and (6.10 e), the source term which produces vorticity fluctuation is

$$\nabla\times\left[S_s\frac{\partial\mathbf{v}_p}{\partial t}\right] + O(\epsilon\alpha^2) = \nabla S_s\times\frac{\partial\mathbf{v}_p}{\partial t} + O(\epsilon\alpha^2) = -a_0^2\nabla S_s\times\nabla P_p.$$

This is a familiar term in the theory of rotational flow. Physically, the vorticity produced by it can be interpreted as the consequence of the fact that the resultant force acting on any lump of fluid fails to pass through the centre of mass, and thus produces a torque and an angular acceleration. This result suggests that the action of pressure field on a stream carrying randomly distributed temperature spots in a turbulent stream may generate turbulent fluctuations and can modify the original turbulent fluctuations in the stream. In the only known experimental realization of this situation (spottily heated air accelerating through the nozzle of a supersonic wind-tunnel) the effect appeared unimportant (see Morkovin 1956, p. 8).

Next consider the sound mode generated by the interaction. The net sound source can be calculated from (3.6 b) and can readily be simplified to

$$\left(\frac{\partial}{\partial t} - \tfrac{4}{3}\mathbf{v}_0\nabla^2\right)m_{ps} - \nabla.\,\mathbf{f}_{ps} + \frac{\partial Q_{ps}}{\partial t} = -\nabla.\left[\frac{\partial}{\partial t}(s_s\,\mathbf{v}_p)\right] + O(\epsilon\alpha).$$

If the disturbance dies down at infinity fast enough, the resultant source strength integrated over the entire flow field is zero, so that the phenomenon can again be interpreted as the scattering of the incident sound wave by the entropy spots.

Finally, consider the generation of the entropy spottiness by the interaction. It follows from (3.7 b) and (6.11 b) that the source of entropy fluctuation is given by the term $-(\mathbf{v}_p \,.\, \nabla)S_s$. It can be regarded as a convection of heat by the motion of the sound field.

Special cases of generation of all three fluctuation modes in the interaction between an entropy disturbance and an infinite or wedge-attached shock wave were discussed theoretically by Chang (1955).

Entropy–vorticity interaction

According to (6.9 f), (6.10 f) and (6.11 c), the entropy–vorticity interaction produces a mass-like and a heat-like effect as well as a slight force-like effect. Consequently, this type of interaction can only produce a very weak (of

	Sound source	Vorticity source	Entropy source
Sound–sound	' steepening ' and ' self-scattering ' $\frac{\partial^2(v_{pi}\,v_{pj})}{\partial x_i\,\partial x_j} + a_0^2\,\nabla^2(P_p^2) + \frac{\gamma-1}{2}\,\frac{\partial}{\partial t^2}\,P_p^2$	$O(\alpha^2\epsilon)$	$O(\alpha^2\epsilon)$
Vorticity–vorticity	' generation ' $\frac{\partial^2(v_{\Omega i}\,v_{\Omega j})}{\partial x_i\,\partial x_j}$	' self-convection ' $-v_{\Omega j}\,\frac{\partial \Omega_i}{\partial x_j} + \Omega_j\,\frac{\partial v_{\Omega i}}{\partial x_j}$	$O(\alpha^2\epsilon)$
Entropy–entropy	$O(\alpha^2\epsilon)$	$O(\alpha^2\epsilon^2)$	$O(\alpha^2\epsilon)$
Sound–vorticity	' scattering ' $2\,\frac{\partial^2(v_{\Omega i}\,v_{pj})}{\partial x_i\,\partial x_j}$	' vorticity convection ' $-v_{pj}\,\frac{\partial \Omega_i}{\partial x_j} + \Omega_j\,\frac{\partial v_{pi}}{\partial x_j} - \Omega_i\,\frac{\partial v_{pj}}{\partial x_j}$	$O(\alpha^2\epsilon)$
Sound–entropy	' scattering ' $\frac{\partial^2}{\partial t\,\partial x_i}\,(S_s\,v_{pi})$	' generation ' $-\alpha_0^2(\nabla S_s)\times(\nabla P_p)$	' heat convection ' $-v_{pi}\,\frac{\partial S_s}{\partial x_i}$
Vorticity–entropy	$O(\alpha^2\epsilon)$	$O(\alpha^2\epsilon)$	' heat convection ' $-v_{\Omega i}\,\frac{\partial S_s}{\partial x_i}$

Table 1. Second-order non-linear interaction between modes of order α.

order $\epsilon\alpha^2$) vorticity fluctuation. The sound field produced turns out to be weak also because the expansion generated by the apparent mass addition is exactly balanced by the contraction following heat subtraction. This can best be seen if we calculate the net source strength for the sound mode produced. From (6.9 f) and (6.11 c), one concludes that

$$\left(\frac{\partial}{\partial t} - \tfrac{4}{3}\nu_0\nabla^2\right)m_{s\Omega} - \nabla.\mathbf{f}_{s\Omega} + \frac{\partial Q_{s\Omega}}{\partial t} = \frac{\partial}{\partial t}\nabla.[\mathbf{v}_\Omega S_s] - \frac{\partial}{\partial t}(\mathbf{v}_\Omega.\nabla)S_s + O(\epsilon\alpha^2)$$
$$= O(\epsilon\alpha^2),$$

since $\nabla.\mathbf{v}_\Omega = 0$. Consequently, the main effects of entropy–vorticity interaction are in the production of the entropy mode. This mode is generated as a result of the convection of the hot spots by velocity fluctuation associated with the vorticity mode. This type of interaction has a leading role in turbulent heat transfer phenomena, see Corrsin (1952).

In order to summarize all second-order effects table 1 was prepared. It gives the source strength for all three modes up to order α^2. Terms of order $\alpha^2\epsilon$ and $\alpha^2\epsilon^2$ are only indicated. Table 1 includes also a more or less intuitive label for each bilateral interaction, like 'generation' or 'scattering'. These are not intended as accurate descriptions but are merely to suggest the corresponding physical processes.

The authors are greatly indebted to Dr Mark V. Morkovin for his constructive criticism during the entire course of this work. The work was supported financially by several government sponsoring agencies: Office of Scientific Research, Contract AF 18(600)–1121; Squid Project, Contract N6ori–105–T.O. III; Navy Bureau of Ordnance, Contract Nord 15872.

References

Carrier, G. F. & Carlson, F. D. 1946 *Quart. Appl. Math.* **4,** 1–12.

Chang, C. T. 1955 Thesis, Johns Hopkins University, ASTIA Document no. AD–95–263.

Cole, J. D. & Wu, T. Y. T. 1952 *Proceedings, Heat Transfer and Fluid Mechanics Institute*, 139–158.

Corrsin, S. 1952 *J. Appl. Phys.* **23,** 113–118.

Favre, A. J., Gaviglio, J. J. & Dumas, R. 1954 *La Rech. Aéro.* **40,** 7–14.

Favre, A. J., Gaviglio, J. J. & Dumas, R. 1957 *J. Fluid Mech.* **2,** 313–342.

Kovásznay, L. S. G. 1953 *J. Aero. Sci.* **20,** 657–674.

Kovásznay, L. S. G. 1955 *Proceedings, Heat Transfer and Fluid Mechanics Institute.*

Lagerstrom, P. A., Cole, J. D. & Trilling, L. 1949 California Institute of Technology, Contract Rep. ONR, Contract N6onr Task Order VIII.

Lighthill, M. J. 1952 *Proc. Roy. Soc.* A, **211,** 564–587.

Lin, C. C. 1953 *Quart. Appl. Math.* **10,** 295–306.

Morkovin, M. V. 1956 Johns Hopkins University Rep., AFORS TN–56–540, ASTIA Document no. AD–110–359.

Ribner, H. S. 1954 *Nat. Adv. Comm. Aero., Wash., Tech. Note* no. 3255.

Trilling, L. 1955 *J. Acoust. Soc. Amer.* **27,** 425–431.

Westervelt, P. J. 1957 *J. Acoust. Soc. Amer.* **29,** 199–203.

Wu, T. Y. T. 1952 Thesis, California Institute of Technology.

A model of supersonic flow past blunt axisymmetric bodies, with application to Chester's solution

By M. D. VAN DYKE

National Advisory Committee for Aeronautics, Ames Aeronautical Laboratory, Moffett Field, California

(*Received* 2 *September* 1957)

SUMMARY

A simple approximate model is set forth for the flow field between the nose of a blunt body of revolution and its detached shock wave. The model tends to explain the poor convergence of Chester's solution, which is based on an improvement of the Newtonian approximation. It suggests a modification of his series for the body shape which appears to improve its convergence considerably.

1. INTRODUCTION

Chester (1956) and Freeman (1956) have recently advanced in this journal an ingenious attack on the problem of supersonic flow past a blunt body. (See also Lighthill 1957, § 3.5 *et seq.*) Their point of departure is the 'Newtonian-plus-centrifugal' solution, which becomes exact as the free-stream Mach number M approaches infinity and the adiabatic index γ approaches unity. After modifying this basic solution to be valid near the body, Chester and Freeman improve upon it by successive approximations, the key to their success being the adoption of von Mises' transformation, in which the stream function is taken as one of the independent variables. The result of Chester (who has carried the approximation several steps further than Freeman for a perfect gas with constant specific heats) is a double series expansion in $\delta = (\gamma-1)/(\gamma+1)$ and M^{-2}.

Unfortunately, the series for the flow variables of interest appear to converge poorly and, surprisingly, less well for axisymmetric than plane flow. For example, for axisymmetric flow of a perfect gas with $\gamma = 7/5$ at $M = \infty$ past whatever body it is that supports a parabolic detached shock wave, Chester's series for the stand-off distance Δ of the shock wave, in terms of its nose radius R_s, is

$$\Delta/R_s = \tfrac{1}{6}(1 - 0{\cdot}6667 + 0{\cdot}4333 - 0{\cdot}3062 + \ldots). \qquad (1)$$

Although the expansion parameter δ is here only 1/6, this series converges so slowly as to be of little practical value. (Chester has used his series only out to $\delta = 1/10$, and then attempted to extrapolate to such 'large' values as 1/6.)

The question naturally arises whether this discouraging behaviour is symptomatic of some basic defect in the approximation, or simply indicates

that the series has an unduly small radius of convergence (if it in fact converges). The present note aims to suggest that the latter is the case, and that by appeal to a simple approximate model of the flow field the series for the shape of the body can be recast in a form that appears to converge much more rapidly.

2. A simple model of the flow field

Consider axisymmetric flow of a perfect gas with constant γ behind a prescribed shock wave. For simplicity we take the shock wave to be a parabola (which is the only case considered in detail by Chester), but other shapes could be treated similarly. According to the Cauchy–Kowalewski theorem, the flow field is analytic in some region downstream of the shock wave, and there is no reason to doubt that this region extends to the surface of the body. One can therefore attempt to expand the flow field in Taylor series starting from the shock wave. It is convenient to work with Stokes's stream function ψ and parabolic coordinates (ξ, η) which are normalized such that the shock wave is described by $\eta = 1$.

On the downstream face of the shock wave, the stream function has the free-stream value, its first derivatives are given by the Rankine–Hugoniot shock relations, and its second derivatives can be found by substituting into the equations of motion. The present model consists of the resulting first three terms of the Taylor expansion starting from the shock wave:

$$\frac{\psi}{\xi^2} = \frac{1}{2} - \frac{(\gamma+1)M^2}{A}(1-\eta) + \left[2\left(\frac{M^2-1}{A}\right)^2 + \frac{(\gamma-1)M^2-2(2+M^2)}{2A} + \right.$$
$$+ 2\frac{M^2+1}{A^2}\xi^2 + \frac{4(\gamma+1)M^4\xi^2}{(M^2-1-\xi^2)A^2} + 2(\gamma-1)M^4\xi^2 \times$$
$$\left. \times \frac{2\gamma M^2-(\gamma-1)(1+\xi^2)}{(1+\xi^2)A^3}\right](1-\eta)^2, \quad (2\,\text{a})$$

where
$$A = 2(1+\xi^2)+(\gamma-1)M^2. \quad (2\,\text{b})$$

Even this approximation is rather unwieldy, but at $M = \infty$ it simplifies to

$$\frac{\psi}{\xi^2} = \frac{1}{2} - \frac{\gamma+1}{\gamma-1}(1-\eta) + \left[\frac{3-\gamma}{(\gamma-1)^2} + \frac{1}{2} + \frac{4\gamma}{(\gamma-1)^2}\frac{\xi^2}{1+\xi^2}\right](1-\eta)^2. \quad (3)$$

In the Newtonian limit, $\gamma \to 1$ (and $\eta \to 1$), this reduces further to

$$\frac{\psi}{\xi^2} \sim \frac{1}{2}\left(1-2\frac{1-\eta}{\gamma-1}\right)^2 + 4\frac{\xi^2}{1+\xi^2}\left(\frac{1-\eta}{\gamma-1}\right)^2. \quad (4)$$

On the axis ($\xi = 0$) the point at which this last expression vanishes (corresponding to the nose of the body) lies at $(1-\eta) = \frac{1}{2}(\gamma-1)$, which is just the result of the first approximation of Chester and Freeman. It is mainly this attribute that qualifies the model as a useful one. Off the axis (4) cannot vanish, which suggests that the model will prove less faithful away from the nose of the body.

It should be remarked that the idea of expanding the flow field in Taylor series from an assumed shock wave is by no means new, but has been followed by a number of workers with uniformly poor results. The innovations in the present model are, first, that the natural coordinates associated with the shock wave are employed, and, second, that the Taylor series is terminated with the parabolic approximation to the stream function; and both of these are essential. Previous investigators, of whom the most assiduous has been Cabannes (1951, 1956), all carried out double Taylor series expansions in Cartesian coordinates. Aside from the inferiority of a double series to the present single expansion, this yields series whose first few terms approach the true result much more slowly than the present series in parabolic coordinates. This is illustrated in figure 1 for a parabolic shock wave at $M = 2$ (with $\gamma = 7/5$), for which Cabannes (1956) has computed seven terms of the double Taylor series.

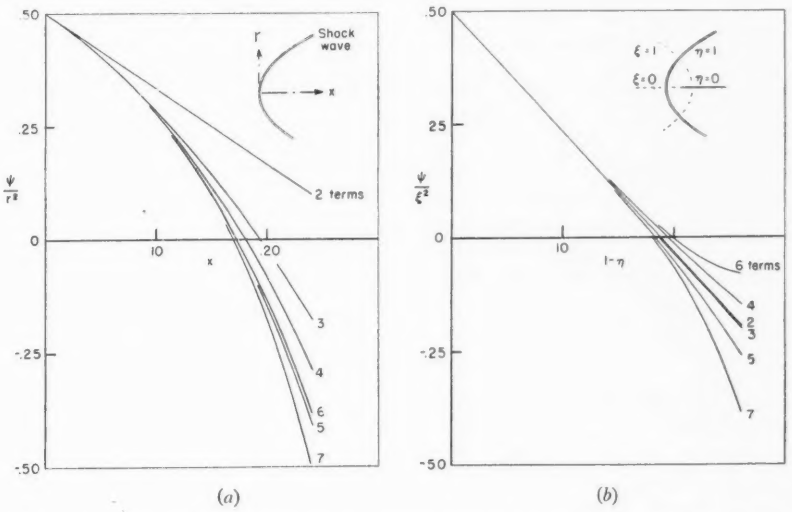

Figure 1. Taylor series expansions for stream function on axis of symmetry behind parabolic shock wave at $M = 2, \gamma = 7/5$. (*a*) Cartesian coordinates; (*b*) Parabolic coordinates.

Figure 1 (*b*) also illustrates the second point that, even in the natural coordinates, adding further terms to the Taylor series worsens rather than improves the approximation. The reason for this is that analytical continuation of the flow field upstream through the detached shock wave leads to a limiting line, or envelope of characteristics, as sketched in figure 2. The continued flow field has a square-root behaviour there. Since the Taylor series represents this analytical continuation, the limiting line determines its radius of convergence. On the axis, the limiting line is about as far ahead of the shock wave as the body is behind it, so that the convergence is

marginal; and in the example of figure 1 it is actually closer, so that the series diverges at the body. (The divergence can be ameliorated by applying the transformation of Shanks (1955).) Off the axis the limiting line is even closer, relative to the distance of the body, so that the convergence deteriorates further.

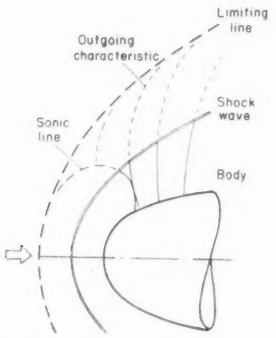

Figure 2. Schematic diagram showing analytical continuation of flow upstream through shock wave.

Poor convergence, or even divergence, is not a fatal flaw, however; though it is for this reason that the truncated series is regarded as a model rather than a systematic approximation. The variation of the stream function is actually very nearly parabolic, so that (somewhat as with asymptotic series) the first three terms of the Taylor series provide a close approximation near the axis.

3. Application to Chester's solution

3.1. *Body shape at infinite Mach number*

Consider first the case of infinite Mach number. Requiring the model stream function (3) to vanish determines the body according to

$$(1-\eta)_{\text{model}} = \frac{\delta}{1+[3\delta(1-\delta)-2(1-\delta^2)\xi^2/(1+\xi^2)]^{1/2}}, \tag{5}$$

where $\delta = (\gamma-1)/(\gamma+1)$. For comparison with Chester's solution, we transform to cylindrical polar coordinates in which the shock wave is described by $x = \frac{1}{2}r^2$, which means that $x = \frac{1}{2}(1+\xi^2-\eta^2)$ and $r = \xi\eta$, and then expand for small δ. Then (with fractions unreduced to facilitate comparison) the body is described by

$$x_{\text{model}} = \delta\left[1-\sqrt{(9\delta/3)}+\frac{25}{10}\delta-\frac{252}{168}\delta\sqrt{(9\delta/3)}+\ldots\right]+$$
$$+\frac{1}{2}r^2\left[1+\frac{2}{3}\sqrt{(9\delta/3)}-2\delta+5\delta\sqrt{(9\delta/3)}-\right.$$
$$\left.-23\delta^2+\frac{343}{12}\delta^2\sqrt{(9\delta/3)}+\ldots\right], \tag{6}$$

whereas Chester's result, of which the leading term was first given by Hayes (1955), is

$$x = \delta\left[1 - \sqrt{(8\delta/3)} + \frac{26}{10}\delta - \frac{463}{168}\delta\sqrt{(8\delta/3)} + \ldots\right] + \\ + \frac{1}{2}r^2\left[1 + \frac{19}{6}\delta - \frac{47}{15}\delta\sqrt{(8\delta/3)} + \frac{11173}{840}\delta^2 - \right. \\ \left. - \frac{2593}{126}\delta^2\sqrt{(8\delta/3)} + \ldots\right]. \quad (7)$$

The agreement is remarkable for the terms independent of r, though (as anticipated) less satisfactory for those in r^2. The model series converges for δ smaller than 3/9, which suggests that Chester's series will converge for δ less than 3/8, corresponding to γ less than 11/5, a value not attained in reality. However, the convergence of both model and prototype is unsatisfactory at $\delta = 1/6$, corresponding to $\gamma = 7/5$. In the model the poor convergence results from expansion of $[1+(3\delta)^{1/2}]^{-1}$ by the binomial theorem, which suggests that the convergence of Chester's series might be considerably accelerated by recasting it as a series for $(1-\eta)^{-1}$. Doing so yields on the axis ($\xi = 0$)

$$(1-\eta)^{-1} = \delta^{-1}\left[1 + \sqrt{(8\delta/3)} - \frac{13}{30}\delta + \frac{187}{840}\delta\sqrt{(8\delta/3)} + \ldots\right]. \quad (8\,a)$$

For $\delta = 1/6$ this gives

$$(1-\eta)^{-1} = 6(1 + 0{\cdot}6667 - 0{\cdot}0722 + 0{\cdot}0247 + \ldots), \quad (8\,b)$$

which appears to be a great improvement over the result of the original series for the related quantity Δ/R_s given in equation (1).

3.2. *Body shape at high Mach number*

Consider now Chester's general case of high Mach number. For simplicity, we restrict the model to the axis, where it is most faithful. Then from (2a) it locates the nose of the body at

$$(1-\eta)_{\text{model}} = [2+(\gamma-1)M^2][(\gamma+1)M^2 + \{6(\gamma-1)M^4 + \\ + 2(\gamma+5)M^2 + 4\}^{1/2}]^{-1}. \quad (9\,a)$$

In terms of Chester's parameters

$$\delta = (\gamma-1)/(\gamma+1), \qquad d = \delta + M^{-2},$$

this is

$$(1-\eta)_{\text{model}} = (\delta + M^{-2} - M^{-2}\delta)\{1 + [(1-\delta)(3\delta + 4M^{-4} - 3M^{-4}\delta)]^{1/2}\}^{-1} \quad (9\,b)$$

or

$$(1-\eta)_{\text{model}} = d(1 - M^{-2} + M^{-4}/d)\{1 + [(1-d+M^{-2})(3d - 3M^{-2} + \\ + 4M^{-4} - 3M^{-4}d + 3M^{-6}]^{1/2}\}^{-1}. \quad (9\,c)$$

Now the last form can be expanded in a series containing only positive powers of $d^{1/2}$ and M^{-2}, as in Chester's solution, only under the assumption that $M^{-2} = O(d^2)$, though Chester assumes merely that $M^{-2} < d$. This minor discrepancy probably indicates a certain lack of fidelity in the present

model. To play safe, however, we shall treat Chester's solution only under the additional assumption that $M^{-2} = O(d^2)$. For $\gamma = 7/5$, this restricts M to values greater than perhaps 4 or 5.

As before, the model suggests recasting Chester's series as an approximation for $(1-\eta)^{-1}$. The result, including now terms in ξ^2, is

$$1-\eta = d\left[1+\sqrt{\left(\frac{8d}{3}\right)}-\frac{13}{30}d+\frac{187}{840}d\sqrt{\left(\frac{8d}{3}\right)}-\ldots\right]^{-1}\times$$
$$\times\left[1+\xi^2\left\{\frac{7}{12}+\frac{1}{60}\sqrt{\left(\frac{8d}{3}\right)}-\frac{299}{1008}d+\frac{M^{-2}}{3d}-\right.\right.$$
$$\left.\left.-\frac{27269}{50400}d\sqrt{\left(\frac{8d}{3}\right)}+\ldots\right\}\right]. \quad (10)$$

(Note that on the axis the solution to this degree of approximation does not depend upon M explicitly, but only in so far as it appears in d.) The apparent convergence of the terms in ξ^2, though again not as rapid as that of the terms independent of ξ, is a great improvement over that of the original series, and probably adequate for practical purposes.

For $\gamma = 7/5$, this modified series (10) leads to ratios of stand-off distance Δ, initial shock-wave radius R_s, and body nose radius R_b, which are compared in table 1 with the results of the model.

M		1·25	1·5	2	3	4	5	6	8	10	∞
$\frac{\Delta}{R_s}$	eqn.(10)	·2815	·2405	·1890	·1429	·1242	·1150	·1098	·1046	·1021	·0976
	model	·2443	·2109	·1693	·1323	·1174	·1100	·1059	·1017	·0997	·0962
$\frac{R_b}{R_s}$	eqn.(10)	·2783	·3608	·4766	·5934	·6450	·6715	·6868	·7025	·7101	·7238
	model	·3080	·3966	·5033	·6014	·6407	·6594	·6695	·6796	·6842	·6923
$\frac{\Delta}{R_b}$	eqn.(10)	1·0112	·6667	·3966	·2408	·1926	·1713	·1599	·1489	·1438	·1349
	model	·7932	·5317	·3364	·2200	·1832	·1668	·1582	·1496	·1458	·1389

Table 1.

For $M = \infty$ an accurate numerical solution of the full equations has been found as the first part of a current programme of calculating the flow field behind a family of detached shock waves. The results are $\Delta/R_s = 0{\cdot}0988$ $R_b/R_s = 0{\cdot}726$, and $\Delta/R_b = 0{\cdot}1360$. Hence the modified series predicts the ratio of stand-off distance to body radius to within a fraction of 1%, and even the model is only 2% off at $M = \infty$. The numerical solution also indicates that the axisymmetric body that supports a parabolic shock wave at $M = \infty$ is itself almost exactly parabolic (whereas in plane flow it is exceedingly close to circular).

The tabulated values of stand-off distance are compared in figure 3 with a number of measurements on spheres in air under conditions such that the adiabatic exponent is close to 7/5. Schlieren photographs show that

for spheres flying at Mach numbers between 2 and 7 the detached shock wave is nearly parabolic over the region that determines the stand-off distance, so that the comparison is justified. At lower Mach numbers the shock wave on a sphere departs significantly from a parabola, and the assumptions of Chester's theory have also been greatly exceeded, so that the agreement shown in figure 3 is undoubtedly coincidental. (No values are shown for Chester's original series, since it converges so poorly that he did not himself suggest using it at $\gamma = 7/5$.)

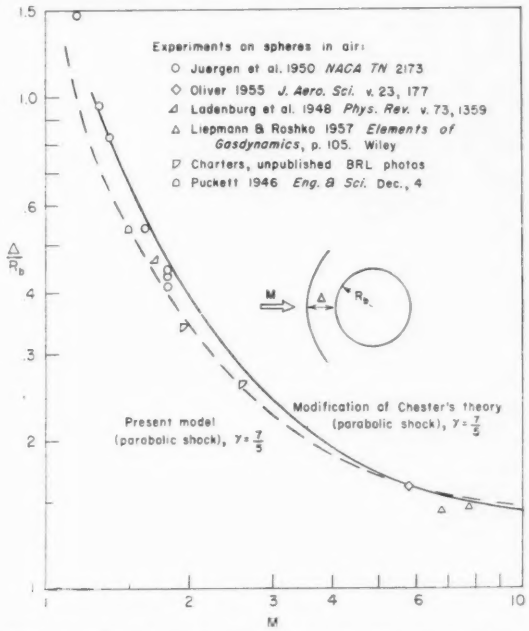

Figure 3. Stand-off distance of shock wave from sphere.

3.3. *Pressure distribution*

Chester's series for the pressure at the surface of the body also suffers from poor convergence (except at the stagnation point). Thus at $M = \infty$ it gives, in units of $\rho_0 V^2$

$$p = \left(1 - \frac{1}{2}\delta + \frac{1}{8}\delta^2\right) - r^2\left[\frac{4}{3} + \frac{253}{63}\delta - \frac{32}{9}\delta\sqrt{(8\delta/3)} + \frac{2\,505\,007}{13\,860}\delta^2\right]. \quad (11)$$

The corresponding result for the model stream function is found, using the Bernoulli equation and the condition of constant entropy along streamlines, to be

$$p = \left(1 - \frac{1}{2}\delta + \frac{1}{8}\delta^2\right) - r^2\left[\frac{3}{2} + \frac{27}{4}\delta - 9\delta\sqrt{(9\delta/3)} + \frac{747}{16}\delta^2\right]. \quad (12)$$

The agreement is fair. In particular, the model confirms that the last coefficient is enormous, though Chester's is still greater by a factor of four.

Unfortunately, the model does not in this case lead to a useful modification of Chester's solution. It actually suggests that his series should be used to calculate the quantity $\eta^4\rho^2(u^2+v^2)$, and that the pressure then be found from the Bernoulli and entropy relations; but working back from Chester's solution for p gives a series for that quantity whose convergence is not appreciably improved.

In the case of plane flow, the convergence of Chester's series is nearly adequate. It would nevertheless be of interest to construct a model, if only to explain the source of the logarithmic terms. (Successively higher powers of logarithms in perturbation series may be the asymptotic representation of Bessel functions, inverse hyperbolic functions, small fractional powers, etc.). However, the author has been unable to devise a useful model, or otherwise to discover an appropriate transformation of the series.

References

Cabannes, H. 1951 Détermination théorique de l'écoulement d'un fluide derrière une onde de choc détachée, *O.N.E.R.A., Note technique* no. 5.

Cabannes, H. 1956 Tables pour la détermination des ondes de choc détachées, *La Rech. Aéro.*, no. 49.

Chester, W. 1956 Supersonic flow past a bluff body with a detached shock, *J. Fluid Mech.* **1**, 353 and 490.

Freeman, N. C. 1956 On the theory of hypersonic flow past plane and axially symmetric bluff bodies, *J. Fluid Mech.* **1**, 366.

Hayes, W. D. 1955 Some aspects of hypersonic flow, Ramo-Wooldridge Corp., Los Angeles, unpublished paper.

Lighthill, M. J. 1957 Dynamics of a dissociating gas, Part I, Equilibrium flow, *J. Fluid Mech.* **2**, 1.

Shanks, D. 1955 Non-linear transformations of divergent and slowly convergent sequences, *J. Math. Phys.* **34**, 1.

The effect of a vertical lapse rate of temperature on the spiral flow of a fluid in a heated rotating cylinder

By G. N. LANCE
Computation Laboratory, University of Southampton

(*Received* 8 *October* 1957)

SUMMARY

Experiments have been performed with a viscous fluid contained in a rotating cylinder heated from below. Previous theoretical explanations of the flow patterns obtained in these experiments assumed that the convective terms in the heat transfer equation were negligible. The present paper gives a treatment which includes one of these convective terms. The results confirm the physical reasoning that, when the lapse rate is positive, the stability is increased and that the motion is therefore decreased.

1. INTRODUCTION

Many experiments have been performed with a fluid in a rotating dish-pan which is heated from below. The case of a shallow fluid has been covered very fully by Fultz (1951, 1956). Several authors have put forward theories which attempt to explain the results. Davies (1953) used a theory which neglected convective terms in the heat transfer equation, whereas Kuo (1954, 1955, 1956) included both horizontal and vertical temperature gradients, but both these theories needed, for their success, the assumption of a shallow fluid.

Experiments with deep fluids have been described by Fultz (1956). Skeib (1953) performed experiments with a value of a, which is effectively a depth parameter (see § 3), very nearly equal to unity. Unity is the value of a which is used, in this paper, to obtain the curves shown in figures 1–3. Davies's theory was extended to cover larger depths by Lance & Deland (1955) but they neglected the convective terms in the heat transfer equation (in the present paper this reference will be referred to as I).

In the dish-pan experiments the fluid was heated near the circumference of the base of the dish-pan and cooled near the axis of rotation. All the theories so far put forward have used the method of small perturbations, the perturbations being superimposed on a steady state of rotation without heating and at constant basic pressure, density and temperature. Previous theories, with the exception of Kuo's (1954), have assumed that the vertical temperature lapse rate was zero but the experimental results have shown that in fact the temperature varies in a manner which is very nearly a linear function of height. The purpose of the present paper is to determine the effect of this vertical lapse rate and to see whether the flow patterns previously given in I are greatly altered by the lapse rate.

2. The equations of motion

The notation used here is the same as that employed in I, where the equations of motion were presented in full. If it is assumed that the motion is axially symmetric and that a steady state has been reached, then the equations can be written, using cylindrical polar coordinates (r, θ, z), in the following form:

$$\rho_1\left(\frac{Du_1}{Dt}-\frac{v_1^2}{r}\right) = -\frac{\partial p_1}{\partial r}+\mu\left(\nabla^2 u_1-\frac{u_1}{r^2}\right)+\tfrac{1}{3}\mu\frac{\partial \psi_1}{\partial r}, \tag{1}$$

$$\rho_1\left(\frac{Dv_1}{Dt}+\frac{u_1 v_1}{r}\right) = \mu\left(\nabla^2 v_1-\frac{v_1}{r^2}\right), \tag{2}$$

$$\rho_1\frac{Dw_1}{Dt} = -\frac{\partial p_1}{\partial z}-g\rho_1+\mu\nabla^2 w_1+\tfrac{1}{3}\mu\frac{\partial \psi_1}{\partial z}, \tag{3}$$

$$\frac{D\rho_1}{Dt} = -\rho_1\psi_1, \tag{4}$$

$$\rho_1 = \rho_0-\alpha(T_1-T_0), \tag{5}$$

$$\rho_1 J c_v\frac{DT_1}{Dt} = Jk\nabla^2 T_1+\Phi_1+p_1\psi_1. \tag{6}$$

In the above six equations, u_1, v_1, w_1 are the components of fluid velocity in the directions of r, θ and z increasing, respectively, relative to an axis system fixed in space with the origin at the centre of the base of the dish-pan. The pressure is denoted by p_1 and the density by ρ_1; μ is the coefficient of viscosity, α is the reciprocal of the coefficient of cubical expansion, J is the mechanical equivalent of heat, c_v is the specific heat at constant volume, k is the thermometric conductivity and Φ_1 is the viscous dissipation function. Also,

$$\frac{D}{Dt} \equiv u_1\frac{\partial}{\partial r}+w_1\frac{\partial}{\partial z}, \qquad \nabla^2 \equiv \frac{\partial^2}{\partial r^2}+\frac{1}{r}\frac{\partial}{\partial r}+\frac{\partial^2}{\partial z^2},$$

and

$$\psi_1 \equiv \frac{\partial u_1}{\partial r}+\frac{u_1}{r}+\frac{\partial w_1}{\partial z}.$$

When the liquid is not heated, rotation of the cylinder causes solid rotation of the fluid and, if heat is supplied, the departures from the state of solid rotation will be small. Thus, if Ω is the angular velocity of the cylinder, we write

$$\left.\begin{aligned} u_1 = u, \qquad v_1 = \Omega r+v, \qquad w_1 = w, \qquad \rho_1 = \rho_0+\rho, \\ p_1 = p_0+p, \qquad T_1 = T_0+T. \end{aligned}\right\} \tag{7}$$

The symbols without suffixes are the six perturbation quantities which determine the departure from the state of solid rotation. It was shown in I that, if attention is confined to slow rates of rotation (as in the experiments), the upper surface of the liquid is approximately the horizontal plane $z = h$, where h is the depth of the fluid.

When the expressions (7) are substituted into (1) to (6), the following equations are obtained for the perturbation variables:

$$-2\Omega\rho_0 v = -\partial p/\partial r+\mu(\nabla^2 u-u/r^2), \tag{8}$$

$$+2\Omega\rho_0 u = \mu(\nabla^2 v-v/r^2), \tag{9}$$

$$-\partial p/\partial z - g\rho + \mu\nabla^2 w = 0, \tag{10}$$

$$r\psi_1 \equiv \partial(ru)/\partial r + \partial(rw)/\partial z = 0, \tag{11}$$

$$\rho = -\alpha T, \tag{12}$$

$$\nabla^2 T = (\rho c_v/k)DT/Dt, \tag{13}$$

where all non-linear terms have been neglected. Now, for the purposes of the present paper, it is assumed that $\partial T_0/\partial z \equiv \Theta = \text{const.}$, so that (13) reduces to

$$\nabla^2 T = (\rho c_v/k)\Theta w, \tag{14}$$

the work of I simply took $\Theta = 0$.

The term containing $\partial T_0/\partial r$ has been omitted and there is, in fact, no real justification for such an omission; however, it does enable the variables r and z to be separated and in this way the equations can be reduced to ordinary differential equations (see (17) to (20) below). Moreover, such a procedure has the advantage that the effect of only one advection term may be obtained and their relative importance may be determined. Finally, if the density is eliminated from (10) and (12) it is found that

$$-\partial p/\partial z + g\alpha T + \mu\nabla^2 w = 0. \tag{15}$$

3. Reduction of the equations to a system of ordinary differential equations

It was shown in I that the variables r and z can be separated by the substitutions

$$\left.\begin{aligned} T(r,z) &= T_1(z)J_0(\beta r), \\ u(r,z) &= U_1(z)J_1(\beta r), \\ v(r,z) &= V_1(z)J_1(\beta r), \\ w(r,z) &= W_1(z)J_0(\beta r), \\ p(r,z) &= P_1(z)J_0(\beta r), \\ \rho(r,z) &= \Pi(z)J_0(\beta r), \end{aligned}\right\} \tag{16}$$

where βr_0 is a zero of $J_1(\beta r_0) = 0$ and r_0 is the radius of the dish-pan.

It is only possible to retain the vertical lapse rate in (14) because the r variation of both T and w is of the form $J_0(\beta r)$. If the form were not the same for both these variables the r coordinate would not cancel from this equation and the system of partial differential equations could not be reduced to a system of ordinary differential equations. As in I, all the quantities may be written in non-dimensional form and the pressure can be eliminated from (8) and (10). The final system of equations is

$$U''' - a^2U' + 2RV' + aW'' - a^3W + aT = 0, \tag{17}$$

$$V'' = 2RU + a^2V, \tag{18}$$

$$W' = -aU, \tag{19}$$

$$T'' - a^2T = (h^2\sigma\Theta/\nu)W \equiv AW, \tag{20}$$

where σ is the Prandtl number, ν is the kinematic viscosity, $a = \beta h$ and R is the rotational Reynolds number $\Omega h^2/\nu$; the dashes denote differentiation with respect to ξ $(= z/h)$.

The boundary conditions are the same as those used in I, since they do not depend on Θ, namely

$$\left.\begin{aligned} U(0) = V(0) = W(0) = 0, \qquad T'(0) = 1, \\ U'(1) = V'(1) = W(1) = T'(1) = 0. \end{aligned}\right\} \tag{21}$$

4. Method of solution

Despite the fact that the system of differential equations (17) to (20) is a linear one, it is not practical to solve them without recourse to numerical methods. A numerical method was also employed in I but, since then, a better method for the solution of a system of linear differential equations subject to two-point boundary conditions has been described by Goodman & Lance (1956). The improved method was used for the present computations and found to be very satisfactory. The calculations were performed on a Ferranti Pegasus digital computer.

Numerical values are required for a, R and $A = (h^2\sigma\Theta/\nu)$. The value of a was taken to be unity. This implies a depth of liquid of about 4 cm in a dish-pan with a radius of 15 cm. Since $\beta r_0 = 3{\cdot}83$ and $a = \beta h$, $h = r_0/3{\cdot}83$ and so, under the conditions of the experiment, for which $r_0 = 15$ cm, $\sigma \doteqdot 7$ for water at a temperature of 15° C, $\nu \doteqdot 0{\cdot}01$ and $\Theta \doteqdot 1$, it follows that $A \doteqdot 10\,737$. In the calculations the Reynolds number R was taken to be 0 (no rotation), 2, 4, 8, 16, 32 and 64.

5. Results and conclusions

Radial velocity component

Figure 1 shows the curves $U(\xi) \times 10^4$ against ξ, for $a = 1$ and $A = 10\,737$. The curves shown are for $R = 0$, 16, 32 and 64. The results for $R = 2$, 4 and 8 were computed, but they are omitted because they lie between those of $R = 0$ and $R = 16$. This figure is to be compared with figure 2 *a* of I, which shows the curves when the lapse rate is zero, i.e. $A = 0$.

The following differences may be noted.

(i) In figure 1, $U \times 10^4$ is plotted, whereas in the corresponding figure of I, $U \times 10^3$ is shown. Hence, there is a considerable drop in the magnitude of the radial velocity component.

(ii) In the present case, for each value of R there is a zero of U when $\xi < 0{\cdot}5$; previously, the zero occurred when $\xi > 0{\cdot}5$.

(iii) For small R the greatest inflow ($U < 0$) is slightly *below* the surface when $A \neq 0$, whereas when $A = 0$, the maximum inflow is *at* the surface. For large R there is a band, for which $0{\cdot}25 < \xi < 0{\cdot}75$, of comparatively slow inflow, but when $\xi > 0{\cdot}75$ the inflow increases and reaches a maximum at the surface.

(iv) In the case of $R = 64$ the radial motion tends to be concentrated in the upper and lower regions of the fluid. Such a behaviour was not apparent in the results of I.

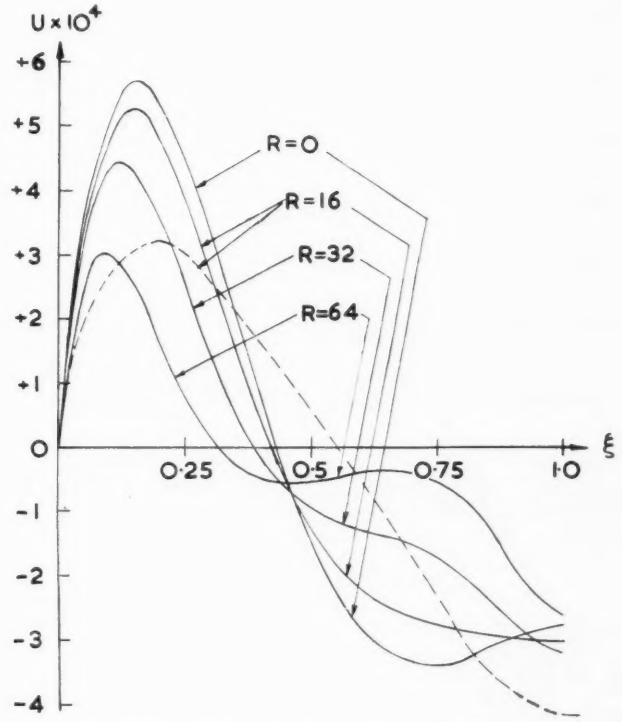

Figure 1. Non-dimensional radial velocity profile plotted against non-dimensional height. Cases for which $A = 10\,737$ are shown as solid lines. The broken curve is $A = 0$, $R = 16$ and is the value of $U \times 10^3$.

Zonal velocity component

Figure 2 shows the curves $V(\xi) \times 10^4$ against ξ, for $a = 1$ and $A = 10\,737$. The curves shown, for $R = 0$, 2, 4, 8, 16, 32 and 64, may be compared with those of figure 3 *a* in I. The following points are notable.

(i) As in the case of $U(\xi)$ there is a reduction in magnitude by a factor of 10.

(ii) The band of easterlies is confined to $\xi < 0{\cdot}2$ when $A = 10\,737$.

(iii) The maximum zonal velocity at the surface continues to increase as R increases, whereas when $A = 0$ the zonal velocity reached a maximum value when $R \doteq 16$. (This is only true for $R \leqslant 64$, which was the limit to which the calculations were taken.)

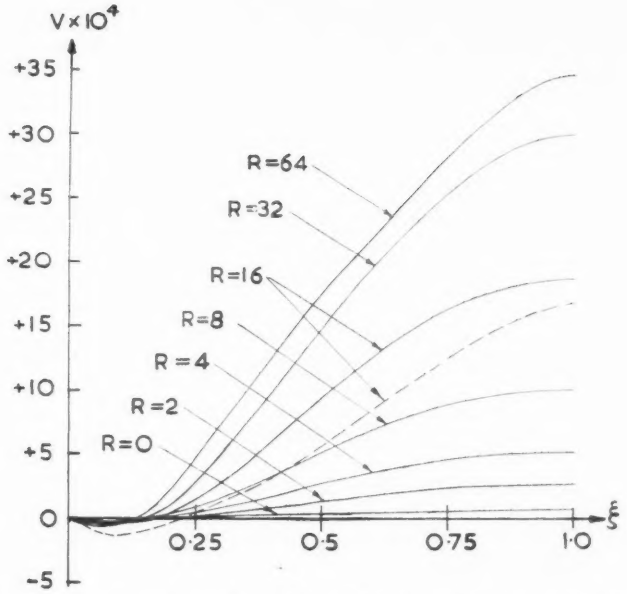

Figure 2. Non-dimensional zonal velocity profile plotted against non-dimensional height. Cases for which $A = 10\,737$ are shown as solid lines. The broken curve is $A = 0$, $R = 16$ and is the value of $V \times 10^3$.

Vertical velocity component

Figure 3 shows the curves $-W(\xi) \times 10^5$ against ξ for $a = 1$ and $A = 10\,737$. The curves for $R = 0$, 16, 32 and 64 are shown, the remainder are omitted for simplicity. The case $A = 0$ is figure 4*a* of I, and the following are the differences between the two cases.

(i) The scale factor is 10^5 in the present case as opposed to 10^3 in the case of $A = 0$.

(ii) The curve $R = 64$ shows a distinct flattening in the range $0{\cdot}25 < \xi < 0{\cdot}75$, when $A = 10\,737$, which implies that w is tending to a constant value at intermediate depths.

(iii) For each value of R the maximum vertical velocity is below $\xi = 0{\cdot}5$ when $A = 10\,737$, but when $A = 0$ the maximum is in each case above $\xi = 0{\cdot}5$.

The results, when looked at *in toto*, show that when a positive vertical lapse rate is present, the whole velocity field is reduced in magnitude. This result agrees with physical reasoning because, if the upper layers of the fluid are the warmest, then greater stability would be expected and consequently less motion.

Since the results obtained here are an order of magnitude smaller than those obtained previously it should be noted that on all the diagrams the comparison curves, which are taken from Lance & Deland, are shown dotted and are plotted to a different scale. Enough has been said in the above remarks, about the results, to make the differences apparent and the interested reader is referred to Lance & Deland for complete diagrams of the case $A = 0$.

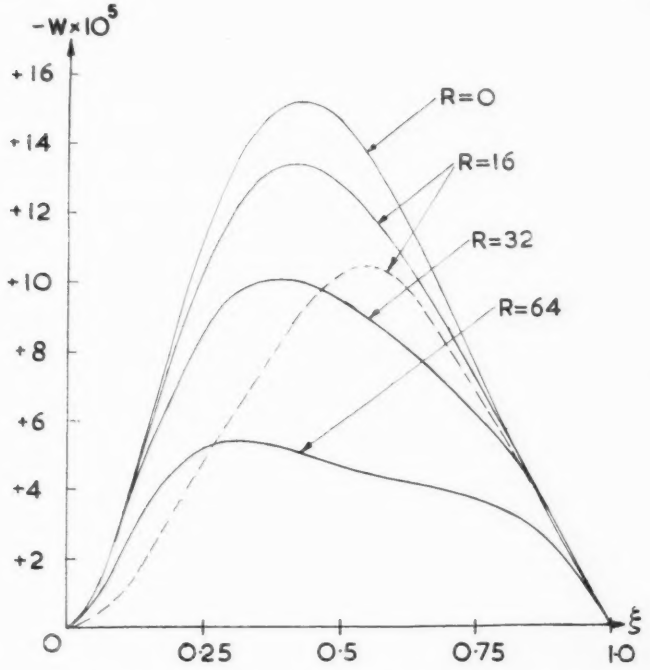

Figure 3. Non-dimensional vertical velocity profile plotted against non-dimensional height. Cases for which $A = 10\,737$ are shown as solid lines. The broken curve is $A = 0$, $R = 16$ and is the value of $-W \times 10^4$.

A detailed comparison with the experimental results of Fultz and Skeib has not been made because, in all the experiments, the value of the Reynolds number does not correspond with any of those used in the present calculations. It is obviously very desirable to extend this work to higher values of R and to other values of the depth parameter a. Such an investigation is at present in hand but it was considered worth while to publish these results as being a valuable extension of the work described in I.

The author wishes to express his thanks to Mr T. V. Davies for his valuable advice.

References

Davies, T. V. 1953 *Phil. Trans.* A, **246,** 81.

Fultz, D. 1951 Article in *Compendium of Meteorology*, p. 1235. American Meteorological Society.

Fultz, D. 1956 *Proceedings of the 1st Symposium on the Use of Models in Geophysical Fluid Dynamics* (Baltimore, 1953), p. 27.

Goodman, T. R. & Lance, G. N. 1956 *Math. Tab., Wash.*, **10,** 82.

Kuo, H. L. 1954 *J. Met.* **11,** 399.

Kuo, H. L. 1955 *J. Mar. Res.* **14,** 14.

Kuo, H. L. 1956 *J. Met.* **13,** 521.

Lance, G. N. & Deland, E. C. 1955 *Proceedings of the Heat Transfer and Fluid Mechanics Institute*, § 16.

Skeib, G. 1953 *Abh. Met. Hydr. Dienst.* **3,** no. 20.

Properties of the Hugoniot function

By ROBERT D. COWAN

Los Alamos Scientific Laboratory of the University of California, Los Alamos, New Mexico

(*Received* 22 *August* 1957)

SUMMARY

Differentiation of the Hugoniot function

$$H(p, v) = E(p, v) - E(p_0, v_0) + \tfrac{1}{2}(p + p_0)(v - v_0)$$

and use of the first and second laws of thermodynamics leads to the relation $dH = T\,dS + dA$, where dA is the element of area in the (p, v) plane swept out (in a counter-clockwise direction) by the line segment $(p_0, v_0) \rightarrow (p, v)$ as the point (p, v) is moved from some point (p_1, v_1) to a neighbouring point $(p_1 + dp_1, v_1 + dv_1)$. This relation, together with rather general assumptions regarding the shape of the isentropic curves $dS = 0$ for the material behind the shock, makes possible the geometrical derivation of a number of properties of the function H and of the Hugoniot curves $dH = 0$.

1. INTRODUCTION

The laws of conservation of mass, momentum, and energy lead to the following relation (first derived by Hugoniot (1889); see also Courant & Friedrichs (1948), pp. 116–146 and 204–218) which must be satisfied across any shock front:

$$E - E_0 = \tfrac{1}{2}(p + p_0)(v_0 - v), \tag{1}$$

where p_0, v_0, and E_0 are the pressure, specific volume, and specific internal energy of the material ahead of the shock front, and p, v, and E are the values of these quantities behind the shock front. (E and E_0 must, of course, be referred to the same energy zero—for example, the energy of the elements in the ideal-gas state at zero temperature.) If the equation of state of the material behind the shock is known so that E and p can be found for any state, then (1) defines all states which can be reached from (p_0, v_0, E_0) by means of a single shock. The locus of all such states can be represented as a curve in the p–v plane, known as the Hugoniot curve.

Even without knowing the equation of state in detail, it is possible to derive several important qualitative properties of the Hugoniot curve on the basis of certain rather general equation-of-state characteristics. This problem has been discussed at length by Bethe (1942) and by Weyl (1949) for the case in which the materials behind and ahead of the shock are chemically identical, and by Courant & Friedrichs (1948) also in the case in which the shock induces a chemical reaction (as in the detonation of

explosives). However, though the assumed equation-of-state characteristics are essentially of a geometrical nature (in terms of the p–v plane), the treatments of the above authors are primarily analytical. The result is that one does not readily obtain much of a feeling for the geometrical relations between the original assumptions and the final deductions. The treatment given below is basically geometrical, and the writer has found it quite useful in dealing with several problems which he has encountered, two of which are mentioned at the end of the paper. Many of the properties discussed below are well known, but are included for the sake of completeness; the proofs given serve to illustrate the simplicity of the geometrical approach.

Two of the basic assumptions made by Courant & Friedrichs in treating the reaction case are rather obscure; these points are cleared up in the discussion following equation (2) and Property 15.

2. Assumptions

It is assumed that there is no external electromagnetic field present, which might affect the problem in the case of shock-induced ionization. The state of the material behind the shock (which may be a mixture of several compounds) is then described completely by the internal energy function $E = E(S, v, n_i)$, where S is the specific entropy and n_i the number of moles of compound i per gram of mixture. The difference in internal energy between two neighbouring states is

$$dE = T\,dS - p\,dv + \sum \mu_i\,dn_i, \tag{2}$$

where μ_i is the chemical potential of the ith component. It is assumed that any shock-induced reaction takes place rather rapidly, and we shall consider only those states which occur to the rear of the reaction zone, where the material is essentially in chemical equilibrium. The term $\sum \mu_i\,dn_i$ in (2) is then zero, the change in internal energy becomes simply

$$dE = T\,dS - p\,dv, \tag{3}$$

and the internal energy can be considered as a function of S and v only. Assuming further that

$$(\partial p/\partial S)_v > 0 \tag{4}$$

so that no two isentropic curves ever cross, the energy can be considered as a single-valued function of pressure and volume

$$E = E(p, v), \tag{5}$$

which will be supposed to be everywhere continuous with continuous derivatives. (Assumption (4) is invalid for water between 0° and 4° C, and for phase changes generally.) Finally, it is assumed that all isentropes have negative slope and positive curvature:

$$(\partial p/\partial v)_S < 0, \tag{6}$$

$$(\partial^2 p/\partial v^2)_S > 0. \tag{7}$$

These two conditions are satisfied rather generally; they have been investigated at some length by Bethe (1942) for substances not reacting chemically and shown to be valid usually except at some phase transformations†. However, (7) is occasionally violated in the case of chemically reacting substances.

From (3) and (4) it follows that

$$(\partial E/\partial p)_v = T(\partial S/\partial p)_v > 0. \tag{8}$$

Since (4) and (6) imply

$$(\partial S/\partial v)_p > 0, \tag{9}$$

it follows from (3) that

$$(\partial E/\partial v)_p > -p. \tag{10}$$

In some cases for $p > p_0$ and $v < v_0$ (which will be mentioned specifically below), the stronger condition

$$(\partial E/\partial v)_p > -\tfrac{1}{2}(p+p_0) \tag{11a}$$

or (from (3))

$$(\partial S/\partial v)_p > \tfrac{1}{2}(p-p_0)/T \tag{11b}$$

will be assumed to hold, and in other cases, the still stronger condition

$$(\partial E/\partial v)_p > 0 \tag{12a}$$

or

$$(\partial S/\partial v)_p > p/T \tag{12b}$$

will be applied. Even this last inequality (which, with (8), is equivalent to $(\partial p/\partial v)_E < 0$) has been shown by Bethe to be usually valid except at some phase transformations.

It is assumed throughout that $p_0 > 0$.

3. Definitions

In order to investigate the properties of the Hugoniot curve defined by (1), it is convenient to define the so-called Hugoniot function

$$H(p,v) \equiv E(p,v) - E(p_0,v_0) - \tfrac{1}{2}(p+p_0)(v_0-v), \tag{13}$$

where $E(p_0,v_0)$ is the internal energy which the material behind the shock would have if it were returned (always under conditions of thermodynamic and chemical equilibrium) to the pressure and specific volume (p_0,v_0) of the unshocked material. By assumption (5), H is a single-valued, continuous, and differentiable function of p and v. In terms of the Hugoniot function, the Hugoniot relation (1) becomes

$$H = E_0(p_0,v_0) - E(p_0,v_0) = \text{constant}. \tag{14}$$

† The inequality examined by Bethe is actually

$$(\partial p/\partial v)_E \equiv (\partial p/\partial v)_S + (p/T)(\partial p/\partial S)_v < 0,$$

which is less general than (6) if (4) holds. (However, Bethe's third assumption $(\partial p/\partial S)_v > -2T/v$ is more general than (4).)

Thus the Hugoniot curve is a curve of constant H, the constant value being zero if the shock induces no chemical reaction (or a reaction such as dissociation or ionization for which the shocked material can be returned reversibly and spontaneously to the original state of the unshocked material), and the constant being greater or less than zero if a reaction is induced which is exothermic or endothermic, respectively. (Note that if the unshocked material is, for example, a complicated organic high explosive in a condensed phase, it may be impossible to reduce to p_0 the pressure of the reaction products at volume v_0 even by reducing the temperature to absolute zero, so that $E(p_0, v_0)$ is undefined. In this case, the zero-temperature isotherm passes above the point (p_0, v_0), and $H(p, v)$ must be defined in terms of say $E(T=0, v_0)$ or $E(T=0, p=0)$ instead of $E(p_0, v_0)$. However, this only changes the value of the constant in (14), and requires no essential revision in the discussion below for Hugoniot curves $H = \text{constant} > 0$. It is convenient to suppose that $E(p_0, v_0)$ does exist so as to permit simultaneous treatment of the cases $H = \text{constant} \gtrless 0$.)

The differential of the Hugoniot function (13) is, on using (3),

$$\begin{aligned} dH &= dE + \tfrac{1}{2}\{(p+p_0)\,dv + (v-v_0)\,dp\} \\ &= T\,dS + \tfrac{1}{2}\{-(p-p_0)\,dv + (v-v_0)\,dp\}. \end{aligned} \tag{15}$$

This is the expression used by Weyl (1949) in his analytical discussion of the problem. However, it is much more convenient for a geometrical treatment to write (15) in the form (Cowan 1953)

$$dH = T\,dS + dA, \tag{16}$$

where dA is the area swept out in the p–v plane by the radius vector $(p_0, v_0) \to (p, v)$ in moving from the point (p, v) to the point $(p+dp, v+dv)$, dA being positive if the radius vector moves in a counter-clockwise direction. That the final term in (15) is the element of area just defined can be seen by noting that this term is just half the alternating (two-dimensional vector) product of the vectors $(v-v_0, p-p_0)$ and (dv, dp), or alternatively by introducing polar coordinates

$$v - v_0 = r\cos\theta, \qquad p - p_0 = r\sin\theta$$

which show that this term is

$$\tfrac{1}{2}r^2\,d\theta = dA. \tag{17}$$

It may be pointed out that although dH is a perfect differential, neither $T\,dS$ nor dA is one. Equation (16) is in fact quite similar to (3), both $p\,dv$ and dA being elements of area in the p–v plane—the one in Cartesian, the other in polar coordinates.

It will be convenient in the discussion below to speak in terms of a coordinate system with origin at (p_0, v_0) and so we introduce the coordinates $p^* = p - p_0$, $v^* = v - v_0$. The isentropic curve which passes through the

origin will be denoted by S_0, and the tangent line to S_0 at the origin will be called T_{S_0}. For each isentrope S lying above S_0, then, as a consequence of assumptions (6) and (7), there exist exactly one point on S in the second quadrant and one point on S in the fourth quadrant at which a straight line through the origin is tangent to S. The locus of all such points of tangency will be denoted by LT, and can be seen to be a continuous curve which is tangent to S_0 at the origin, but otherwise lies entirely above S_0 (figure 1). Because of assumptions (4) and (7), any straight line through the origin cuts LT in at most one point, and it is evident from the definition that entropy increases monotonically in travelling along LT outward from the origin in either direction.

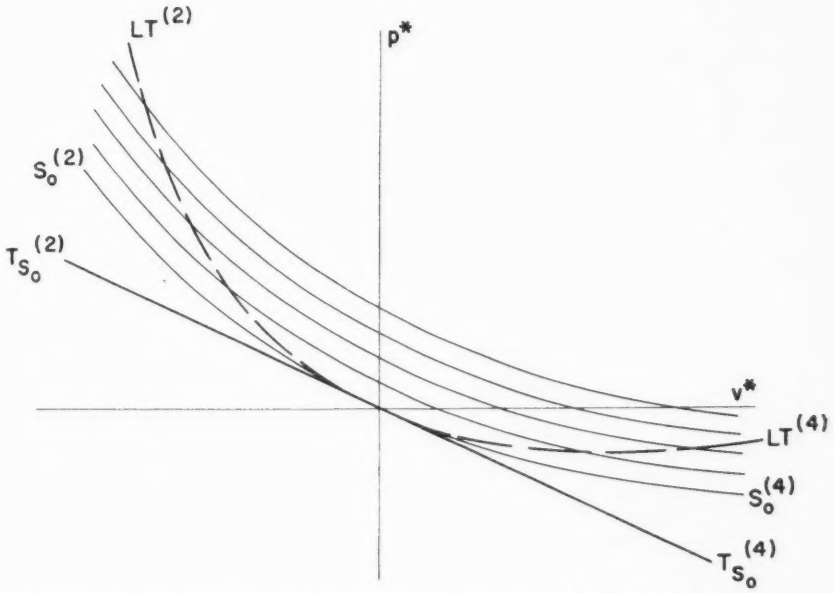

Figure 1. The isentrope S_0, the tangent to S_0 at the origin T_{S_0}, and the locus LT of all points at which a ray through the origin is tangent to an isentrope.

The curves LT, S_0, and T_{S_0} each pass through the origin but are otherwise confined to the second and fourth quadrants. The portions of these curves lying in the second and fourth quadrants will be denoted by the superscripts (2) and (4), respectively.

It should, of course, be kept in mind that the region of the (p^*, v^*)-plane in which H is defined is bounded from below by the zero-temperature isotherm. This (along with any regions in which the assumptions (3) to (7) are invalid) may introduce certain limitations on the validity of some of the statements made below.

4. Properties of the Hugoniot function

General properties of $H(p^*, v^*)$

Property 1. $H(0, 0) = 0$, by definition.

Property 2. For $p^* < 0$, $(\partial H/\partial v)_p > 0$; for $v^* > 0$, $(\partial H/\partial p)_v > 0$.

Travelling to the right along an isobar $p^* < 0$ or upward along an isochor $v^* > 0$, both dS and dA are positive, and hence $dH > 0$ from (16).

Property 2′. Wherever condition (11) is satisfied, $(\partial H/\partial v)_p > 0$ even though $p^* > 0$.

This follows immediately from (15).

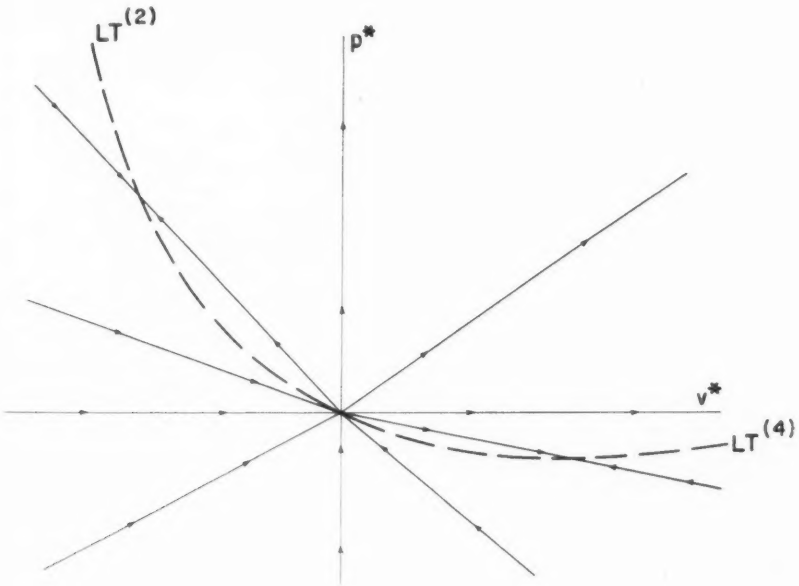

Figure 2. On any straight line through the origin, H increases away from the origin on the first-quadrant side of LT and increases toward the origin on the third-quadrant side of LT (Property 3).

Property 3. On any ray through the origin travelling away from the origin, $dH > 0$ on the first-quadrant side of LT and $dH < 0$ on the third-quadrant side of LT (figure 2). Thus H passes through a maximum at LT.

On such a ray, $dA = 0$, and hence from (16), $dH = T\,dS$. The qualitative behaviour of H is thus identical to that of S and follows immediately from the definition of LT.

PROPERTY 4. Travelling along an isentrope in the direction of increasing pressure, $dH > 0$ on the first-quadrant side of LT and $dH < 0$ on the third-quadrant side of LT (figure 3). Thus H passes through a minimum at $LT^{(4)}$ and through a maximum at $LT^{(2)}$.

Along an isentrope, $dS = 0$, and hence $dH = dA$.

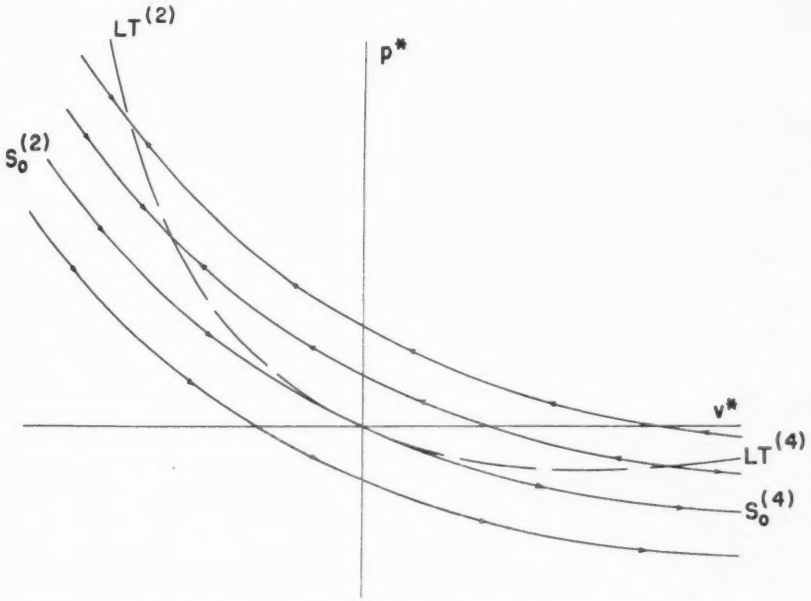

Figure 3. On an isentrope, H increases in the direction of increasing pressure on the first-quadrant side of LT and increases in the direction of decreasing pressure on the third-quadrant side of LT (Property 4).

PROPERTY 5. Except for the origin, $H > 0$ on LT and on $S_0^{(1)}$ and $H < 0$ on $S_0^{(2)}$ and T_{S_0}. Travelling away from the origin, $dH > 0$ on $LT^{(4)}$ and $S_0^{(4)}$ and $dH < 0$ on $S_0^{(2)}$, $T_{S_0}^{(2)}$ and $T_{S_0}^{(1)}$.

The statements regarding $LT^{(2)}$ and T_{S_0} follow from Properties 1 and 3, and those regarding S_0 from Properties 1 and 4. Travelling away from the origin on $LT^{(4)}$, both dS and dA are positive and hence $dH > 0$. Note, however, that a similar statement cannot be made on $LT^{(2)}$ since dS and dA have opposite signs; $H > 0$ on $LT^{(2)}$, but does not necessarily increase monotonically in a direction away from the origin—see the discussion following Property 15.

Properties of the curve $H = 0$

In the case of a shock which includes no chemical reaction (in the sense described in § 3), the possible thermodynamic states behind the shock are those for which $H = 0$; such states are thus of considerable physical interest.

PROPERTY 6. There exists a continuous curve $H = 0$ (denoted by H_0 for brevity) which passes through the origin O, but is otherwise confined to the second quadrant between $LT^{(2)}$ and $S_0^{(2)}$ and to the fourth quadrant between $S_0^{(4)}$ and $T_{S_0}^{(4)}$. For any point P on $S_0^{(2)}$, the ray $O \rightarrow P$ cuts H_0 in exactly one point; for P on $S_0^{(4)}$, $O \rightarrow P$ cuts H_0 in at most one point and a vertical or a horizontal line through P cuts H_0 in exactly one point.

It is evident from Properties 3 and 5 that $H > 0$ on the first-quadrant side of $LT^{(2)}$ and $S_0^{(4)}$, and $H < 0$ on the third-quadrant side of $S_0^{(2)}$ and $T_{S_0}^{(4)}$. Thus any points for which $H = 0$ must lie in the portions of the second and fourth quadrants stated above. For any point P on $S_0^{(2)}$, the ray $O \rightarrow P$ cuts $LT^{(2)}$ in exactly one point Q; since the values of H at P and Q are less than and greater than zero, respectively (Property 5), and since H increases monotonically from P to Q (Property 3), the line segment $P \rightarrow Q$ contains exactly one point at which $H = 0$. Similarly, for any point P on $S_0^{(4)}$ (where $H > 0$), a vertical or a horizontal line through P intersects T_{S_0} at a point Q (where $H < 0$)†, and by Property 2 there exists exactly one point between P and Q at which $H = 0$. Continuity of the curve H_0 follows from that of the curve S_0 and that of the function (13). For P on $S_0^{(4)}$, $O \rightarrow P$ cuts H_0 in at most one point by Property 3.

Note that there is nothing which precludes the possibility of maxima and minima in volume along $H_0^{(2)}$; Bethe has, in fact, discussed phenomena (molecular rotation, vibration, dissociation, ionization) which tend to produce just such effects. The question of pressure maxima and minima on $H_0^{(2)}$ is dealt with in Property 10 below‡.

PROPERTY 7. $H > 0$ on the first-quadrant side of the curve H_0, and $H < 0$ on the third-quadrant side of H_0.

This is evident from the statements made in proving Property 6.

PROPERTY 8. As a point P moves along H_0 in the direction from fourth to second quadrant, the straight line through O and P turns continuously clockwise with no stationary values of its slope.

In the vicinity of the origin, H_0 has positive curvature. On the second-quadrant side of the origin, this follows from Property 6 and assumption (7); on the fourth-quadrant side, H_0 cannot have negative curvature because of Property 6, and it cannot have zero curvature because to the second order dS (and hence also dH) is negative going down $T_{S_0}^{(4)}$. Thus Property 8 holds in the vicinity of the origin. Since the line $O \rightarrow P$ cannot cut H_0 in two different points (Property 6), the direction of rotation of $O \rightarrow P$

† If Q lies below the zero-temperature isotherm (isentrope), then the line through P must be terminated at the $S = 0$ curve, where H may or may not be negative (Property 4). This indicates the likelihood of an upper limit to volume on H_0. Such a limit indeed exists (as pointed out by Bethe) since the final term in (13) tends to plus infinity with v whereas $E(p, v)$ certainly has a finite lower bound.

‡ Bethe states that pressure maxima and minima may occur on $H_0^{(4)}$. This is a result of his assumption $(\partial p/\partial S)_v > -2T/v$, which is less restrictive than (4).

can never reverse itself. A point of inflection P at which H_0 is tangent to $O \to P$ is also impossible, from Properties 3 and 6.

PROPERTY 9. Travelling along H_0 in the direction from fourth to second quadrants, S increases monotonically ($dS > 0$) except for a stationary value at the origin, where ΔS is of the third order in shock strength.

Since $dH = 0$ along H_0, then, from (16) and (17),

$$T\,dS = -dA = -\tfrac{1}{2}r^2\,d\theta.$$

In the vicinity of the origin

$$\tan\theta = \frac{p^*}{v^*} \doteq \left(\frac{\partial p}{\partial v}\right)_H + \frac{1}{2}\left(\frac{\partial^2 p}{\partial v^2}\right)_H v^*$$

and

$$d\tan\theta = \frac{r^2}{v^{*2}}\,d\theta \doteq \frac{1}{2}\left(\frac{\partial^2 p}{\partial v^2}\right)_H dv^*,$$

so that

$$S(v^*) - S(0) \doteq -\frac{1}{12T_0}\left(\frac{\partial^2 p}{\partial v^2}\right)_H (v^*)^3 = -\frac{1}{12T_0}\left(\frac{\partial^2 p}{\partial v^2}\right)_S (v^*)^3 \qquad (18)$$

which is of the third order in v^*†. It may be noted that the change of entropy along H_0 near the origin is directly related to the non-zero curvature of the isentrope S_0. (In fact, if S_0 were a straight line, then along S_0, $dS = dA = 0$ and hence $dH = 0$; thus H_0 would be coincident with S_0 along the entire length of the latter.)

PROPERTY 10. In travelling along $H_0^{(2)}$ away from the origin, the pressure and energy vary as follows: (*a*) if $dv < 0$, then $dp > 0$ and $dE > 0$; (*b*) if $dv > 0$, then $dp > 0$ if and only if the inequality (11) is satisfied on H_0, and $dE > 0$ if the inequality (12) is satisfied on H_0.

If $dv < 0$ in travelling up $H^{(2)}$, then Property 8 implies $dp > 0$, and from (3)

$$dE = T\,dS - p\,dv > 0$$

since $dS > 0$ from Property 9. If $dv > 0$ in travelling up $H_0^{(2)}$, then $T\,dS > 0$ and $-p\,dv < 0$ and nothing definite can be said about the sign of dE. However, if the inequality (11) is satisfied, then $(\partial H/\partial v)_{\prime\prime} > 0$ from (15), and this implies $dp > 0$ from Property 7. If the even stronger condition (12) is satisfied, then $dv > 0$ and $dp > 0$ along H_0 imply from (8) and (12) that also $dE > 0$ along H_0. (Note that assumption (12) is a sufficient but not a necessary condition for $dE > 0$.)

Properties of a curve $H = -c$ (c = constant > 0)

Constant-H curves for $H < 0$ are not of great interest since such a curve (which will be denoted by H_-) represents the locus of possible states

† This expression can also be obtained by direct differentiation of (15) at constant H to give the coefficients $(\partial^{(n)}S/\partial v^{(n)})_H$ in a Taylor series expansion for S.

behind a shock which has induced an endothermic chemical reaction, and such cases are not of much physical importance. The properties of such curves are similar to those of H_0 and will only be summarized briefly.

PROPERTY 11. H_- lies everywhere on the third-quadrant side of H_0; $H > -c$ everywhere on the first-quadrant side of H_- and $H < -c$ everywhere on the other side (Properties 7 and 3). For $p^* < 0$, a horizontal line cuts H_- at most once; for $v^* > 0$, a vertical line cuts H_- at most once (Property 2). Any ray from the origin cuts H_- at most once (Property 3). In travelling along H_- in the direction from fourth to second quadrant, $dA < 0$ and $dS > 0$ (see (16)). On $H_-^{(2)}$, the behaviour of pressure and energy is as described in Property 10.

Properties of a curve $H = +c$ ($c = constant > 0$)

Constant-H curves for $H > 0$ are of great physical interest since one such curve (which will be denoted by H_+) includes the locus of possible states behind a shock-induced exothermic chemical reaction (as in the detonation of an explosive, either gaseous, liquid, or solid) or behind such a reaction which is not shock-induced (slow combustions or deflagrations); see, for example, Courant & Friedrichs (1948).

PROPERTY 12. H_+ lies everywhere on the first-quadrant side of H_0, or, if H is not defined at the origin, then everywhere above the zero-temperature isentrope. In any case, H_+ is confined to the second, first, and fourth quadrants.

If H is defined at the origin, this follows from Property 7; if not, then it follows from the physical requirement $T > 0$. In addition, it can be shown (Courant & Friedrichs 1948) that the only physically significant parts of H_+ are those in the second and fourth quadrants, and so we shall not consider $H_+^{(1)}$ in any detail.

PROPERTY 13. Given any point P on LT, then, according as the value of H at P is less than, equal to, or greater than c, the ray $O \to P$ cuts H_+ not at all, at the one point P, or at (at most) one point on either side of P. Similarly, the isentrope through P cuts H_+ zero, one, or (at most) two times according as $H(P) \lessgtr c$ if P is on $LT^{(2)}$ or according as $H(P) \gtrless c$ if P is on $LT^{(4)}$.

These statements follow immediately from Properties 3 and 4. Note the essential difference between these properties of H_+ and the corresponding properties of H_0 and H_-, directly connected with the fact that only H_+ can intersect LT at a point other than the origin (Property 5).

PROPERTY 14. For any point P on $LT^{(4)}$, there exists a continuous curve H_+ through P, which at P is tangent from below to $S_0^{(4)}$ and tangent from above to $O \to P$; $(\partial^2 p/\partial v^2)_S > (\partial^2 p/\partial v^2)_H > 0$. On $H_+^{(4)}$, the entropy

has a maximum value where it crosses $LT^{(4)}$ and decreases monotonically on either side of this point.

The statements regarding tangency follow directly from Properties 4, 3, and 2, and the continuity of the Hugoniot function (13). The entropy maximum follows from the tangency relations, and the absence of any other stationary points in entropy is obvious since only at points on LT can dS and dA be simultaneously zero (see (16)).

The intersection of $H_+^{(1)}$ and $LT^{(4)}$ represents the state of the reaction products for a Chapman–Jouguet deflagration (Courant & Friedrichs 1948).

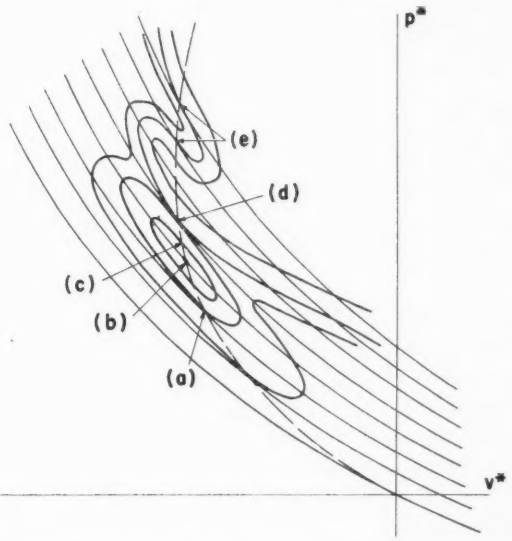

Figure 4. Diagram showing the mutual relation of isentrope, $LT^{(2)}$, and curves H_+ defined by $H =$ constant > 0. Under the assumptions (4) to (10), the relations shown at (*a*), (*b*), (*c*), and (*d*) are possible (Property 15), but those at (*e*) are not (Property 3). Under assumption (11), only (*a*) is possible.

PROPERTY 15. For any point P on $LT^{(2)}$, the constant-H curve, H_+, which passes through P may behave in any of several ways: (*a*) H_+ may be tangent from above to the isentrope through P; (*b*) H_+ may consist of the single point P; (*c*) H_+ may be tangent from below to the ray $O \rightarrow P$; (*d*) H_+ may have two branches, one of the form (*a*) and one of the form (*c*). H_+ cannot have a point of inflection at P, behaving as in (*a*) on one side of $LT^{(2)}$ and as in (*c*) on the other side.

At any point P on LT, then along $O \rightarrow P$ (or along the isentrope through P) $dS = dA = 0$ and hence $dH = 0$ from (16); thus H_+ must be tangent to $O \rightarrow P$ (and to the isentrope S_P). However, H_+ cannot lie in between $O \rightarrow P$ and S_P because, travelling away from P on such a curve, $dS < 0$ and $dA < 0$ and hence dH cannot be zero. Thus H_+ must behave

as shown at (*a*), (*b*), (*c*), or (*d*) in figure 4. An inflection point at P is not possible; see figure 4 and Property 3.

It is evident from figure 4 (which may be viewed as a contour-map of a three-dimensional (v, p, H) surface) that H_+ has the form (*a*), (*b*), (*c*), or (*d*) according as in travelling up $LT^{(2)}$ H increases, passes through a maximum, decreases, or passes through a minimum, respectively. Thus the necessary and sufficient condition that only the relation (*a*) prevail is that H increase monotonically in travelling up $LT^{(2)}$ (see the discussion following Property 5). Since on $LT^{(2)}$ $(\partial p/\partial v)_H = (\partial p/\partial v)_S < 0$, an equivalent condition is that $(\partial H/\partial p)_v > 0$ or $(\partial H/\partial v)_p > 0$. This last inequality, from (15), is equivalent to (11). *In all the following discussion of the properties of H_+, it will be assumed that on $LT^{(2)}$*

$$\left(\frac{\partial E}{\partial v}\right)_p > -\tfrac{1}{2}(p+p_0) \qquad \text{or} \qquad \left(\frac{\partial E}{\partial p}\right)_v > \tfrac{1}{2}(v_0-v).$$

Proofs of most of the following statements have already been given or are obvious.

PROPERTY 16. In travelling along $LT^{(2)}$ in the direction away from the origin, $dH > 0$.

PROPERTY 17. For any point P on $LT^{(2)}$, there exists a continuous curve H_+ passing through P which is tangent from above to the isentrope through P $((\partial^2 p/\partial v^2)_H > (\partial^2 p/\partial v^2)_S > 0)$ and which meets $LT^{(2)}$ *only* at P. For any point P' on $LT^{(2)}$ between O and P and for any point P'' on $LT^{(2)}$ beyond P, the ray $O \to P'$ and the isentrope $S_{P'}$ intersect $H_+^{(2)}$ not at all, $O \to P$ and S_P meet $H_+^{(2)}$ only at P, and $O \to P''$ and $S_{P''}$ each intersect $H_+^{(2)}$ at most twice (once on either side of $LT^{(2)}$).

PROPERTY 18. In travelling along $H_+^{(2)}$ away from $LT^{(2)}$ in either direction, S increases monotonically with no stationary values except at the point of intersection P of $H_+^{(2)}$ and $LT^{(2)}$, where S is a minimum. For a point Q near P, the difference $S(Q)-S(P)$ is of the second order in $\Delta v = v_Q - v_P$.

Similarly to the derivation of Property 9, one has†

$$\tan\theta \doteq \left(\frac{\partial p}{\partial v}\right)_H + \frac{1}{2}\left(\frac{\partial^2 p}{\partial v^2}\right)_H \frac{(\Delta v)^2}{v^*},$$

and

$$d\tan\theta = \frac{r^2}{v^{*2}}\,d\theta \doteq \left(\frac{\partial^2 p}{\partial v^2}\right)_H \frac{\Delta v}{v^*}\,d(\Delta v),$$

$$S(Q)-S(P) \doteq \frac{(v_0-v)}{4T}\left(\frac{\partial^2 p}{\partial v^2}\right)_H (\Delta v)^2. \tag{19}$$

PROPERTY 19. At the point of intersection of $H_+^{(2)}$ and $LT^{(2)}$, the internal energy increases in the direction of increasing pressure. On the part of $H_+^{(2)}$

† See the footnote to Property 9.

which lies to the left of $LT^{(2)}$, the behaviour of pressure and energy are as given in Property 10 for $H_0^{(2)}$.

The first statement follows from (3) and (6);

$$(\partial E/\partial p)_H = (\partial E/\partial p)_S = -p(\partial v/\partial p)_S > 0.$$

Proof of the remainder is exactly as that for Property 10.

The intersection of $H^{(2)}$ and $LT^{(2)}$ represents the state of the reaction products for a Chapman–Jouguet detonation (Courant & Friedrichs 1948).

5. Summary and applications

In figure 5 is sketched a series of constant-H curves illustrating the most important properties developed above, assuming that condition (11) holds for $p^* > 0$. These properties—subject to limitations which may

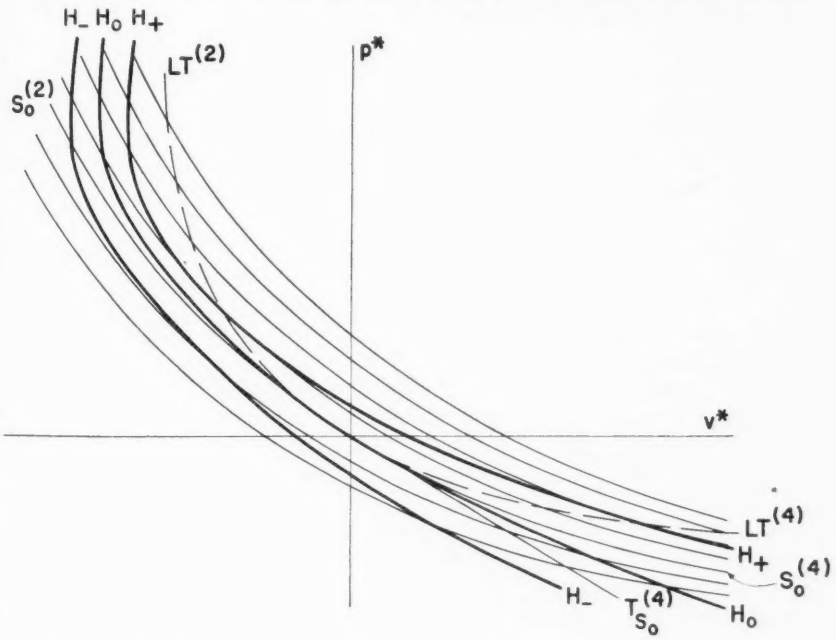

Figure 5. Diagram showing isentropes, the curve LT, and the general form of the constant-H curves assuming conditions (4) through (11) to be valid. (In order to illustrate volume minima on $H^{(2)}$ on the scale of this figure, the upper part of $H_0^{(2)}$ has been drawn in such a way that the requirements of (21) are violated.)

arise from the fact that the zero-temperature isotherm does not pass below the origin, or from phase transformations or other causes of violation of assumptions (4) to (10)—are briefly as follows.

The (p^*, v^*)-plane can be thought of as divided into three parts by the half-line $(v^* = 0, p^* < 0)$, and by the curves $LT^{(2)}$ and $LT^{(4)}$, the loci of

all possible Chapman–Jouguet states for exothermic detonations and deflagrations, respectively. No constant-H curve has pressure maxima or minima anywhere, nor volume maxima or minima for $v^* > 0$. No constant-H curve is cut by a straight line through the origin nor by an isentropic curve more than once in each of the three regions of the (p^*, v^*)-plane. The curve $H = 0$ passes through the origin, in the second quadrant lies between $LT^{(2)}$ and $S_0^{(2)}$, and in the fourth quadrant lies between $S_0^{(4)}$ and $T_{S_0}^{(4)}$. Above and to the right of any constant-H curve $H = c$, the value of H is greater than c; on the other side of this curve, H is less than c. Travelling up $H = 0$ in the direction from fourth to second quadrant, the entropy increases monotonically except for a point of inflection at the origin. Travelling up a curve $H = \text{constant} < 0$, $dS > 0$ everywhere. A curve $H = \text{constant} > 0$ in general crosses both $LT^{(4)}$ and $LT^{(2)}$; in travelling up this curve, starting below $LT^{(4)}$, entropy increases monotonically until it reaches a maximum value at $LT^{(4)}$, then decreases monotonically to a minimum value at $LT^{(2)}$, after which it again increases monotonically.

Two applications of the properties developed above will be given. Both pertain to the curve $H_0^{(2)}$ (the case in which the shock produces no chemical reaction), and serve to elaborate on certain characteristics of this curve.

1. The equation of state of a gas may be written in the form

$$E = pv/(\gamma - 1). \tag{20}$$

In the case of a monatomic ideal gas, $\gamma = 5/3$ for all p and v; the effect of excitation and ionization in a real gas is to increase E for given p and v and thus produce an effective value of γ which is less than 5/3. Thus for a point (p, v) which lies on the Hugoniot curve for the ideal gas, it is seen from (13) that $H > 0$ for the real gas. From Property 7, it follows that the Hugoniot curve for the real gas lies to the left of (or below) the ideal-gas curve. At very high pressures, the real gas is completely ionized and the potential energy becomes negligible relative to the kinetic energy, so that the equation of state of the real gas becomes identical with that of the ideal one and, consequently, the two Hugoniot curves also become identical; the possibility of a volume minimum on the Hugionot curve of the real gas (due to ionization, etc., as mentioned earlier) is thus evident.

2. For a certain problem which the author once encountered, it was important to know for an arbitrary point (p_1, v_1) on $H_0^{(2)}$ whether the isentrope through this point intersected the chord $(p_0, v_0) \rightarrow (p_1, v_1)$ or lay everywhere above it. It is immediately evident from Property 6 that the former is the case. In fact, the point of intersection is closer to (p_0, v_0) than to (p_1, v_1) as can be seen in the following way. In figure 6, S_1 is the isentrope through (p_1, v_1) and (p_2, v_2) is the point on S_1 for which $p_2 = p_0$. Then from the Hugoniot relation (1)

$$E_1 - E_0 = \tfrac{1}{2}(p - p_0)(v_0 - v_1) + p_0(v_0 - v_1),$$

and from (3)

$$E_2 - E_1 = -\int_{v_1}^{v_2} p_{S_1}\, dv,$$

so that

$$E_2 - E_0 = A_1 - A_2 - p_0(v_2 - v_0), \tag{21}$$

where A_1 and A_2 are the shaded areas in figure 6. From assumption (10), it follows that $A_1 > A_2$. Thus it may be seen that not only does $H_0^{(2)}$ lie between $LT^{(2)}$ and $S_0^{(2)}$, but tends to lie closer to the latter than to the former (see figure 5).

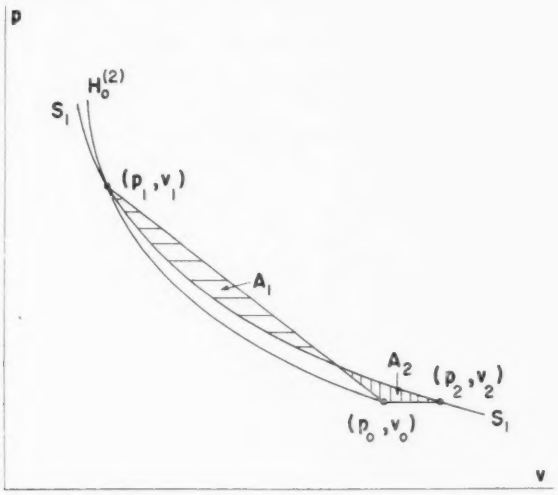

Figure 6. Relation of the Hugoniot chord $(p_0, v_0) \rightarrow (p_1, v_1)$ to the isentrope through (p_1, v_1); the area A_1 is greater than the area A_2.

This work was performed under the auspices of the U.S. Atomic Energy Commission. The author wishes to acknowledge numerous helpful discussions with Drs Wildon Fickett and William W. Wood of this laboratory.

References

Bethe, H. A. 1942 The theory of shock waves for an arbitrary equation of state, *OSRD Report* no. 545 (unclassified).

Courant, R. & Friedrichs, K. O. 1948 *Supersonic Flow and Shock Waves*. New York: Interscience.

Cowan, R. D. 1953 *Phys. Rev.* **92,** 1079 (A).

Hugoniot, H. 1889 *J. Éc. polyt. Paris* **58,** 1.

Weyl, H. 1949 *Comm. Pure Appl. Math.* **2,** 103.

REVIEWS

Viscous Flow Theory, II—Turbulent Flow, by SHIH-I PAI. Princeton: D. Van Nostrand Co., 1957. 277 pp. $6.75 or 48*s*.

In a time which most people would find barely adequate for the writing of one book, Professor Pai has published no fewer than three on different branches of fluid mechanics. Beginning with *Fluid Dynamics of Jets* (1954), he followed up with *Viscous Flow Theory, I—Laminar Flow* (1956), and now we have this new work on turbulent flow. The two parts of the treatise on viscous flow theory are really separate books, since there is not much in common, pedagogically speaking, between laminar and turbulent flow; indeed, there is not even much of a case for the use of a common title in view of the relatively unimportant part played by viscosity in most cases of turbulent flow. It is no mean achievement for a man to find the determination and knowledge needed for three books in rapid succession, and it might be supposed that they have a purpose which is obvious. I have not in fact been able to discern clearly the purpose served by the present book or to classify it as one of the common types. I do not think that it can be called a research monograph on turbulent flow; the author does not reveal important new advances, and his book does not have the physical insight and critical appraisal that would be needed for it to say anything new to those in touch with the subject. Nor can it be said to be an exposition for students; the material is too raw and incomplete, and includes too many unrelated items of current research which are of unknown significance, for the book to be suitable for teaching purposes. There is undoubtedly a need for a textbook on turbulent flow, but the present work does not have the regard for fundamentals and for logical coherence that such a text should have. Despite the claim made on the dust-jacket (with characteristic punctuation and spelling) that " Engineers, research scientists as well as advanced students will find this complete treatment of turbulent flow an indispensible source of fresh information", it seems to me to lack both the indispensability of a good textbook and the freshness of a good research monograph.

So far as technique of writing is concerned, the author has acted simply as a reporter, absorbing large masses of paper and regurgitating it in a uniform style in the manner of a journalist. The present book, like a good newspaper, can fairly be said to be comprehensive in scope, up to the minute, impartial, and discursive. It also has the defects of some journalistic reporting—a limited respect for the truth, haste in composition and printing, some irresponsibility, and an apparent reluctance to think about the material for longer than it takes to read it and write it down in different (not always!) words. Professor Pai does have a genuine flair for reporting scientific developments; as many visitors to the University of Maryland have found, he makes a creditable job of writing up their lectures for later reproduction and distribution by the University. This kind of writing requires mental agility and elasticity to an unusual degree. But though the rapid reporting of many different

scientific subjects demands considerable skill, the job encourages superficiality and this is unfortunately the hall-mark of the book under review. Passing lightly from one snippet of news to another, the text always stops short of the point of illumination and fails completely to provide a clear picture of the basic mechanics of turbulent flow.

The scope of the book is wide, and embraces all aspects of turbulent motion; the classical cases of turbulent shear flow, mixing-length theories, boundary layers with pressure gradients, compressible turbulent flow, turbulent diffusion, decaying isotropic turbulence, spectrum theory, Kolmogoroff's similarity theory, and even turbulence in an electrically conducting fluid, all find some kind of place in the book. The treatments of these topics are not thorough (nor could they be in a book of this size), and a more cautious author would have hesitated to try to compress a whole subject like turbulent diffusion into 18 pages. But granted that it is useful to say something about everything within the space of one book, there is an acute problem of selection of material to be faced. The pieces of work which Professor Pai chooses for inclusion show him to be attracted strongly by those having a mathematical form and hardly at all by physical thought; for instance, the book includes fairly full accounts of Reichardt's "inductive theory of turbulence" (pp. 37, 129), the method of determining profile drag from wake measurements (p. 135), Goldstein's hyperbolic diffusion equation (p. 186), correlation and spectrum tensor relations (pp. 214–230), and Chandrasekhar's 'propagation' of density fluctuations (p. 256), but on the other hand makes no mention whatever of what is perhaps the most fundamental (and practically useful) formula in the theory of turbulence, namely, that the rate of dissipation of energy is of the same order of magnitude as u^3/l, where u and l are representative velocity and length scales of the turbulence. The more straightforwardly mathematical investigations in any subject are undoubtedly the easiest to comprehend, and are often seized upon with relief by students; for that very reason, it is desirable always to explain their significance, the assumptions on which they are based, their implications, and their agreement with observation. I am sure Professor Pai would agree with that precept, but I do not think he has done much about it; he says (p. 209), "... we have no general methods for solving such nonlinear equations. At the present time, we try to obtain an understanding of the mechanism of turbulence by studying experimental results ...", but in fact he does not provide a single diagram or table of observations relating to homogeneous turbulence even though about half the book is concerned with that case. His bias toward highly theoretical enquiries sometimes leads him into rather pretentious and irrelevant generalities, as for instance when (ch. 8) he drags in phase space and Liouville's theorem and other concepts of statistical mechanics.

The book falls into two non-overlapping and non-interacting parts, the first being concerned with "semi-empirical theories of turbulence" and the standard cases of turbulent shear flow, and the second with the "statistical theory of turbulence" and isotropic turbulence in particular. This dichotomous approach to the subject of turbulent flow was remarked

in a recent review of *Momentum Transfer in Fluids* by Corcoran, Opfell and Sage (*J. Fluid Mech.* **2**, 1957, 204); indeed, had Professor Pai's book appeared a little earlier, it would have been convenient to review them together since they have a good deal in common quite apart from their concern with turbulent flow. The division is made quite sharply here, the mean velocity distribution in jets, wakes, etc. being regarded as belonging to the "semi-empirical theories" and velocity fluctuations in those same flows as belonging to the "statistical theories". Unless someone soon writes a book which integrates the old and the new, the means and the fluctuations, the "semi-empirical" and the "statistical", we shall have a generation of students who believe that there must be some basis in nature for this dual approach and that jets and wakes really do have two faces. Mixing-length theories and the statistical terminology represent the contributions of two separate periods of research (both of them now past), and we ought by now to be able to make up our minds about what is good in each and to allow what is not good to be quietly forgotten.

The first part of the book on the "semi-empirical theories" follows a familiar and appropriate pattern. There is first a chapter introducing the momentum and vorticity transfer theories and hypotheses about the mixing length, and containing a rather perfunctory account of the facts that they are intended to explain. The two key empirical laws concerning the mean velocity are the universality of the distributions in the central region of a channel and near a rigid plane boundary. These two laws deserve prominence, as any number of writers have pointed out, but Professor Pai passes over them lightly and does not even distinguish them clearly (p. 28). The next five chapters consider in turn the cases of channel flow, a flat plate without and with a pressure gradient, a compressible boundary layer, and what the book calls "turbulent jet mixing regions and wakes". I cannot see here any improvement on the corresponding parts of the books by Schlichting (1950) and Goldstein (1938), any advantage conferred by the date of the present book being more than balanced by the greater perspicacity of these earlier writers. The author perpetuates the misleading half-truth that near a wall "there is a laminar sub-layer in which the flow behaves as a laminar flow" (p. 40) and that the relative velocity fluctuations fall to zero at the wall (p. 242). He makes the calculation of turbulent boundary layer parameters seem even more like a set of arbitrary rules than it usually does, and even though the chapter on the compressible boundary layer is a brave attempt to be up-to-date, he has not succeeded in giving the various contributions to that problem any order and coherence. In his description of free turbulent flows, the wonderful phenomenon of the sharp transition from rotational to irrotational flow at an irregular fluctuating boundary is mentioned only once (p. 75) and it is there referred to as a postulate.

The second part of the book, on the "statistical theory", is evidently more congenial to the author, and he makes full use of the greater opportunities for presenting mathematical analysis. He has had the useful idea of including an account of elementary probability theory, and he has taken particular trouble over the account of harmonic analysis of random

functions. He uses the box device of first imagining the random function to be zero outside some distant boundary in order that the Fourier coefficients should exist, and of allowing the boundary to recede to infinity at an appropriate stage of the analysis. The approach has the advantage of directness, although in Professor Pai's hands it is rather lengthy (and he surely unnerves his readers when he says (p. 217)—wrongly—that the shape of the box in three dimensions could affect the results after the limit is taken). He makes a number of portentous remarks about ergodicity in general and about the relation between theoretical and experimental averages in turbulence, but he fails to say clearly (indeed it is not evident that he knows it) that stationarity in the variable concerned in a necessary, and usually in practice a sufficient, condition for equality of the ensemble average and an integral average. The whole treatment of stationary random functions is poor, and there is confusion (pp. 161–164) between the various values taken by a random variable and the various values taken by a random function of t at different values of t in one realization of the function. There are several gaffes, as when he states that an auto-correlation function is positive definite (p. 213) and that non-normality of the probability distributions of velocity derivatives indicates that "they are not entirely random in nature".

After these mathematical preliminaries, most of the standard analysis of homogeneous turbulence is presented. Provided no physical arguments are involved, Professor Pai gets by without much error, although the selection of material is curious and undiscriminating. Where physical justification of the analysis is needed, as in the account of Kolmogoroff's similarity theory, and in the brief excursion into turbulence in a conducting fluid, the text is quite inadequate. The introduction to chapter 13 reflects confusion between the various wave-number ranges of the spectrum and the various stages of decay; it may have been this confusion which led Professor Pai into the persistent error that inertia forces have no effect on the smallest eddies (p. 234) and that as a consequence the energy spectrum has a Gaussian form at large wave-numbers (p. 238). Nowhere does one hear about the law of decay of turbulent energy and the spectral distribution that are actually observed in real wind tunnels. As for the chapter on turbulent diffusion, I can say only that evidently Professor Pai and I have quite different views about what are the real problems involved.

I am sure that my general opinion of this book has already revealed itself sufficiently. Like the book by Corcoran, Opfell and Sage, I do not think it can be recommended, either as a text for postgraduate students or as a source of information or enlightenment to more senior people. Again like this earlier book, it is written in rudimentary English, and with little regard for the rules of grammar and punctuation.

As a less sober postscript to this review, I, like the reviewer of Part I of the present work (*J. Fluid Mech.* **2**, 1957, 515), was struck by Professor Pai's diverting habit of incorporating slices of other people's papers in his book. This is perhaps carrying the reporting technique a little too far. I was able to recognize three whole paragraphs and some odd sentences from two of my own papers in the chapter on diffusion, and more of my

own paragraphs in other chapters (with no hint that a direct quotation was being given and often without reference to the source). He even uses this strange technique on his own writing, and on page 146 reproduces what he has given on page 10. How many other writers are represented in this book? As a method of constructing a book it is so absurd that one cannot be indignant at being copied in this way. Scissors and paste may be useful accessories at a lower level of writing, but at this level it is impossible to integrate existing pieces of prose into a continuous reasoned narrative. An author cannot avoid mastering a subject and rewriting it himself.

G. K. BATCHELOR

Magnetohydrodynamics, by T. G. COWLING. New York: Interscience Publishers, Inc., 1957. 115 pp. $3.50.

The motion of a fluid or a gaseous medium possessing electrical conductivity in the presence of a magnetic field has become of great importance in the last decade. The theoretical treatment is variously designated as 'magneto-hydrodynamics' or 'magneto-gasdynamics', or more generally 'magneto-fluid dynamics', and sometimes, less characteristically, as 'hydromagnetics'. Although a few experimental investigations on the influence of magnetic forces on the motion of a conducting liquid date from the previous century and the discovery of the magnetic field of sunspots was made in the first decade of the present century, it has taken some time for a wider interest to develop. One feature leading to this wider interest seems to have been the discovery of interstellar polarization of light, which for its explanation required the assumption of interstellar magnetic fields of wide extension. Problems connected with cosmic radiation led to the same conclusion. Once the presence of such fields was recognized, many other problems called for investigation. Almost at the same time the wide application of shock waves for the investigation of high temperature gas motion with its consequent ionization led to the problem whether such flows could be influenced by means of magnetic fields; research on the behaviour of magnetically driven plasmas arose out of this. Perhaps two landmarks in the development of the subject were the first Symposium on Cosmical Gas Dynamics (Paris, 1949, later followed by meetings at Cambridge, England, 1953, and Cambridge, Massachusetts, 1957); and H. Alfvén's book *Cosmical Electrodynamics*, published in 1950. From 1950 onward papers on astrophysical problems and on results of experimental work have come out in rapid succession; the number of conferences is multiplying, and now technical applications are in view. Thus there is a need for a treatise which may help interested scientists and engineers to become acquainted with the many aspects of magneto-fluid dynamics.

Professor Cowling's book is not intended as a treatise, but as a condensed survey. The topics treated are briefly as follows. Chapter 1 gives the basic equations and general ideas, stressing the distinction between cases

where the electrical resistance of the medium is a determining influence, and those cases where the conductivity of the medium can be considered as being practically infinite. The meanings of the magnetic Reynolds number and of other non-dimensional quantities are pointed out. Since one of the factors occurring in the magnetic Reynolds number is the length scale of the field, the case of 'infinite conductivity' is of great importance in astrophysical and geophysical systems with their large dimensions, the decay times for electric current systems being here of cosmical duration. As an illustration of a different case a simple treatment is given of laminar flow under the combined influence of ordinary viscosity and what is sometimes termed 'magnetic viscosity'. Chapter 2 is about 'magneto-statics' and considers equilibrium states in which the mechanical forces are balanced by magnetic stresses. Applications are made to some astronomical problems (sunspots, streamers and filaments, and spiral arms of the galaxy). Chapter 3 treats wave motion, mainly for an incompressible fluid where the velocity of propagation is wholly determined by magnetic effects (the so-called 'Alfvén waves', connected with the effective tension along the lines of magnetic flux). Again some astrophysical applications are mentioned. Chapter 4 considers the influence of magnetic forces on the stability or instability of fluid motion, with examples taken from cases of laminar (incompressible) flow and from problems of convection. Chapter 5 is entitled 'Dynamo theories' and considers the question whether fluid or gas motions in the presence of an originally weak magnetic field can lead to an increase of the field strength, in the way in which this occurs in a self-exciting dynamo. Elsasser's, Bullard's, and Parker's theories of the origin of the magnetic field of the earth are considered and criticized. The chapter also includes a brief discussion of turbulent fields of motion and of the distribution of energy between turbulent motion and magnetic field. Finally chapter 6 gives attention to the effects of molecular structure, as they appear in ionized gases. Each chapter is concluded with a short list of the most important and relevant publications.

From this summary it will be seen that Cowling's book is of value to all who wish to become acquainted with various topics of magneto-fluid dynamics. But on the other hand, considered from the point of view of the needs of this moment, the book leaves many things to be desired. Although it is evident that in the short space set for the Interscience Tracts on Physics and Astronomy (of which this book is one) there is no room for the writing of a textbook, one has the feeling that in preparing it the author has limited himself mostly to a critical discussion of a series of selected topics, in order to point out where theories are incomplete. Professor Cowling, who is an authority in the field of gas motion under the influence of magnetic fields, of course has full right to do so, but as a result of this the reader is not greatly stimulated to enter into the subject and to attempt to work out problems for himself. It is clear moreover that the emphasis in the selection is on the geophysical and astronomical applications, as Professor Cowling himself observes in his preface; although he adds the hope that the

publication of the book may expedite developments also in the engineering aspects, one cannot say that he is giving much help in this respect.

Chapter 6, for instance, on ionized gases, indeed gives the relevant equations and puts them into various forms, and these forms are discussed from a number of points of view, but at the end the reader still may ask: where do I stand? How can I apply this to a particular problem? Mean collision times are introduced, but there is no indication concerning the methods in use for calculating or estimating them (although some of these methods are considered in *The Physics of Fully Ionized Gases*, by L. Spitzer, Jr., which appeared earlier in the same series of tracts and which may in a sense be regarded as a companion volume). In some of the other chapters of Professor Cowling's book, in the treatment of problems concerning the sun, the magnetic field of the galaxy, the magnetic field of the earth, and turbulence theory, the ultimate impression obtained is rather a negative one; it looks as if almost nothing fruitful can be done in these matters.

Problems concerning the behaviour of acoustic waves, and still less problems referring to shock waves in a magnetic field, have not been considered at all. Here a great many cases are awaiting adequate treatment and it would have been useful if at least some indications had been given. There are, for instance, three-dimensional problems concerning the propagation of shock waves approaching a magnetic field (in experimental situations one always has to do with non-uniform fields); there is also the problem of a shock wave in a cold gas subjected to a magnetic field, the electrical conductivity appearing only behind the wave front as a consequence of the high temperatures generated there. There is the problem of stationary supersonic flow of an ionizable gas around a magnetized body. Boundary layer flow under conditions leading to ionization and with magnetic field influencing the motion likewise calls for attention. Still another group of problems refers to plasmas driven by magnetic fields; this is under investigation at present on account of the very high temperatures which can be produced in them. The magnetic field due to the plasma current itself, as well as fields derived from outside sources, are both of importance in guiding the motion of the plasma. The question of the stability of the plasma current involves the so-called 'pinch effect' (the lateral contraction of a plasma current as a consequence of its own magnetic field); Professor Cowling does make two short references to this effect (pp. 27, 29) without, however, making any reference to the intriguing questions connected with it. (Some discussion of the 'pinch effect' is to be found in Spitzer's book.)

Certainly we are grateful for the material Professor Cowling has put so lucidly in 115 pages. The book seems well adapted to the needs of astrophysicists and geophysicists who wish to obtain a rapid view of the present state of the application of magneto-fluid dynamics to their field. But one who comes from the aerodynamical side still feels the need for a work of more comprehensive character, which can serve as a guide for those who wish to develop their ability to work in this interesting domain.

J. M. Burgers

JOURNAL OF FLUID MECHANICS

Volume 3, Part 5 February 1958

CONTENTS

The behaviour of a Pitot tube in transverse shear
by P. O. A. L. DAVIES 441

Flow in shock tubes with area change at the diaphragm section
by R. A. ALPHER and D. R. WHITE 457

The effects of a sound wave on the compressible boundary layer on a flat plate
by C. R. ILLINGWORTH 471

Non-linear interactions in a viscous heat-conducting compressible gas
by BOA-TEH CHU and LESLIE S. G. KOVÁSZNAY 494

A model of supersonic flow past blunt axisymmetric bodies, with application to Chester's solution
by M. D. VAN DYKE 515

The effect of a vertical lapse rate of temperature on the spiral flow of a fluid in a heated rotating cylinder
by G. N. LANCE 523

Properties of the Hugoniot function
by ROBERT D. COWAN 531

Reviews 546

Printed in Great Britain by Taylor & Francis Ltd.